

5-2018

Spatial Analysis of Air Particulate Pollution Distributions and Its Relation to Real Property Value in Beijing, China

Yingyu Zhang

State University of New York College at Buffalo - Buffalo State College, zhangy07@mail.buffalostate.edu

Advisor

Tao Tang, Ph.D., Professor of Geography

First Reader

Tao Tang, Ph.D., Professor of Geography

Second Reader

Stephen Vermette, Ph.D., Professor of Geography

Third Reader

Catherine Lange, Ph.D., Associate Professor of Earth Science and Science Education

Department Chair

Alexander Karatayev, Ph.D., Director of the Great Lakes Center

Recommended Citation

Zhang, Yingyu, "Spatial Analysis of Air Particulate Pollution Distributions and Its Relation to Real Property Value in Beijing, China" (2018). *Great Lakes Center Masters Theses*. 7.

http://digitalcommons.buffalostate.edu/greatlakes_theses/7

Follow this and additional works at: http://digitalcommons.buffalostate.edu/greatlakes_theses



Part of the [Earth Sciences Commons](#), [Environmental Education Commons](#), and the [Environmental Health and Protection Commons](#)

Abstract:

Air particulate pollution contributes the major air pollution in Beijing, China. In this research, concentrations of air particulate pollutants were measured at a total of twenty-three field locations in the urban districts of Beijing applying a laser particle counter in June and December 2015. Geographic Information System (GIS) was utilized to study the two and three-dimensional spatial distributions of air particulate pollution ($PM_{0.5}$, $PM_{1.0}$, $PM_{2.5}$, $PM_{5.0}$, PM_{10}). Geostatistical or spatial statistical models were applied to interpolate the spatial distributions of air particulate pollution and real property values in the study area. Geographically Weighted Regression (GWR) was applied to analyze the spatial relationships of air particulate pollution and distribution of real property values. The three-dimensional analysis was conducted to illustrate vertical spatial distributions of air particulate pollution for each of the twenty-three field survey profiles in ArcGIS. Temporal distributions of air particulate pollution within 10 hours daytime at two field survey locations were analyzed. The results show that the concentrations of different sizes of air particulate pollutants in urban areas of Beijing distribute differently with different spatial patterns. The spatial distributions of real property values indicate that the highest value occurred in the northwestern and the central parts of Beijing both in the June and December 2015. There is no significant relationship of real

property values and the intensity of air particulate pollution. Therefore, we suggest that the spatial distribution factors of air particulate pollution in Beijing is not a major factor for people to purchase real properties as homes.

State University of New York
College at Buffalo
Great Lake Center

Spatial Analysis of Air Particulate Pollution Distributions
and Its Relation to Real Property Value in Beijing, China

A Thesis in
Great Lakes Ecosystem Science

by

Yingyu Zhang

Submitted in Partial Fulfillment
of the Requirements
for the Degree of

Master of Arts
May 2018


Approved by:

Tao Tang, Ph.D.
Professor of Geography
Chairperson of the Committee/Thesis Adviser

Alexander Y. Karatayev, Ph.D.
Professor of Biology and Director of Great Lakes Center

Kevin J. Miller, Ed.D.
Dean of the Graduate School

Committee Member Signatures:

Dr. Tao Tang, Advisor :  Date: 04/20/2018

Dr. Stephen Vermette:  Date: 4/20/2018

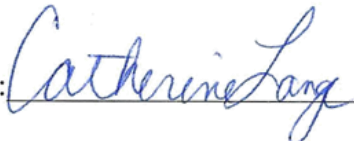
Dr. Catherine Lange:  Date: 4/20/2018

TABLE OF CONTENTS

1.	Introduction.....	1
1.1	Significance of the Study.....	1
1.2	Objectives of the Study.....	4
2.	Literature Review.....	7
2.1	The Research of Air Particulate Pollution	7
2.2	The Studies of Characteristics and Chemical Component of Air Particulate Pollution.....	10
2.3	The Studies of Temporal and Spatial Distribution of Air Particulate Pollution and Its Influential Factors	12
2.3.1	Temporal Distribution of Air Particulate Pollution.....	13
2.3.2	Spatial Distribution of Air Particulate Pollution.....	14
2.4	The Studies of Real Property Value and Its Influential Factors	15
2.5	Applications of GIS	18
2.5.1	GIS Application in Air Particulate Pollution Studies.....	18
2.5.2	GIS Application in the Real Property Analyses	20
2.6	Applications of Remote Sensing to Air Particulate Pollution and Land Use and Land Cover (LULC) Studies.....	21
3.	Methodology.....	22
3.1	The Study Area	23
3.2	Field Data Collection	25
3.3	Data-mining of Real Property Values Online	32
3.4	Spatial Analyses in ArcGIS Environment.....	33
3.4.1	Kriging Interpolation	33
3.4.2	Geographically Weighted Regressions (GWR)	36
3.5	Land Use and Land Cover (LULC) Analyses.....	37
4.	Results.....	41
4.1	Results of Temporal Distribution.....	42
4.2	Result of Spatial Distribution.....	53
4.2.1	Two-Dimensional Spatial Distributions of Air Particulate Pollution	53
4.2.2	Three-Dimensional Spatial Distributions of Air Particulate Pollution	68
4.2.3	Spatial Distributions of Real Property Values.....	121

4.2.4 Spatial Relations to Distributions of Air Particulate Pollution and Real Property Values	125
5. Conclusion	129
5.1 Temporal Distributions of Air Particulate Pollution	129
5.2 Two Dimensional (2D) Spatial Distributions of air particulate and Real Property Values.....	129
5.3 Three Dimensional (3D) Spatial Distributions of Air Particulate Pollution ...	130
5.4 The Further Research of Studying Spatial Relationships of Air Particulate Pollution and Real Property Values	131
5.5 Limitations of the Study.....	134
6. Bibliography	135
Appendix A	151
Appendix B.....	154

ILLUSTRATIONS

Figure 1: The Size of Air Particle Pollutants (EPA, 2016)	1
Figure 2: Average Housing Prices in Beijing (Fangjia, 2015)	17
Figure 3: Beijing's Location in China Map	24
Figure 4: The Map of Urban Districts in Beijing Municipality	25
Figure 5: Handheld GrayWolf Laser Particle Counter Model: 3016-IAQ.....	26
Figure 6: Positions and the Sequence of Data Collection.....	29
Figure 7: Locations at Yiyuanju and Shuixingyuan.....	32
Figure 8: The Original Imagine of Beijing	39
Figure 9: A Sample of Supervised Classification	41
Figure 10: Attribute Table after Supervised Classification.....	41
Figure 11: Temporal Distribution of Fine PM Concentrations at Yiyuanju.....	45
Figure 12: Temporal Distribution of Total PM Concentrations at Yiyuanju.....	46
Figure 13: Temporal Distribution of Fine PM Concentrations at Shuixingyuan	47
Figure 14: Temporal Distribution of Total PM Concentration at Shuixingyuan	48
Figure 15: PM _{0.5} Spatial Interpolation Map	58
Figure 16: PM _{1.0} Spatial Interpolation Map	60
Figure 17: PM _{2.5} Spatial Interpolation Map	62
Figure 18: PM _{5.0} Spatial Interpolation Map.....	64
Figure 19: PM ₁₀ Spatial Interpolation Map	66
Figure 20: Change of PM Concentration in Summer 2015	69
Figure 21: Change of PM Concentration in Winter 2015	69
Figure 22: PM _{0.5} Spatial Distribution Map in Summer.....	75
Figure 23: PM _{0.5} Spatial Distribution Map in Winter	80
Figure 24: PM _{1.0} Spatial Distribution Map in Summer.....	85
Figure 25: PM _{1.0} Spatial Distribution Map in Winter	90
Figure 26: PM _{2.5} Spatial Distribution Map in Summer.....	95
Figure 27: PM _{2.5} Spatial Distribution Map in Winter	100
Figure 28: PM _{5.0} Spatial Distribution Map in Summer.....	105
Figure 29: PM _{5.0} Spatial Distribution Map in Winter	110
Figure 30: PM ₁₀ Spatial Distribution Map in Summer	115
Figure 31: PM ₁₀ Spatial Distribution Map in Winter.....	120
Figure 32: Spatial Distribution of Real Property Value	124
Figure 33: GWR Regression Residual Map.....	128
Figure 34: LULC Classification of Beijing Urban Area.....	133
Figure 35: LULC Classification of Beijing (including urban and suburban areas)...	134

TABLES

Table 1: Data Collections in 2015 a)summer, b)winter	27
Table 2: Mean of Air Particulate Pollution ($\mu\text{g}/\text{m}^3$).....	42
Table 3: 24-hours mean in Standards ($\mu\text{g}/\text{m}^3$)	43
Table 4: Statistical Data of Air Particulate Pollution (Yiyuanju, $\mu\text{g}/\text{m}^3$).....	44
Table 5: Statistical Data of Air Particulate Pollution (Shuixingyuan, $\mu\text{g}/\text{m}^3$)	46
Table 6: Temporal Distributions of PM Concentrations	51
Table 7: Temporal Profiles of Three-three Sites	53
Table 8: Coefficients of Each PM Concentration of a)Yiyuanju b)Shuixingyuan.....	54
Table 9: Data of Air Particulate Pollution (summer 2015, $\mu\text{g}/\text{m}^3$).....	56
Table 10: Data of Air Particulate Pollution (winter 2015, $\mu\text{g}/\text{m}^3$)	56
Table 11: Data of Real Property Values (USD/m^2).....	121

1. Introduction

1.1 Significance of the Study

Air particulate pollution, which is also called pollution of particulate matter (PM), is the term for a mixture of extremely small solid particles and liquid droplets found in the air (EPA Particulate Matter, 2016). According to EPA (United States Environmental Protection Agency), there are two categories of air particulate pollutants (Figure 1): inhalable coarse particles and fine particles (EPA Particulate Matter, 2016). Inhalable coarse particles are larger than 2.5 micrometers and smaller than 10 micrometers in diameter. Fine particles are 2.5 micrometers in diameter and smaller (EPA Particulate Matter, 2016).

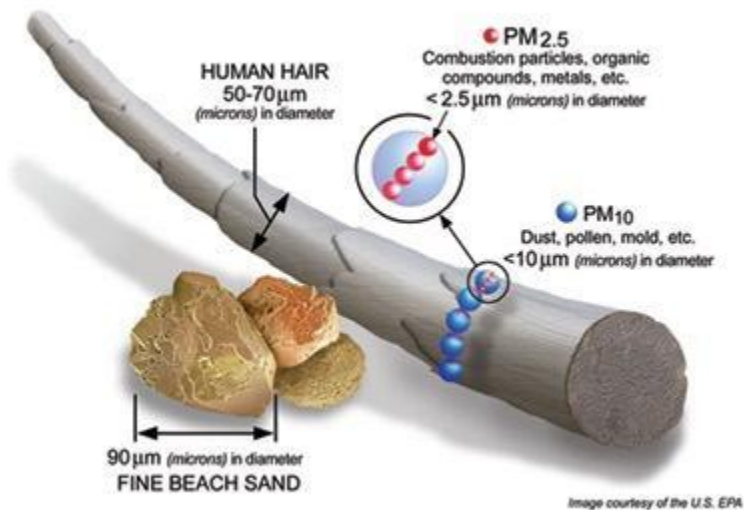


Figure 1: The Size of Air Particle Pollutants (EPA Particulate Matter, 2016)

Air pollution is one of environmental problems in recent decades, which has a serious toxicological impact on human health (Robinson, 2005; Habre et al., 2014; Adel et al., 2016). According to the US National Ambient Air Quality Standards (NAAQS) and World Health Organization (WHO), air particulate pollution is one of the six criteria air pollutants (air particulate pollution, ground-level ozone, carbon monoxide, sulfur oxides, nitrogen oxides, and lead). EPA calls these pollutants “criteria” air pollutants because it sets NAAQS for them based on the criteria, which regard their effects on health or welfare (EPA, 2017). Particles with a diameter of less than 10 microns (PM_{10}), including fine particles less than 2.5 microns ($PM_{2.5}$) pose risks to health, because they are capable of penetrating peoples’ lungs and entering their bloodstream (WHO, 2018). The health effects of air particulate pollution include respiratory and cardiovascular morbidity (such as aggravation of asthma, respiratory symptoms and an increase in hospital admissions); mortality from cardiovascular and respiratory diseases and from lung cancer (WHO, 2013; EPA, 2017). The health effects of air particulate pollution due to the exposure levels: short term (hours, days) and long term (months, years). Short-term exposure to particulate matter (PM) is a risk factor on respiratory health, and long-term exposure to PM may lead to a marked reduction in life expectancy. The increase of cardiopulmonary and lung cancer mortality are the main reasons for the reduction in life expectancy (Pelucchi et al., 2009; Jerrett et al., 2009; Zhou et al., 2014; Adel et al., 2016)

Rapid economic growth and industrial development have been taken place in China in recent years (He et al, 2001). Beijing, the capital of the country and one of the largest cities, encounters serious air particulate pollution (Tang et al., 2010). According to the data from Beijing Municipal Environmental Protection Bureau, the annual average concentration of PM_{2.5} was 80.6µg/m³ in 2015, which was eight times higher than WHO air quality standards of PM_{2.5} (10µg/m³ annual mean), 2.3 times higher than the China Air Quality Standards (35µg/m³ annual mean, Class 2) and five times higher than National Ambient Air Quality Standards (NAAQS, 15µg/m³ annual mean). The annual average concentration of PM₁₀ was 101.5µg/m³ in 2015, which was five times higher than WHO air quality standards of PM₁₀ (20µg/m³ annual mean), 1.5 times higher than the China Air Quality Standards (70µg/m³ annual mean, Class 2).

With the development of economy and the growing population, demands of residents for real property increase dramatically in Beijing, which lead to relative growth of real property values (Chivakul et al., 2015). Consumer demands, the level of income, social security, residential environment have significant impacts on real property values (Liu et al., 2016). Nikolaos et al. (2011) suggested that the natural environment has an impact on real property values, however, there are very few studies show the relationships between air particulate pollution and real property values of the area, especially spatial

relationships in large or super large municipalities, such as Beijing.

Geographic information systems (GIS) offer researchers a powerful method of managing, analyzing, and displaying spatial information (GISGeography, 2017). Therefore, GIS was utilized in this research to analyze spatial distribution of air particulate pollutants in the urban area of Beijing and the spatial relationships between air particulate pollutants and real property values. Remote sensing is also a powerful tool to extract spatial information on Land Use Land Cover (LULC) changes over a large area (Carlson et al., 1999; Guerschman et al., 2003; Rogana and Chen, 2004; Zsuzsanna et al., 2005; Reis, 2008). LULC classification is one of the most widely and commonly used applications in remote sensing (Saadat et al., 2011).

1.2 Objectives of the Study

The objectives of this research are:

- a) to visualize the spatial patterns in two dimensions of air particulate pollutant ($PM_{0.5}$, $PM_{1.0}$, $PM_{2.5}$, $PM_{5.0}$, PM_{10}) concentrations and analyze the spatial relationships between the air particulate pollution and its distributions of real property values.

Some studies indicate that air particulate pollution of different particle sizes in Beijing have different characteristics of spatial distribution and pollution sources (Zhu et al.,

2016, Wang et al.,2013b). Cheng et al. (2014) and Pearce et al. (2009) mentioned that the characteristics of spatial distribution and sources of air pollution are affected by many factors, such as meteorological (wind directions, humidity etc.) and anthropic (transportation etc.) factors. In order to analyze the spatial distribution of PM in different particle sizes, we applied particle counters with concentrations of PM to collect data at twenty-three locations in Beijing urban area. Geospatial models were established by using GIS in this study. In recent years, real property values have increased dramatically in the City of Beijing (Glaeser 2016). Geographic locations, residential environment, favorite floors, etc. are the main factors affecting real property prices (Corsini, 2009). More researches about the spatial relationships between air particulate pollution and its relations to the distributions of real property are needed, in particular, for the large city like Beijing. The goal of this research is to test spatial statistically if there is a strong correlation between the concerning of relative low air particulate concentrations and high real estate prices (or appreciations of the real estate locations). The original hypothesis is that air particulate pollution is not a criterion of real estate choice. The alternative hypothesis is that air particulate pollutions contribute the values or appreciations of real properties in the study area.

b) to visualize the spatial distributions in three dimensions on air particulate pollution

(PM_{0.5}, PM_{1.0}, PM_{2.5}, PM_{5.0}, PM₁₀) concentrations and compare the different spatial patterns at different levels of elevations.

Data from Beijing Municipal Environmental Protection Bureau (2015) indicated that the concentrations of PM_{2.5} were very high in 2015 with the average 80.6µm per cubic meter. A survey made by Institute of Public and Environmental Affairs in 2012 showed that 87.5% of local residents in Beijing concerned about air quality, that is to say, air quality got attentions from more than two-thirds (2/3) of population in Beijing. Yang et al. (2005) studied the vertical distributions of PM_{2.5} concentrations at fourteen days in the autumn and winter in Beijing. They found the vertical distribution of PM_{2.5} concentrations decreased with the increase of the altitude in the autumn and winter. Therefore, this study visualized the three-dimensional (3D) spatial distributions of air particulate pollution and compare the spatial profiles of air particulate pollution in different elevations.

c) to help the local government mitigate and control the air particulate pollution.

Air particulate pollution became a serious problem and pushed government to mitigate and control it. The Five-Year Plan of Chinese government which is a draft economic plan for the next five years, contains new targets that will need to be met to solve the environmental crises (China's National People's Congress, 2016) This study would be a useful guidance for the government to understand the spatial distributions of air

particulate pollution and to control and reduce the air pollution.

2. Literature Review

The literatures relevant to this study has been reviewed into the following sections: 1) the researches of air particulate pollution, 2) the studies of characteristics and chemical component of air particle pollutants, 3) the studies of temporal and spatial distribution of air particulate pollution and its influential factors, 4) the studies of real property value in Beijing and its influential factors, 5) applications of GIS in analyzing air particulate pollution and the real properties, 6) applications of remote sensing to air particulate pollution and land use and land cover (LULC) studies.

2.1 The Research of Air Particulate Pollution

In 2005, WHO established the air quality guidelines of annual mean and 24-hour mean concentrations of PM_{2.5} and PM₁₀. The annual mean concentration of PM_{2.5} is 10 $\mu\text{g}/\text{m}^3$ and the 24-hour mean concentration is 25 $\mu\text{g}/\text{m}^3$; the annual mean concentration of PM₁₀ is 20 $\mu\text{g}/\text{m}^3$ and its 24-hour mean concentration is 50 $\mu\text{g}/\text{m}^3$. In 1982, ambient air quality standard was regulated in China, when initial limits were set for TSP (Total Suspended Particulates), SO₂, NO₂, lead and Benzopyrene. In 1996, the standard was both strengthened and expanded from 1982 standard; in February 2012, China released a new national air quality standard (GB3095-2012), which sets limits for the first time on PM_{2.5}.

The new standards took effect nationwide in 2016, but Beijing required to implement the standards in 2012. China Air Quality Standards (GB3095-2012) divided standards into classes: Class 1 applies to special regions (including national parks) and Class 2 applies to all other areas. The annual mean concentration of $PM_{2.5}$ in China Air Quality Standards (GB3095-2012, Class 2) is $35\mu\text{g}/\text{m}^3$ and the 24-hour mean concentration is $75\mu\text{g}/\text{m}^3$; the annual mean concentration of PM_{10} is $70\mu\text{g}/\text{m}^3$ and its 24-hour mean concentration is $150\mu\text{g}/\text{m}^3$. In 1990, The Clean Air Act required EPA to set National Ambient Air Quality Standards (NAAQS) for pollutants which were considered harmful to public health and the environment. EPA established the National Ambient Air Quality Standards (NAAQS) for the six criteria air pollutants (air particulate pollution, ground-level ozone, carbon monoxide, sulfur oxides, nitrogen oxides, and lead). In NAAQS, annual mean concentration of fine particle ($PM_{2.5}$) to be less or equal to $15\mu\text{g}/\text{m}^3$ (Primary) and the 24-hour mean concentration of $PM_{2.5}$ is $35\mu\text{g}/\text{m}^3$ (Primary and Secondary); the 24-hour mean concentration of PM_{10} is $150\mu\text{g}/\text{m}^3$.

China has experienced severe air pollution these years (Chen et al., 2013; Guan et al., 2016; Guo et al., 2014; Huang et al., 2014; Li et al., 2016; Sun et al., 2014; Wang et al., 2016; Zhang et al., 2015; Song et al. 2017a). Wang et al. (2000) studied the characteristics of air particulate matter and found there was a heavy air particulate

pollution in most areas in China. Song et al. (2017) analyzed data of particulate matter concentrations ($PM_{2.5}$ and PM_{10}) from 1300 national air quality monitoring sites in a period of three years (January 2014 to December 2016). They found that $PM_{2.5}$ pollution was much heavier in winter than in summer, especially in the Northern China (Song et al., 2017a). $PM_{2.5}$ has become the most frequent and major pollutant in China followed by PM_{10} and O_3 (Song et al., 2017a). The first study of air particulate pollution was done in Beijing during the year between 1989 and 1990 (Chen et al., 1994). At present, researches on air particulate pollution in China are carried out by departments and institutions of environmental research and management across the nation (Wang et al., 2014).

With the rapid development of science and new technologies, various methods such as GIS and remote sensing were used to study air particulate pollutants and analyze the spatial distributions of air pollution (Zhang et al., 2015). Gorai et al. (2014) utilized GIS to analyze the spatial patterns of asthma hospitalization and air pollutants in New York State. Spendley and Brehme (2014) applied GIS for topographic analysis and modeling air pollutant concentrations in the study of influencing factors on particulate pollution in Keene, New Hampshire.

2.2 The Studies of Characteristics and Chemical Component of Air Particulate Pollution

Particulate Matter (PM), a mixture of solids and liquid droplets floating in the air, affects human living environments in terms of air quality, public health, climate effects and ecosystems (Watson, 2003; AirNow, 2014). High concentrations of air particulate pollution may cause respiratory diseases and cardiovascular diseases (Lee et al., 2014).

Air particulate pollution has become one of the major environmental problems in the City of Beijing (He et al, 2001). Air particulate pollution acts as a trigger for haze events (light attenuation) which relate to both meteorological conditions and pollutant levels in the atmosphere (Song et al. 2017). Fine particles are believed to be one of the major reasons in scattering of visible light and a cause of the degradation of visibility (Sloane et al., 1991; Zhao et al. 2013).

Many studies indicated that elemental carbon (EC), organic carbon (OC), ionic species (i.e., sulfate $[\text{SO}_4^{2-}]$, nitrate $[\text{NO}_3^-]$, ammonium $[\text{NH}_4^+]$, chloride $[\text{Cl}^-]$, sodium $[\text{Na}^+]$, etc.), crustal elements, and water are the major constituents in PM (Lee et al., 2002; Pathak et al., 2003; Shen, 2010; Tsai et al., 2011). EC and OC particles are released from the incomplete combustion of carbonaceous fuels; EC is a primary pollutant that is emitted directly during the combustion processes; OC consists of primary and secondary carbons;

primary OC is emitted in the particulate phase, and secondary OC is formed via gas-to-particle processes of volatile organic compounds (VOCs) in the atmosphere (Lee et al., 2002; Pathak et al., 2003; Aneja et al., 2006; Shen, 2010; Tsai et al., 2011). In addition, SO_4^{2-} , NO_3 , and NH_4 are the common components of secondary inorganic aerosols in the atmosphere, and the particles are formed via the reactions of the precursors of sulfur dioxide (SO_2), oxides of nitrogen (NO_x ; nitric oxide [NO] and nitrogen dioxide [NO_2]), and ammonia (NH_3) in the atmosphere (Lee et al., 2002; Pathak et al., 2003; Aneja et al., 2006; Shen, 2010; Tsai et al., 2011). Particulate matter (PM) is composed of various chemical elements (Seinfeld 1989). Zhang et al. (2013) found twenty main chemical elements (Al, As, Br, Ca, Cl, Cr, Cu, Fe, K, Mg, Mn, Ni, P, Pb, S, Se, Si, Ti, V and Zn) in Beijing using X-Ray Emission (PIXE).

Air quality models which use mathematical and numerical techniques simulate the physical and chemical processes that affect dispersion and reaction of air pollutants in the atmosphere (EPA, 2017). These models are utilized to characterize primary pollutants that are emitted directly into the atmosphere and secondary pollutants that are formed as a result of complex chemical reactions within the atmosphere (EPA, 2017). Dispersion modeling, photochemical modeling and receptor modeling are the three commonly used air quality models (EPA, 2017). Dispersion modeling use mathematical formulations to

characterize the atmospheric processes that disperse a pollutant emitted by a source; photochemical models are large-scale air quality models which simulate the changes of pollutant concentrations in the atmosphere by using mathematical equations characterizing the chemical and physical processes in the atmosphere; receptor models are mathematical or statistical procedures for identifying and quantifying the sources of air pollutants at a receptor location (EPA, 2017). Zhang et al. (2013) collected 121 daily $PM_{2.5}$ samples from an urban site in Beijing between April 2009 and January 2010 (four seasons). They utilized chemical mass balance (CMB) and positive matrix factorization (PMF) to characterize aerosol speciation, identify likely sources and their contributions (Zhang et al., 2013). CMB and PMF are receptor models to identify the likely sources and quantify source contributions (EPA, 2017). In their research, the PMF model identified six main sources: soil dust, coal combustion, biomass burning, traffic and waste incineration emission, industrial pollution, and secondary inorganic aerosol in Beijing urban area (Zhang et al, 2013). Each of these sources has an annual mean contribution of $PM_{2.5}$ is 16%, 14%, 13%, 3%, 28%, and 26%; however, the relative contributions of these identified sources significantly vary with changing seasons (Zhang et al, 2013).

2.3 The Studies of Temporal and Spatial Distribution of Air Particulate Pollution and

Its Influential Factors

2.3.1 Temporal Distribution of Air Particulate Pollution

In these recent years, air particulate pollution occurred many times in winter in Beijing (Zhao et al., 2014). Seasonal variation of air particulate pollution was significant, with the highest concentration in the winter and the lowest in the summer (He et al, 2001).

Using PM_{2.5} and PM₁₀ as examples, the maximum values of PM_{2.5} and PM₁₀ mass concentrations appeared in January, while the minimum values in April in 2012 in Beijing urban area (Zhao et al., 2014). Both these two sizes of particulate matter were significantly influenced by meteorological conditions (Zhao et al., 2014). Meteorological factors, such as daily average temperature (°C), relative humidity (%), wind speed (wind scale) and precipitation (mm), were the main factors influenced the daily changes of PM_{2.5} and PM₁₀ (Zhao et al., 2014). However, seasonal changes of PM_{2.5} and PM₁₀ mass concentrations demonstrated that they were positively correlated with temperature and relative humidity, respectively, and strongly negatively correlated with wind speed (Zhao et al., 2014). Wind speed and relative humidity are two major factors affecting the temporal distributions of PM_{2.5} and PM₁₀ mass concentrations (Zhao et al., 2014).

In addition, anthropogenic factors are also important that cannot be ignored (Shi et al., 2012). Shi et al. (2012) discussed diurnal variations trends of PM_{2.5} concentrations which

showed a distinctive bimodal pattern with two marked peaks during the morning and evening rush hour times, that can be explained as the impact of high volume of traffic on the streets. Higher concentrations of $PM_{2.5}$ were observed in rush hours on weekdays compared to weekends, suggesting the influence of anthropogenic activities on the fine particulate levels, for example, traffic-related local $PM_{2.5}$ emissions (Shi et al., 2012). Bernosky and Vermette (2012) monitored PM_{10} along Phnom Penh roads and created road-side temporal profiles. They established “commuter profile” and “business district profile” to study temporal relationships between PM_{10} and field survey locations.

2.3.2 Spatial Distribution of Air Particulate Pollution

Air particulate pollutions have significant spatial characteristics which are very important for us to study. In general, the $PM_{2.5}$ pollution is higher in the south and east part of Beijing and is lower in the north and west, but when south or southeast wind is blowing, the situation could be totally the opposite (Hu et al., 2013). Meanwhile, Beijing is surrounded from the north, west, and east by the Yanshan Mountains (Yang et al., 2011). Due to the mountain terrain, it is not beneficial to the horizontal diffusion of air pollutants and leads to higher $PM_{2.5}$ concentrations (Chen et al., 2016).

A GRIMM 180 aerosol particle spectrometer which measures both the dust mass in

real-time and simultaneously the according particle sizes and their distribution in different size ranges can be used to analyze the vertical distributions of air particulate pollution (GRIMM Aerosol Technik, 2016). The concentrations of PM₁₀, PM_{2.5}, and PM_{1.0} decreased with height in vertical profiles (Deng et al., 2015). PM, especially PM_{2.5} showed complex vertical distributions and they had distinct layered structures with elevated levels extending to the 100, 200 and 300m heights (Chan et al., 2005). The meteorological evidence suggested that atmospheric layers over urban Beijing were featured by strong temperature inversions close to the surface (< 50m) and more stable conditions aloft. They enhanced the accumulation of pollutants and probably caused the complex vertical distributions of PM over urban Beijing (Chan et al., 2005).

Other factors such as measuring sites near main traffic roads (bus or subway stations), densely inhabited district or factories influence the concentrations of air particulate pollution (Phuleria et al., 2007). Because individual organic compounds such as hopanes and steranes and selected polycyclic aromatic compounds (PAHs, generated via combustion) were found in emissions of vehicles, they were considered as sources of particulate matter (Phuleria et al., 2007).

2.4 The Studies of Real Property Value and Its Influential Factors

China has become one of the world's fastest growing economies and has the most active as well as interesting real estate markets in the world (Deng et al., 2009). In the past decade, the Chinese real estate market had dramatic growth (Qiao, 2010). The data from National Bureau of Statistics of China and Bank of China showed that the average price of commercial houses in Beijing area (including urban and suburban districts) in 2015 was 22633.00 CNY/m², about 3478.79 USD/m² (Exchange rate: 100USD=650.6CNY). While in 2014, the average price of real estate was 18833.00 CNY/m², about 3019.56 USD /m² (Exchange rate: 100USD=621.64CNY). From the average housing price map (Figure 2), Xicheng District, Dongcheng District and Haidian District which are the developed regions and had the highest average housing prices. While Fangshan district which is one of the Beijing suburb regions had the lower prices (Fangjia, 2015).

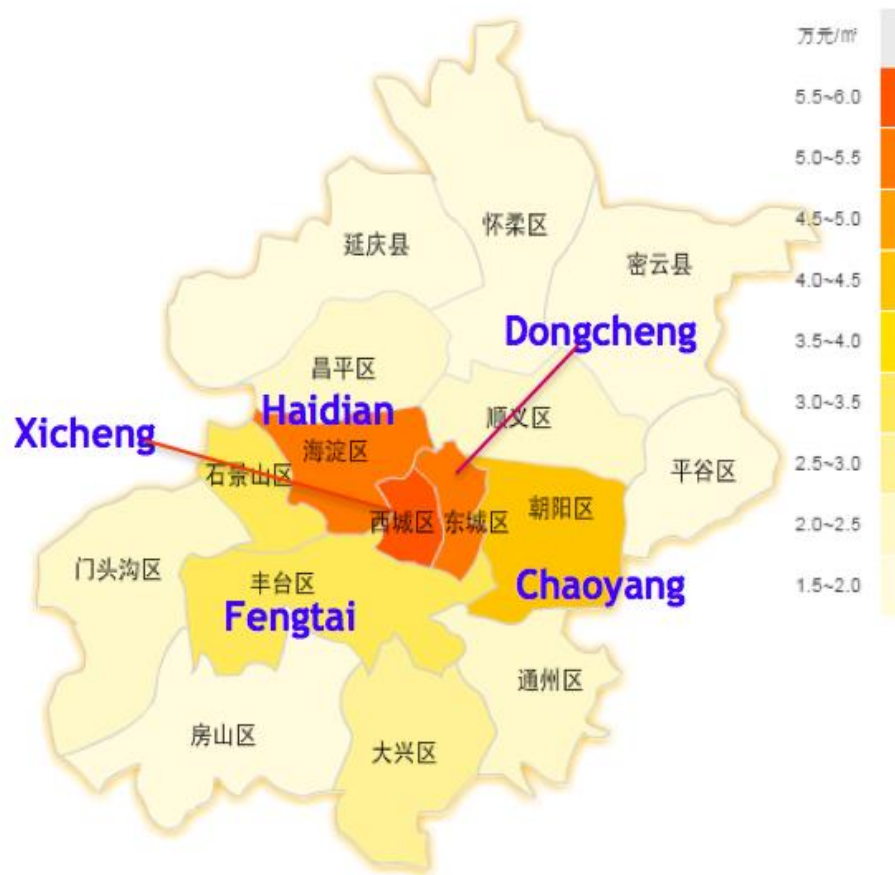


Figure 2: Average Housing Prices in Beijing (Fangjia, 2015)
 in the figure, 万元/m² represents 10,000 CNY/m²,
 according to the exchange rate in 2015:
 100USD=650.6CNY, 10,000 CNY/m²=1537 USD/m²

Case and Shiller (1990) found that housing prices had the positive relationship with some economic factors such as construction costs, population growth, and income (Case et al., 1990). Potepan (1996) further analyzed more factors, including social environmental factors such as rent, land prices, household income, population, quality of public services, crime rate, air pollution, non-housing prices, mortgage, interest rates, property tax rates, construction costs, agricultural land prices, and legal land use constraints. Yang et al.

(2015) concluded that the natural landscape characteristics had the significant impact on housing price, especially the cottages and villas. Cui et al. (2010) analyzed the influential factors of housing prices in Beijing, and he summarized three major factors that were consumers, the real estate agencies and the government.

2.5 Applications of GIS

2.5.1 GIS Application in Air Particulate Pollution Studies

Geographic Information System (GIS) is one of the powerful technologies that can be used to map and model the distributions of air particulate pollution (Zhang et al., 2015). In order to conduct spatial analyses in GIS, various geostatistical methods, such as inverse distance weighting (IDW) and Kriging have been developed to interpolate pollutant values at locations where data are unavailable collected (Wong et al., 2004; Moore et al., 2007). Dashtpajardi et al. (2012) utilized IDW and ordinary kriging (OK) interpolation to interpolate data for evaluating the distribution of air pollutant (NO₂) in the south west of Iran. They found ordinary kriging had less error (Dashtpajardi et al., 2012). Tang et al. (2010) applied universal kriging (UK) to analyze the spatial distributions of concentrations for PM_{0.3}, PM_{0.5}, PM_{1.0}, PM_{3.0} and PM_{5.0}. UK was selected as the interpolation tool because it does not assume that the predicted value on average is a constant in study area (Tang et al. 2009). UK also was suggested as potential prediction

methods for evaluating the health effects of long-term exposure to ambient air pollution (Mercer et al. 2011).

Geographically weighted regression (GWR) is an exploratory tool that can generate a separate regression equation to address spatial variation (Fotheringham et al., 2002).

GWR provides a spatial statistical model of the variables for predicting if a variable can fit the separate regression equation to every feature (Brunsdon et al., 1996;

Ogneva-Himmelberger et al., 2009; Tang et al., 2009). Tang et al. (2009) conducted GWR model for analyzing the coefficients or relationships between spatial concentrations of air particulate pollution and residential respiratory diseases in Beijing in 2008. Li et al.

(2015) developed a GWR model to examine the impacts of urban structure and activities on PM_{2.5} concentrations in Beijing.

Traditional two-dimensional (2D) maps require the creation of many scenes, one at each height for studying the change of pollution concentrations with elevations (Sears and Jacko, 2008). In 2008, University College London (UCL) Centre for Advanced Spatial Analysis (CASA) and Environmental Research Group (ERG) in Kings College London created an interactive three-dimensional (3D) air pollution map (CASA and ERG, 2008).

They produced the 3D virtual scenes of Central London and air pollution predictions of

NO₂, NO_x and PM₁₀ which were fused in these 3D virtual scenes to build the 3D air pollution map (CASA and ERG, 2008; Zahran et al., 2010). Meike (2016) made 3D models of air pollutants data in the “Project Sky Nose” by using ArcGIS. The data was collected by a quadcopter with a sensor payload. Meike (2016) visualized the data points and created a 3D map.

2.5.2 GIS Application in the Real Property Analyses

GIS can be used in scientific investigations, resource management, and development planning (He, 2001). The real estate designing and planning is one of the essential applications of GIS. The GIS model has become a main tool in real estate designing and planning (Lin et al., 2001). Lin et al. (2001) introduced the technology of GMN which abbreviating GIS+MIS (Management Information Systems)+Network in developing real estate management software. GIS provides geographic information and 3D visualization capabilities to traditional real estate software system (Lin et al., 2001). GIS technology is particularly fitting to the application of real estate analyses because the real estate property is geospatial in nature (Donlon, 2007). Amaneddine and Chmait (2009) developed another tool called UGIS (“You Get It Simply”) for helping customers and real estate agents to search and explore different types of real estates around Lebanon. UGIS is based on GIS platform and enhanced with GIS to build indexed search engine and

visualize the spatial distribution of real properties (Amaneddine and Chmait, 2009).

2.6 Applications of Remote Sensing to Air Particulate Pollution and Land Use and

Land Cover (LULC) Studies.

Remote sensing has been widely used for environmental applications such as for air quality and water quality studies (Penner, et al. 2002). Lim et al. (2009) utilized Landsat satellite images to test the algorithm which was developed to map the spatial distribution of PM₁₀ concentrations. Hadjimitsis et al. (2002) investigated the potential of using satellite remotely sensed imagery for assessing atmospheric pollution. Aerosol optical thickness was detected from Landsat-5 TM band 1 images (Hadjimitsis et al., 2002). Zhai et al. (2015) utilized high resolution remote sensing images to estimate the spatial distribution of PM_{2.5} concentrations in Shijiazhuang, China.

Barrett and Ben-Dov (1967) stated LIDAR (laser radar) could meet the needs of measuring vertical profiles of atmospheric particulate concentrations. Warren (1969) discussed the fundamental capabilities and limitations of the LIDAR in observing particulate concentrations in atmosphere. The accuracies of return signal of backscatter and attenuation as well as the optical parameters related to the characteristics of the aerosol limited the technique (Warren, 1969). The main areas of utility for LIDAR in air

pollution are observing the structure and height of mixing layers; measuring the transport and diffusion of clouds of particulates; detecting the opacity of smoke-plume (Warren, 1969).

Land use and land cover (LULC) are two important geographic categories record socio-economic activities and land management practices (Comber, 2008). Anderson et al. (1976) utilized remote sensor data to identify nine basic classes in United States: “Urban or Built-up Land”, “Agricultural Land”, “Rangeland”, “Forest Land”, “Water”, “Wetland”, “Barren Land”, “Tundra” and “Perennial Snow or Ice”. Colditz et al. (2011) did a LULC study in both South Africa and Germany. They identified five categories, which were “urban”, “agriculture”, “forested and semi-natural land”, “wetland”, and “water” (Colditz et al., 2011). Han et al. (2015) did simulation and projection of land use changes in Beijing in 1985, 2000 and 2010. They found that cultivated land converts to urban built-up land, which will become the main feature of LULC changes (Han et al., 2015). Tian et al. (2014) also developed LULC datasets for Beijing in 1978, 1987, 1992, 2000 and 2010 from Landsat images and Sun et al. (2016) mentioned LUCC is a key factor affects atmospheric particulate pollution.

3. Methodology

3.1 The Study Area

Beijing is located in the northern tip of the North China Plain, the latitude and longitude in Beijing are 39.9042°N and 116.4074°E (Figure 3). The Yan Mountain surrounds the area of city in the north, northwest and west sides. The climate in Beijing is a monsoon-influenced humid continental climate which is characterized by relative high humidity, hot and moist in the summers; and cold, windy, and dry in the winters (People's Daily, n.d.). The municipality covers $16,410\text{ km}^2$ and is composed by 16 urban and suburban districts and 2 counties (Figure 4). The major urban transportation framework in the city is shaped by circular freeways that are called the 'Ring Roads': starting from the "Second Ring Road" and expanding to the "Sixth Ring Road". Owing to the economic development, landscape and density of residential and commercial buildings, the "Fourth Ring Road" could be regarded as the boundary between the urban and the suburban regions in Beijing (Yang et al, 2013). Six urban districts are within the "Fourth Ring Road" namely Xicheng, Dongcheng, Chaoyang, Haidian, Fengtai and Shijingshan.

In this research, we conducted the field measurements and analyzed spatial distributions of air particulate pollution and real property values in the urban areas of Beijing that are within the "Fourth Ring Road". According to the most recent (6th) census of China, the total municipal population in 19.6 million, and 86% of this population are considered as

urban residents (Beijing Statistic Bureau, 2011) or people who live in these six districts. In addition, Beijing has estimated more than 6 million migrant workers (people from other provinces and cities). These people traveled to Beijing for better economic opportunities (Yang et al, 2013).



Figure 3: Beijing's Location in China Map
(ChinaHIGHLIGHTS, 2012)



Figure 4: The Map of Urban Districts in Beijing Municipality (CHINATouristMaps, 2010); the orange lines represent the Beijing “Ring Roads”

3.2 Field Data Collection

The concentrations of air particulate pollutants ($PM_{0.5}$, $PM_{1.0}$, $PM_{2.5}$, $PM_{5.0}$, PM_{10}) were collected by a team of the graduate students and faculty of Capital Normal University and SUNY Buffalo State College. A handheld GrayWolf Laser Particle Counters 3016-IAQ which was made by GrayWolf Company in U.S. (Figure 5) was used to collect and record air particulate data during the two-time periods without precipitations: June 15th to June 24th, 2015, and December 24th to December 26th, 2015 (in this research, “summer” and

“winter” refer to these dates, including tables and graphs). Table 1 and Figure 6 show both the positions and the sequence of data collection in different seasons.



Figure 5: Handheld GrayWolf Laser Particle Counter Model: 3016-IAQ (the data inside the red circle show concentrations of air particulate pollution)

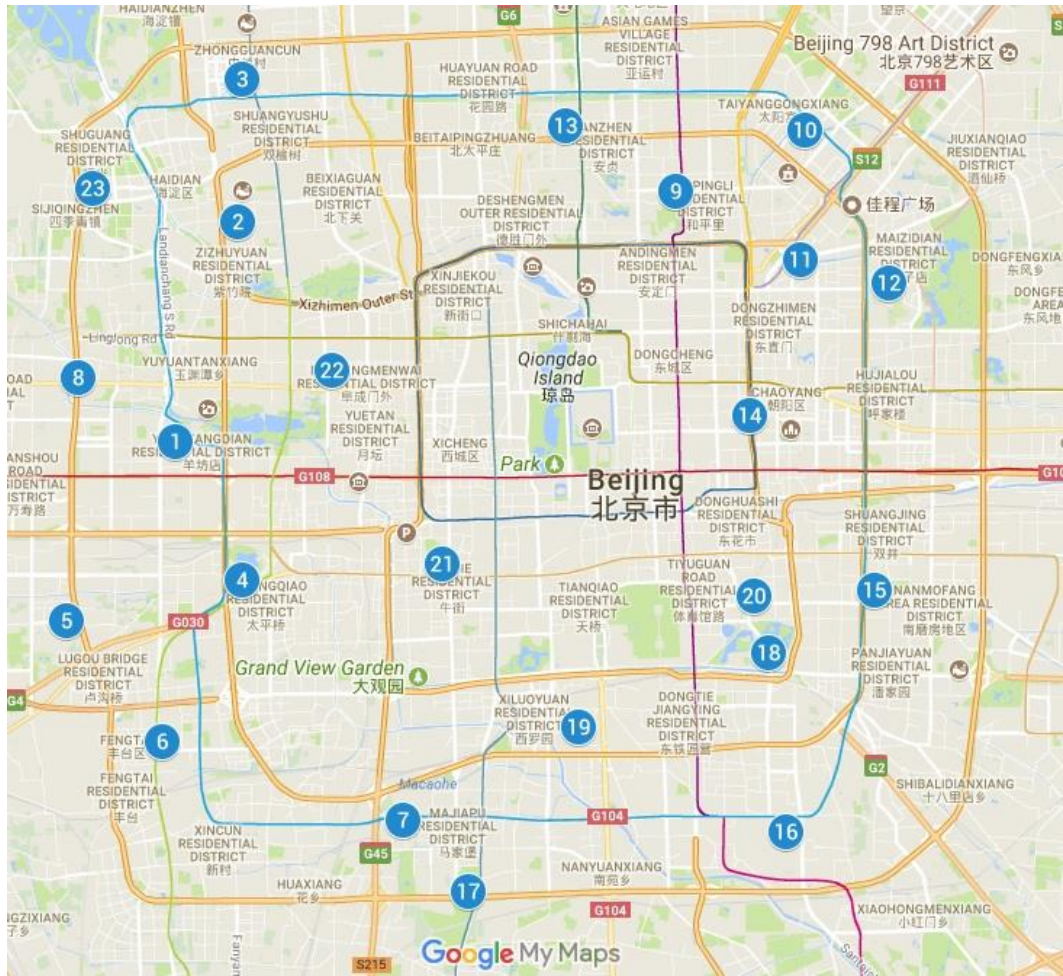
Table 1: Data Collections in 2015 a)summer, b)winter

Site/Profile Number of					
Jun.15 th	Jun.16 th	Jun.17 th	Jun.22 th	Jun.23 th	Jun.24 th
1	2,3	4-8	9-12	13-18	19-23

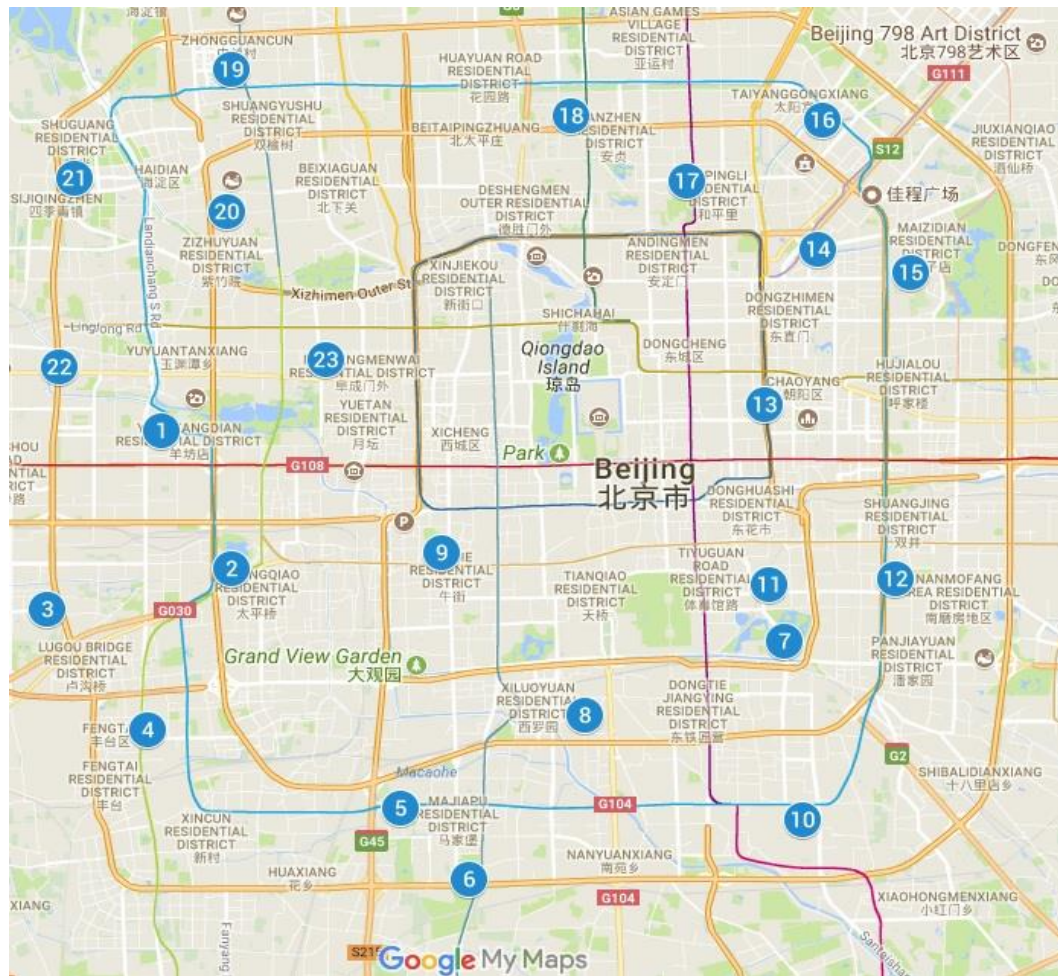
a)

Site/Profile Number of		
Dec. 24 th	Dec. 25 th	Dec.26 th
1-7	8-14	15-23

b)



a)



b)

Figure 6: Positions and the Sequence of Data Collection
in a) summer 2015 and b) winter 2015
(Printed in Google My Maps)

The handheld GrayWolf Laser Particle Counter 3016-IAQ provides up to six particle sizes (PM_{0.3}, PM_{0.5}, PM_{1.0}, PM_{2.5}, PM_{5.0}, PM₁₀) simultaneously in counting and displaying the cumulative and differential particle count and concentration data (GrayWolf Sensing Solutions, 2011). The concentrations of PM that were recorded are the cumulative data. In this study, the concentrations of PM_{0.5} are the concentrations of

particles equal to and less than $0.5\mu\text{m}$ ($\leq \text{PM}_{0.5}$); the concentrations of $\text{PM}_{1.0}$ are the concentrations of particles equal to and less than $1.0\mu\text{m}$ ($\leq \text{PM}_{1.0}$). $\text{PM}_{2.5}$ concentrations mean the concentrations of particles less than (includes $\text{PM}_{0.5}$, $\text{PM}_{1.0}$) and equal to $2.5\mu\text{m}$. The concentrations of $\text{PM}_{5.0}$ also mean the concentrations of particles equal to and less than $5.0\mu\text{m}$ ($\leq \text{PM}_{5.0}$); The concentrations of PM_{10} mean the cumulative concentrations which include the concentrations of particles equal to and less than $10\mu\text{m}$ ($\leq \text{PM}_{10}$). The laser particle counter was operated for the default one- minute sampling period, with a set flow rate of 2.83 L/min ($0.00283 \text{ m}^3/\text{min}$). Three one-minute samplings run were taken simultaneously, and the mean concentrations were reported in microgram per cubic meter ($\mu\text{g}/\text{m}^3$).

Twenty-three field survey sites were selected randomly in the Beijing urban districts within the “Fourth Ring Road”. The conditions of these sites are selected in densely populated residential areas which are not close to the main transportation roads or streets.

Twenty-three vertical profiles were surveyed in the randomly selected locations with a total of 115 air pollution sampling points. Five samples were collected on each vertical profile, and the three one-minute continuous samplings were conducted at each five samples. Twenty-three high-rise residential buildings were used to collect the samples from the ground (1st floor) to the elevation of 44.8 meters (16th floor) to form

twenty-three vertical profiles: each of the vertical profiles from the ground to 44.8 meters elevation has been divided into 5 levels, that means one sampling measurement was conducted every 11.2 meters (four building stories increase) elevation increase.

According to the Harmonized Building Modulus Standard (2014), in China, the standard height of one story of high-rise residential buildings in the country is 2.8 meters.

In order to normalize the twenty-three profiles monitoring data collected at different times in a day with possible varying background conditions, temporal analyses were conducted at two field survey sites (Yiyuanju, Shuixingyuan) that were chosen randomly in the west and east areas in Beijing (Figure 7). The two fields measured air particulate pollution datasets were also recorded by using a GrayWolf Laser Particle Counter. The data of air particulate concentrations were collected 10 hours (without precipitations) from 8:00 am to 6:00 pm in the winter of 2016 (January 15th, Yiyuanju; January 19th, Shuixingyuan). The three one-minute continuous samplings were taken every half-hour through the 10 hours a day and the mean concentrations of each three one-minute sampling were also reported in microgram per cubic meter ($\mu\text{g}/\text{m}^3$). Student's T-Test were utilized to test if the two datasets which collected at the two locations were similar or dissimilar; and Mann-Whitney U-Test were utilized to test the data collected at different time periods in 10 hours were similar or dissimilar. The statistical analyses were

conducted in R 3.4.3 and Mann-Whitney U Test Calculator (Social Science Statistics, 2018). Based on the statistical results, the temporal data were utilized to normalize the data collected at the twenty-three profiles and the two temporal profiles (Yiyuanju Profile and Shuixingyuan Profile) were defined.

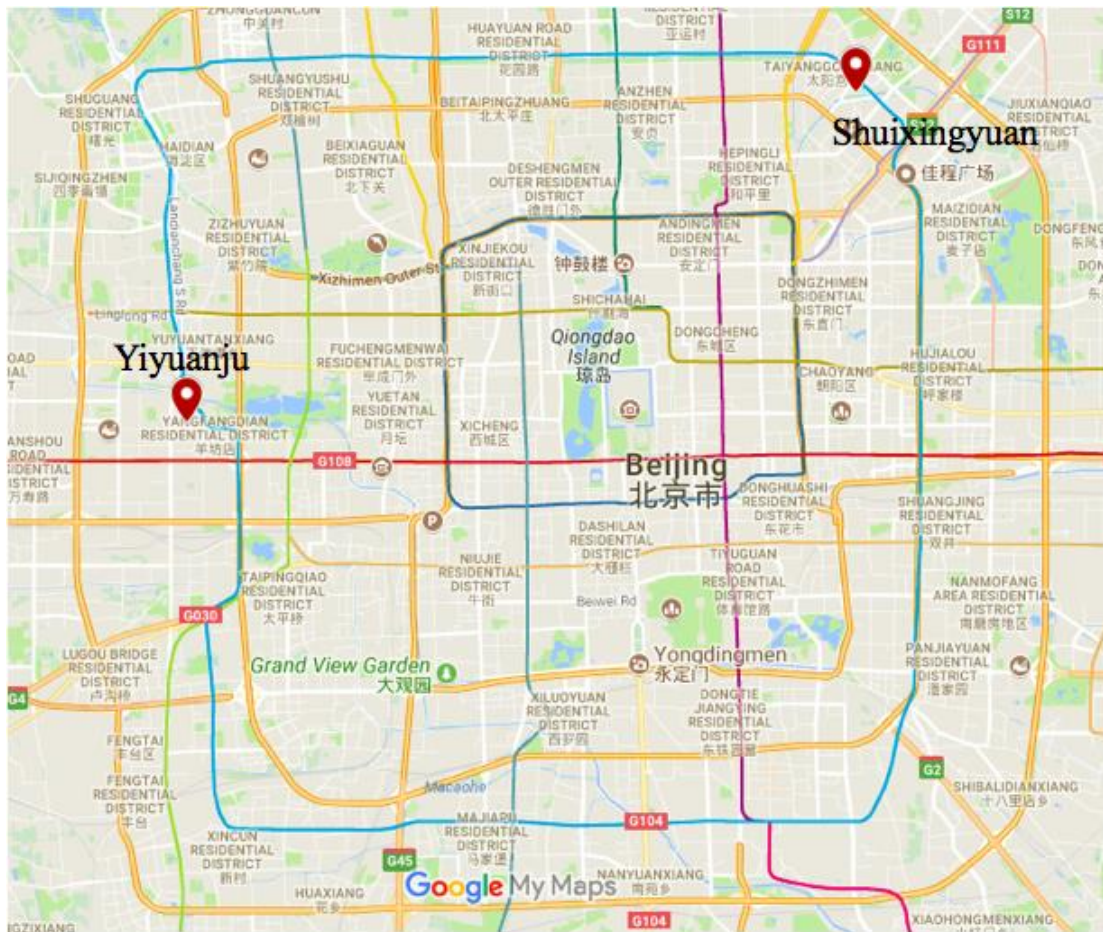


Figure 7: Locations at Yiyuanju and Shuixingyuan (red points; printed in Google My Maps)

3.3 Data-mining of Real Property Values Online

The real property values in the study area of urban Beijing were collected from the three

main and official websites in the real property market in China. They are Fangjia.com, 58.com and Lianjia.com. The real property data from these three websites have been certified by the National Bureau of Statistics, the Notary Office of the central government and other government agencies in China. The three real estate websites provide the housing prices of the different apartments at the twenty-three field survey locations as a reference to research. We collected the housing prices of apartments at each the twenty-three field survey locations and calculated the mean price of these apartments at each the twenty-three field survey locations. The unit price per square meter in US dollars (USD) were utilized, converting from Chinese Yuan (CNY). The price values are concurrent values at the twenty-three field survey locations both in June and December of 2015 (in this research, “June” and “December” stand for the field survey periods: June 15th to June 24th, 2015, and December 24th to December 26th, 2015, including tables and graphs).

3.4 Spatial Analyses in ArcGIS Environment

3.4.1 Kriging Interpolation

Spatial interpolation is the procedure of estimating the values of the variable under study at unsampled locations, using point observations within the same region (Lozano et al., 2009; Mofarrah & Husain, 2010; Nejadkoorki et al., 2011; Deligiorgi and Philippopoulos,

2011). Statistical interpolation methodologies which based on data provided from air quality monitoring sites are applied in air pollution modeling for estimating the spatial distribution of pollutants (Lozano et al., 2009; Mofarrah & Husain, 2010; Nejadkoorki, 2011; Deligiorgi and Philippopoulos, 2011). Inverse-Distance-Weighting (IDW) interpolation, Kriging, Natural Neighbor, Spline, Trend, etc are used commonly as spatial interpolation methods. Kriging is similar with IDW in that it weights the surrounding measured values to derive a prediction for each new location in the output raster dataset (Jensen and Jensen, 2013). In addition, Kriging is the best choice for phenomena with a strong random component or for estimation of statistical characteristics (Mitas and Mitasova, 1999). In this study, the field survey sites/profiles were selected randomly from the urban area in Beijing. Therefore, kriging interpolation was applied to analyze the concentrations of air particulate pollution. The weights come from a semivariogram model that was developed by looking at the spatial structure of the data (Deligiorgi and Philippopoulos, 2011). To create a continuous surface or map of the phenomenon, predictions are made for locations in the study area based on the semivariogram model and the spatial arrangement of measured values that are nearby (Tyagi and Singh, 2013). Goovaerts (1997): “All kriging estimators are but variants of the basic linear regression estimator $Z^*(u)$ defined as

$$Z^*(u)-m(u) = \sum_{\alpha=1}^{n(u)} \lambda_{\alpha} [Z(u)-m(u)].”$$

with

u, u_α : location vectors for estimation point and one of the neighboring data points, indexed by α ;

$n(u)$: number of data points in local neighborhood used for estimation of $Z^*(u)$;

$m(u), m(u_\alpha)$: expected values (means) of $Z(u)$ and $Z(u_\alpha)$;

$\lambda_\alpha(u)$: kriging weight assigned to datum $z(u_\alpha)$ for estimation location u ; same datum will receive different weight for different estimation location;

$Z(u)$ is treated as a random field with a trend component, $m(u)$, and a residual component,

$R(u) = Z(u) - m(u)$. Kriging estimates residual at u as weighted sum of residuals at

surrounding data points. Kriging weights, λ_α , are derived from covariance function or

semivariogram, which should characterize residual component. Distinction between trend

and residual somewhat arbitrary; varies with scale (Goovaerts, 1997).

Three Kriging interpolation methods are widely used: Simple Kriging (SK), Ordinary

Kriging (OK) and Universal Kriging (UK). Simple Kriging (SK) requires the stationary,

constant and known mean value (m_u) of the quantity to be predicted to be known (Bezzi

and Vitti, 2005, Bohling, 2005; Gundogdu and Guney, 2007). Ordinary Kriging (OK)

assumes the mean is constant but an unknown spatial value (Luo et al., 2008, Wang et al.,

2014). Universal Kriging (UK) is used to estimate means when the data have a strong

trend which can be modeled by simple functions (Lefohn et al., 2005, Yamamoto,2005; Gundogdu and Guney, 2007). In this study, raster surfaces of concentrations for each of the five particle sizes were generated by applying universal kriging (UK) model. The reason of using UK model is the predicted value on average is not a constant in the study area. Because of that, SK model and OK model were not chosen in this study. The concentration surfaces were converted to vector map layers with tangible attribute databases of value distributions.

3.4.2 Geographically Weighted Regressions (GWR)

The spatial relationships between the concentrations of air particulate pollution and real property data can also be analyzed and tested by using the newly developed Geographic Weighted Regression (GWR) model. In ArcGIS, a dependent variable and one or more explanatory or independent variables need to be provided when using Geographic Weighted Regression (GWR; Charlton and Fotheringham, 2009). Universal kriging (UK) raster surfaces of air particle concentrations were converted to vector polygons and intersected to the distributions of real property data. In essence, the major difference of GWR with most of other spatial statistical analyses, such as UK is that the GWR model test and predict the spatial relations of two variables. If the GWR predictions are not significant at the most locations in the study area, it approves there is no strong relations

of the two variables. The purpose of using GWR is to spatially quantify the relations between air particulate pollution and the real property data in order to evaluate the impacts of former to the latter.

GWR generates a regression residual feature map. It shows the standard deviation values of modeling errors. The ideal GWR regression model presents randomly distributed over or under predictions across the study area. In this case, GWR were conducted in ArcGIS for the concentrations of all sizes air particulate pollution and real property data. The real property values at twenty-three sites were used as dependent variable and the concentrations of all sizes air particulate as the explanatory or independent variables.

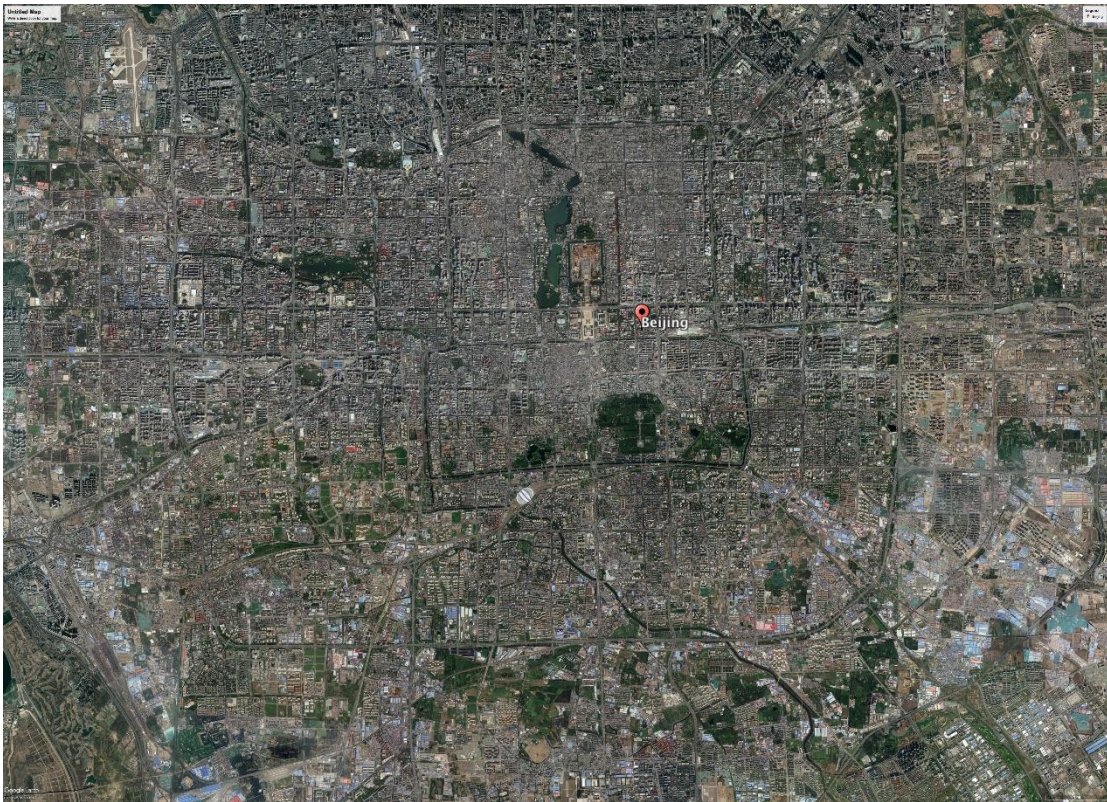
Regression coefficients (β) were computed by the regression models imbedded in the GIS software. These are values, one for each explanatory variable, that represent the strength and type of relationship between the predicted variable and the dependent variable.

Positive coefficient indicates a positive relationship. By contrast, negative coefficient represents a negative relationship. The larger the coefficient, the stronger the relationship is.

3.5 Land Use and Land Cover (LULC) Analyses

Land use and land cover (LULC) are two important geographic categories record

socio-economic activities and land management practices (Comber, 2008). In this research, we discussed the spatial relationships of LULC, the concentrations of air particulate pollution. The supervised classification was conducted in the environment of the remote sensing software, ERDAS IMAGINE 2016, for exploring the LULC of the field survey area in Beijing and producing classification maps of geographic features. The original images were download from Google Earth Pro 7.3.1.4507 (download in March 17, 2018) with the spatial resolution of 4800*3059 grid cells (Figure 8).



a)

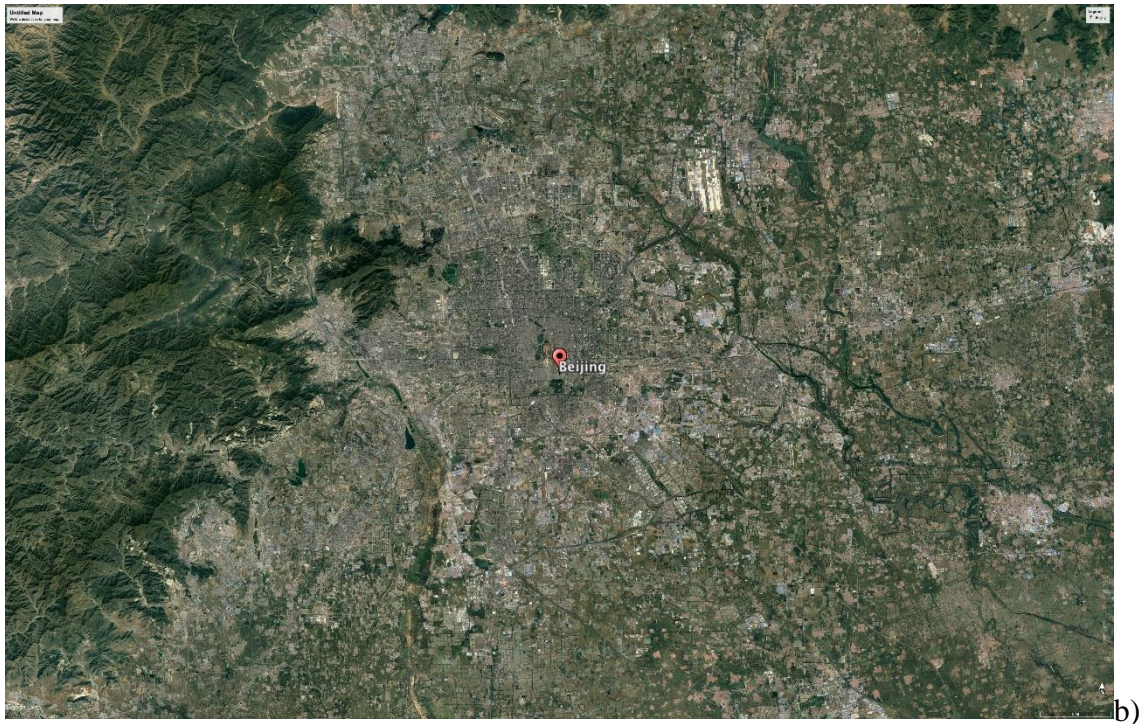


Figure 8: The Original Imagine of Beijing
a) the urban districts of Beijing within the “Fourth Ring Road”;
b) the area of Beijing within the urban and suburban districts
(Printed in Google Earth Pro 7.3.1.4507)

Classification is the most popularly used information extraction techniques in digital remote sensing (Richards, 1986; Lillesand and Kiefer, 2000). There are several methods to classify the geographic features on the images in ERDAS Imagine software environment. Supervised and unsupervised classifications are two commonly used approaches of digital image classification (Rundquist, 2010). Unsupervised classification groups pixels into “clusters” based on their properties using image clustering algorithms such as K-means and the Iterative Self-Organizing Data Analysis Technique (ISODATA; Rundquist, 2010). While in supervised classification, representative samples need to be

selected for each land cover class and then ERDAS software uses these representative samples and applies them to the entire image (GISGeography, 2017). The supervised classification was used to analyze the images and we classified four features of land use (river, street and highway, building and green belt) in this research to explore the spatial relationships of LULC, the concentrations of air particulate pollution. Because the unsupervised classification was used for the unknown areas and it is hard to identify the ground features from the satellite images (Rundquist, 2010), and the supervised classification method was adopted.

The supervised classification makes the signature files of the different geographic features and five areas of each class (geographic feature) were selected as the samples for classification (Figure 9). The green represents the green belts (vegetation); black shows the streets and highways; blue areas are rivers and grey stands for buildings (Figure 10).

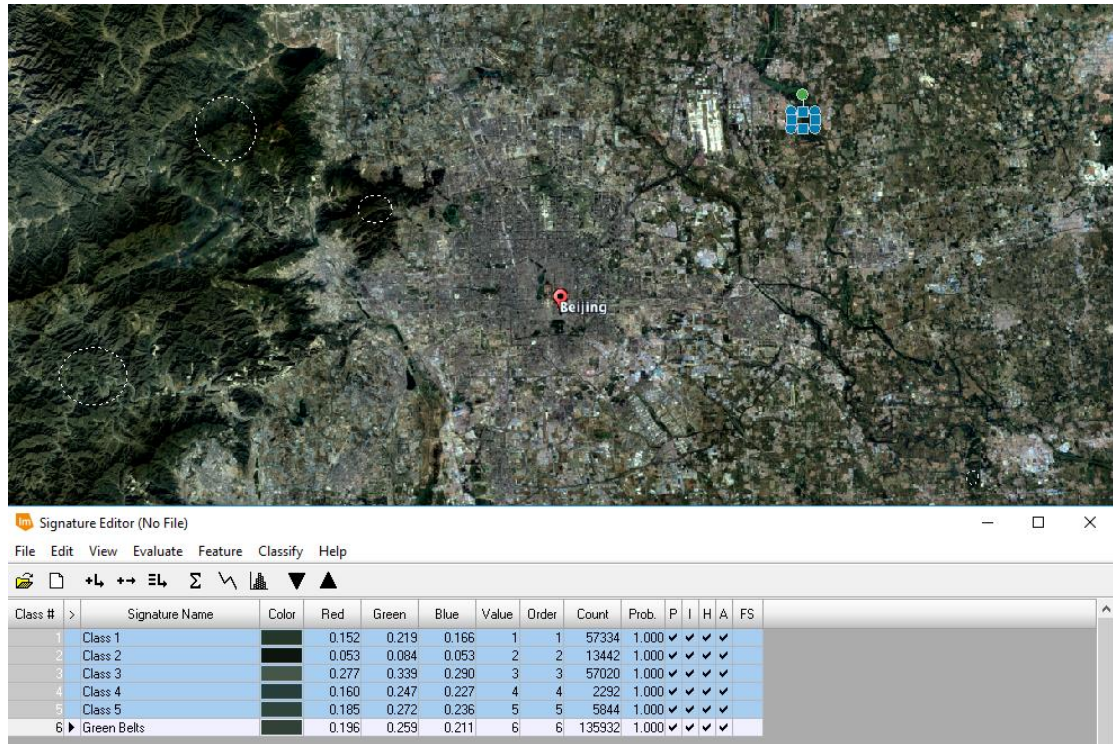


Figure 9: A Sample of Supervised Classification

Row	Histogram	Color	Red	Green	Blue	Opacity	
1	0	Black	0	0	0	0	
2	0	Black	0	0	0	0	
3	0	Black	0	0	0	0	
4	0	Black	0	0	0	0	
5	1345120	Green	0	1	0	1	Green belt
6	2702165	Black	0	0	0	1	Street and highway
7	1128629	Blue	0	0	1	1	River
8	11432086	Grey	0.565	0.522	0.522	1	Building

Figure 10: Attribute Table after Supervised Classification

4. Results

Temporal distributions of air particulate pollution concentrations in the two sites of Beijing (Yiyuanju, Shuixingyuan) were described and analyzed; the results of two-dimensional spatial distributions of air particulate pollution were analyzed and the

differences were compared; spatial patterns in two dimensions of real property values were conducted and the spatial relationships between the air particulate pollution and its distributions of real property values were analyzed. The results from three-dimensional vertical distributions of air particulate pollution were visualized and the differences of each five stories in the twenty-three profiles were compared.

4.1 Results of Temporal Distribution

Table 2 shows the mean of each particulate matter (PM) in 10 hours daytime in the west of Beijing (Yiyuanju) and east of Beijing (Shuixingyuan). The mean of PM_{2.5} and PM₁₀ in 10 hours at the two sites were compared with 24 hours mean in WHO standards, National Ambient Air Quality Standards (NAAQS) and China Air Quality Standards (Table 3).

Table 2: Mean of Air Particulate Pollution ($\mu\text{g}/\text{m}^3$)

	Size of				
	PM _{0.5}	PM _{1.0}	PM _{2.5}	PM _{5.0}	PM ₁₀
Mean value in 10 hours daytime, Yiyuanju (West of Beijing)	23.48	42.26	64.79	124.09	287.72
Mean value in 10 hours daytime, Shuixingyuan (East of Beijing)	23.52	47.17	76.9	127.14	285.17

Table 3: 24-hours mean in Standards ($\mu\text{g}/\text{m}^3$)

Standards	Size of	
	PM _{2.5}	PM ₁₀
WHO	25	50
NAAQS	35	150
China Air Quality Standards (GB3095-2012)	75	150

Based on Table 2 and Table 3, the mean of PM_{2.5} concentrations in 10 hours is 64.79 $\mu\text{g}/\text{m}^3$ at Yiyuanju (west of Beijing) and at Shuixingyuan (east of Beijing) is that 76.90 $\mu\text{g}/\text{m}^3$, both of the two means are two times more than the 24-h mean in WHO standard; the mean of PM₁₀ concentrations in 10 hours is 287.72 $\mu\text{g}/\text{m}^3$ at Yiyuanju and 285.17 $\mu\text{g}/\text{m}^3$ at Shuixingyuan, almost six times more than WHO standard and two times more than NAAQS and China Air Quality Standards. The means of PM_{2.5} and PM₁₀ concentrations were much higher than all the three standards, that is to say, the PM concentrations in 10 hours measured at the two sites in Beijing urban area were very high.

Table 4: Statistical Data of Air Particulate Pollution (Yiyuanju, $\mu\text{g}/\text{m}^3$)

	Size of				
	PM _{0.5}	PM _{1.0}	PM _{2.5}	PM _{5.0}	PM ₁₀
Mean	23.48	42.26	64.79	124.09	287.72
Median	23.68	41.27	69.39	128.55	250.52
Standard deviation	6.77	15.18	23.25	38.98	112.03

It is clearly to see the mean, median and standard deviation of each size PM. The fine particles (PM_{2.5}) taken at Yiyuanju (west of Beijing urban area) had a mean concentration of $64.79\mu\text{g}/\text{m}^3$, a median concentration of $69.39\mu\text{g}/\text{m}^3$ and a standard deviation of $23.25\mu\text{g}/\text{m}^3$ (Table 4). Concentrations of PM taken at two field survey sites from 8:00 am to 6:00 pm, incorporating morning, afternoon and evening traffic flow. PM_{2.5} rose from 8:00 am to 9:00 am and fall before noon. There was a sharp increased from 12:00 pm to 12:30 pm, reaching a peak of $77.72\mu\text{g}/\text{m}^3$ and then decreased sharply from 12:30 pm to 1:30 pm. The PM_{2.5} trend upward after 1:30 pm, reaching the highest value at $116.51\mu\text{g}/\text{m}^3$. The results from the line chart (Figure 11) show the trend of PM_{0.5} and PM_{1.0} concentrations are similar with PM_{2.5}.

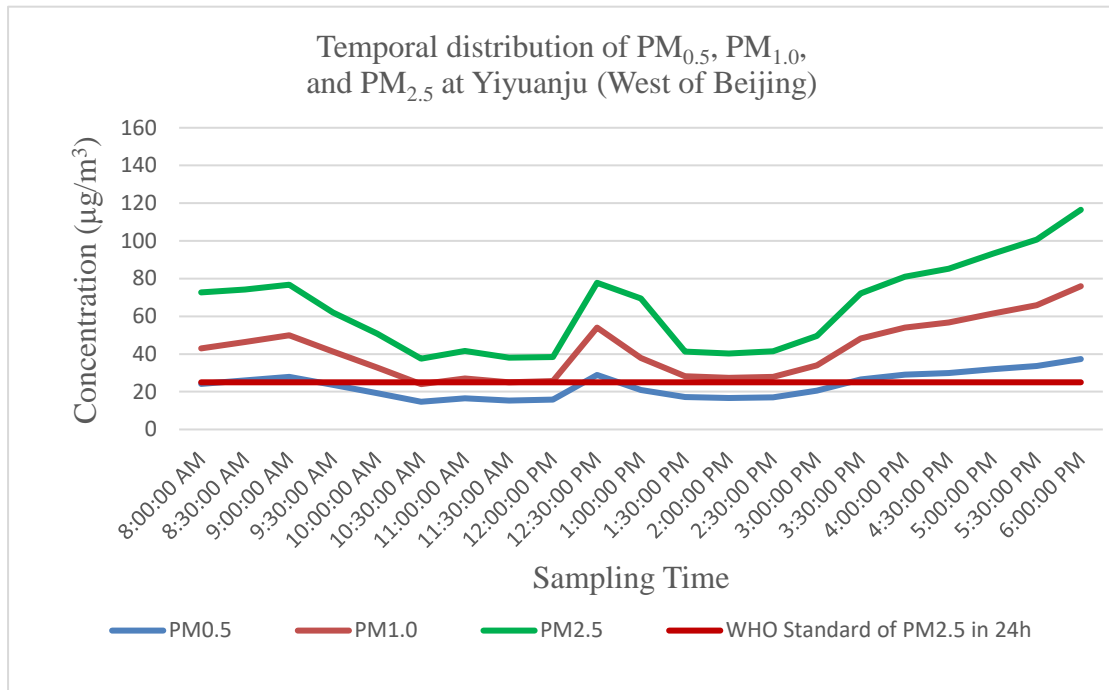


Figure 11: Temporal Distribution of Fine PM Concentrations at Yiyuanju

The PM_{10} taken at Yiyuanju (west of Beijing urban area) had a mean concentration of $287.72\mu\text{g}/\text{m}^3$, a median concentration of $250.52\mu\text{g}/\text{m}^3$ and a standard deviation of $112.03\mu\text{g}/\text{m}^3$ (Table 4). Trend of PM_{10} concentrations from 8:00 am to 6:00 pm at Yiyuanju is shown in Figure 12. There was a dramatic decrease of total PM concentrations from 8:00 am to 10:00 am and then it rose up slightly. The temporal distribution of $PM_{5.0}$ concentrations displays the same as PM_{10} concentrations.

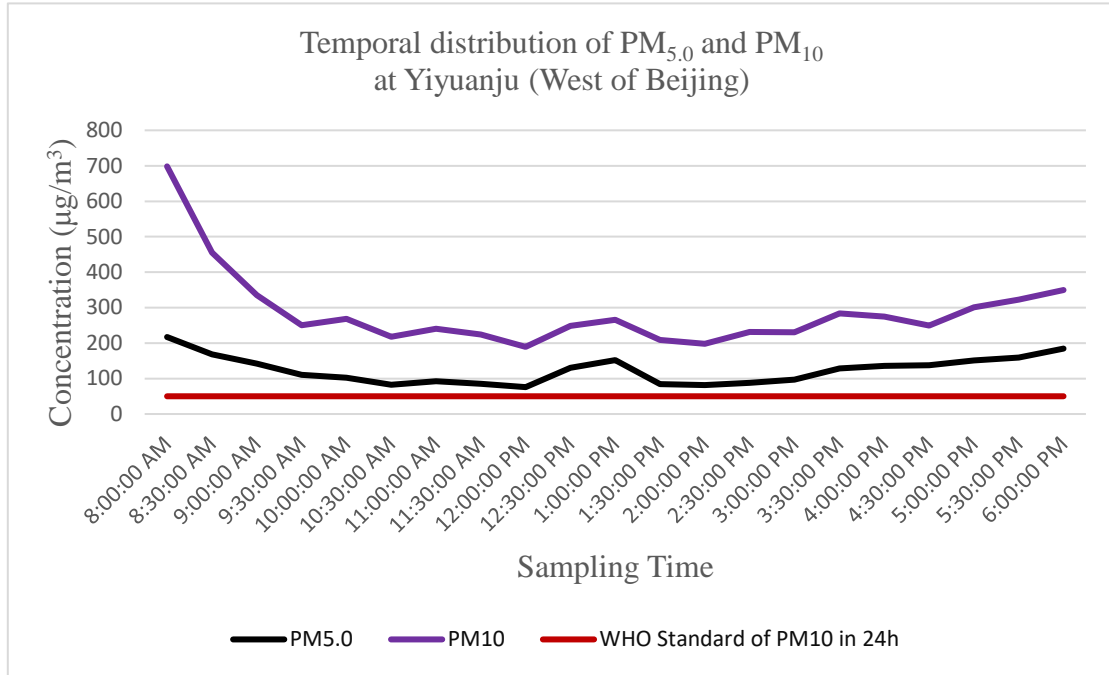


Figure 12: Temporal Distribution of Total PM Concentrations at Yiyuanju

The mean of $PM_{2.5}$ concentrations of Shuixingyuan (east of Beijing urban area) is $76.90\mu\text{g}/\text{m}^3$, with a median of $70.05\mu\text{g}/\text{m}^3$ and a standard deviation of $39.72\mu\text{g}/\text{m}^3$ (Table 5).

Table 5: Statistical Data of Air Particulate Pollution (Shuixingyuan, $\mu\text{g}/\text{m}^3$)

	Size of				
	$PM_{0.5}$	$PM_{1.0}$	$PM_{2.5}$	$PM_{5.0}$	PM_{10}
Mean	23.52	47.17	76.90	127.14	285.17
Medium	23.99	45.61	70.05	118.08	276.30
Standard deviation	9.47	23.66	39.72	50.15	79.91

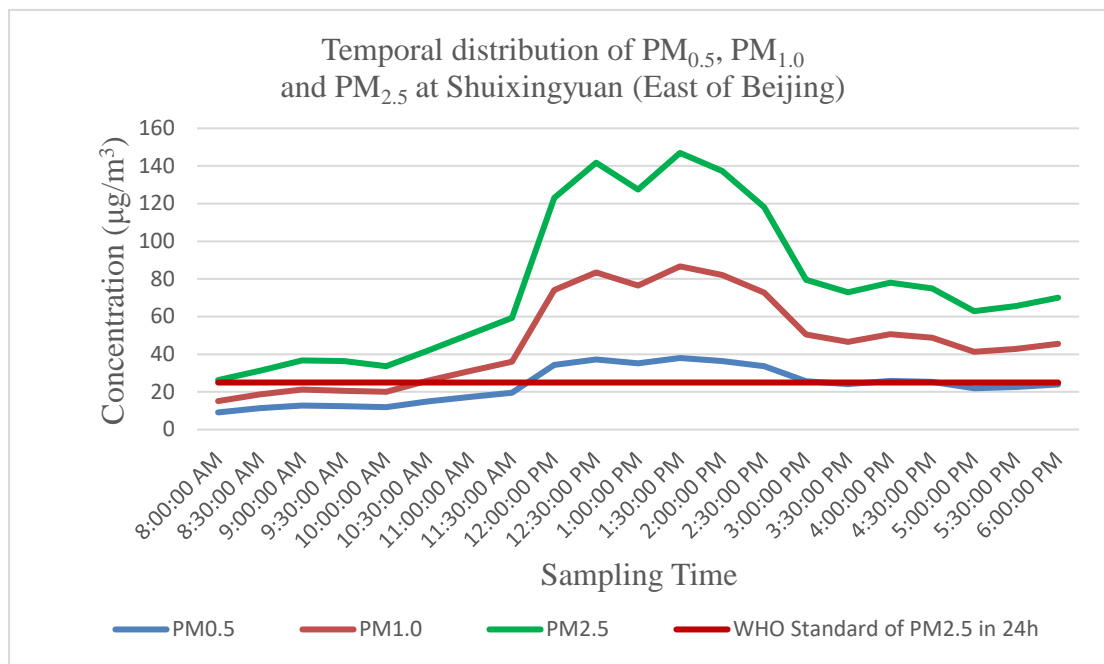


Figure 13: Temporal Distribution of Fine PM Concentrations at Shuixingyuan

Based on Figure 13, PM_{2.5} concentrations at Shuixingyuan rose steadily from 8:00 am to 11:30 am; while from 11:30 am to 12:30 pm, they increased dramatically and reached a peak of 141.79µg/m³ at 12:30 pm; the concentrations of PM_{2.5} fall from 12:30 pm to 1:00 pm before rising until another peak which was reached at 146.95µg/m³. PM_{2.5} concentrations sharply fall again from 1:30 pm to 3:30 pm. They fluctuated for the following two and a half hours until 6:00 pm. Concentrations of PM_{0.5} and PM_{1.0} displayed the similar trend with PM_{2.5}.

Table 5 indicates a mean concentration of PM₁₀ is 285.17µg/m³, with a median

concentration of $276.30\mu\text{g}/\text{m}^3$ and a standard deviation of $79.91\mu\text{g}/\text{m}^3$. As shown in Figure 14, concentrations of PM_{10} kept an upward tendency before 1:00 pm; and gradually went down from 1:00 pm to 6:00 pm. The temporal distribution of $\text{PM}_{5.0}$ concentrations displayed similar trend with concentration of PM_{10} .

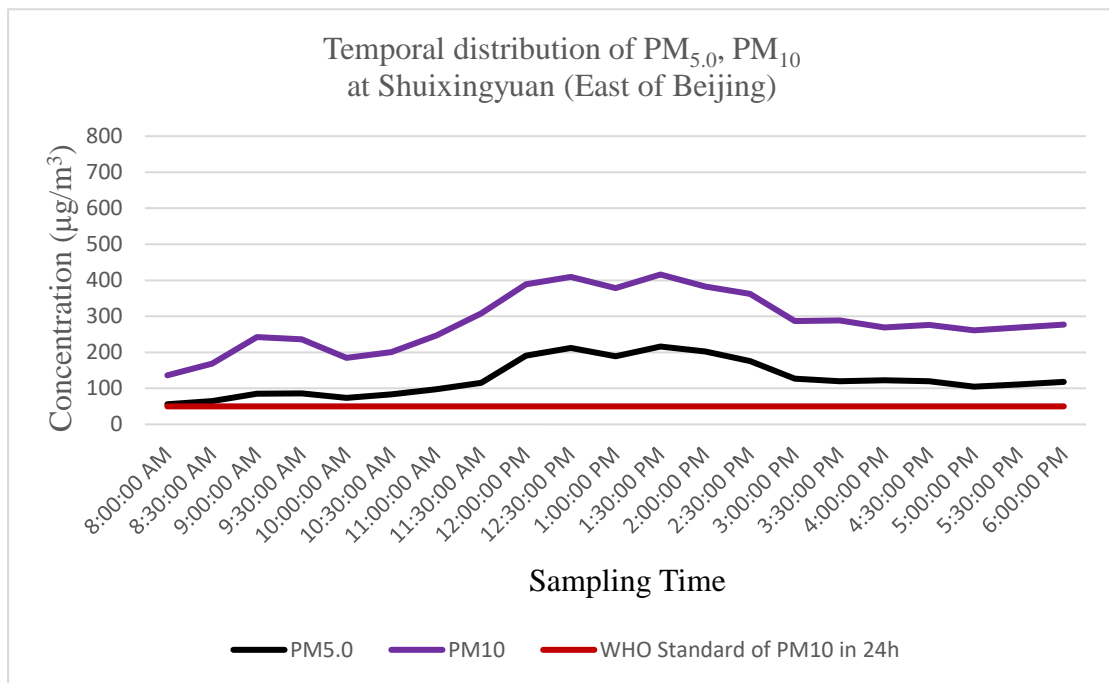


Figure 14: Temporal Distribution of Total PM Concentration at Shuixingyuan

Since the different temporal patterns of PM concentrations appeared at the two field survey sites of Beijing urban area (Yiyuanju, Shuixingyuan). Student's T-Test was utilized in order to test if there is a significant difference of each site's mean of each PM concentration (the codes of Student's T-Test in R were attached in Appendix A).

Student's T-Test is a method of testing hypotheses about the mean of a small sample

drawn from a normally distributed population when the population standard deviation is unknown (Fisher, 1987). The results show that all the p-values are above 0.05, which means the mean of each PM concentration do not have significant difference between the two field survey sites (Yiyuanju, Shuixingyuan).

The Mann-Whitney U-Test was also be used to test if the temporal distributions of PM concentrations are similar in shape. The Mann-Whitney U-Test is a non-parametric test were utilized in place of an unpaired Student T-Test (Shier, 2004). Based on Figure 11, concentrations of PM_{2.5} taken at Yiyuanju from 8:00 am to 12:00 pm gradually goes down, however, they reach a peak in the period between 12:00 pm and 1:30 pm, and then go up. In order to study the temporal distribution of the PM_{2.5} concentrations at Yiyuanju, the Mann-Whitney U-Test was used to test if there is a significant difference of the time periods. The results from Mann-Whitney U Test Calculator indicate that the concentrations of PM_{2.5} from 1:30 pm to 6:00 pm have significant difference to the concentrations of PM_{2.5} from 8:00 am to 1:30 pm (the U -value is 19, the critical value of U at $p < .05$ is 24). From Figure 13, we found that the temporal distribution of PM_{2.5} concentrations at Shuixingyuan also need to be analyzed. The results show that PM_{2.5} concentrations at Shuixingyuan from 11:30 am to 3:00 pm are significant different from other survey periods (the U -value is 6, the critical value of U at $p < .05$ is 24). The same

method was also used to test if there is significant difference of PM₁₀ concentrations at the two survey sites. The results indicated that PM₁₀ concentrations at Yiyuanju from 8:00 am to 10:00 am are significant different from the PM₁₀ concentrations from 10:00 am to 6:00 pm (the U -value is 12, the critical value of U at $p < .05$ is 15); however, at Shuixingyuan, PM₁₀ concentrations from 11:30 am to 3:30 pm have a significant difference of other survey periods (the U -value is 15, the critical value of U at $p < .05$ is 26).

Because the concentrations of PM_{0.5} and PM_{1.0} display the similar trend with PM_{2.5} at Yiyuanju and Shuixingyuan, the differences also be tested by using the Mann-Whitney U-Test. The results indicate that the concentrations of PM_{0.5} and PM_{1.0} from 1:30 pm to 6:00 pm have significant difference to the concentrations of them from 8:00 am to 1:30 pm at Yiyuanju (the U -value is 24, the critical value of U at $p < .05$ is 26, both PM_{0.5} and PM_{1.0}); PM_{0.5} and PM_{1.0} concentrations at Shuixingyuan from 11:30 am to 3:00 pm are significant different from other survey periods (the U -value is 7, the critical value of U at $p < .05$ is 24, both PM_{0.5} and PM_{1.0}). The temporal distribution of PM_{5.0} concentrations at Yiyuanju and Shuixingyuan also have the similar trends with the PM₁₀ concentrations measured at the two sites, that is to say, the differences of temporal distributions of PM_{5.0} concentrations also need to be analyzed. The results show that PM_{5.0} concentrations at

Yiyuanju do not have significant difference in 10 hours. However, PM_{5.0} concentrations at Shuixingyuan from 11:30 am to 3:30 pm are significant different from other survey periods (the *U*-value is 4, the critical value of *U* at $p < .05$ is 26). Table 6 shows the different temporal distributions of each PM concentrations at the two sites.

Table 6: Temporal Distributions of PM Concentrations

Size of	Profile	
	Yiyuanju	Shuixingyuan
PM _{0.5}	8:00am-1:30pm; 1:30pm-6:00pm	11:30am-3:00pm; 8:00am-11:30am, 3:00pm-6:00pm
PM _{1.0}	8:00am-1:30pm; 1:30pm-6:00pm	11:30am-3:00pm; 8:00am-11:30am, 3:00pm-6:00pm
PM _{2.5}	8:00am-1:30pm; 1:30pm-6:00pm	11:30am-3:00pm; 8:00am-11:30am, 3:00pm-6:00pm
PM _{5.0}	No significant difference	11:30am-3:30pm; 8:00am-11:30am, 3:30pm-6:00pm
PM ₁₀	8:00am-10:00am; 10:00am-6:00pm	11:30am-3:30pm; 8:00am-11:30am, 3:30pm-6:00pm

In summary, there is no significant difference of each PM concentration at the two field survey sites measured in 10 hours. However, the PM concentrations are significantly different at the different time periods in 10 hours. The reasons of this situation may be the traffic flow; but there are no enough evidences to prove. Two temporal profiles (Yiyuanju Profile and Shuixingyuan Profile) were conducted in order to normalize entire field

survey data collected at different times in a day of the twenty profiles. Based on the distances between each twenty-three profile and the two sites (Yiyuanju or Shuixingyuan), the temporal profile can be determined to normalize field survey data (Table 7).

Table 7: Temporal Profiles of Three-three Sites

Locations	Distance of Yiyuanju (m)	Distance of Shuixingyuan (m)	Profile
Yiyuanju	0.00	14307.07	Yiyuanju
Weigongcun	4586.63	11571.18	Yiyuanju
Huangzhuangxiaoqu	7451.26	11394.16	Yiyuanju
Taipingqiaoxili	3106.03	14548.47	Yiyuanju
ZiChenyuan	4168.20	17895.91	Yiyuanju
Zhouzhuangzijiayuan	6035.04	18040.75	Yiyuanju
Caoqiao	8996.23	16061.25	Yiyuanju
Dinghuisi	2365.74	15546.26	Yiyuanju
Huafujingyuan	11361.97	2832.45	Shuixingyuan
Shuixingyuan	14307.07	0.00	Shuixingyuan
Xinyuannan Road	13228.81	2591.04	Shuixingyuan
Zaoyingnanli	14902.53	3508.37	Shuixingyuan
Anzhenxili	10203.24	4779.75	Shuixingyuan
Shichang Street	11716.02	5874.11	Shuixingyuan
Hexieyayuan	14516.28	9398.57	Shuixingyuan
Zhonghaicheng	14661.12	14194.41	Shuixingyuan
Fengzhuyuan	10863.07	16914.21	Yiyuanju
Xinanzhongli	12810.38	10509.02	Shuixingyuan
Gexinnanlu	10010.12	12906.94	Yiyuanju
Yinghuazuo	12166.64	9462.94	Shuixingyuan
Laoqianggen	5970.67	11442.44	Yiyuanju
Baiwanzhuang Street	3492.28	10718.23	Yiyuanju
Chuihongyuan	5407.40	14468.00	Yiyuanju

4.2 Result of Spatial Distribution

4.2.1 Two-Dimensional Spatial Distributions of Air Particulate Pollution

Based on the two temporal profiles, the coefficients (α) which were used to normalize the

field survey data were defined as:

$$\alpha = (M/m) * 100\%$$

With

m: mean of each PM concentration at each survey period (Table 6) within 10 hours at the two sites (Yiyuanju, Shuixingyuan);

M: mean of each PM concentration at the two sites (Yiyuanju, Shuixingyuan) in 10 hours.

Table 8 shows the coefficients (α) used to normalize the field data collected at the twenty-three profiles.

Table 8: Coefficients of Each PM Concentration of a)Yiyuanju , b)Shuixingyuan

Time	Size of				
	PM _{0.5}	PM _{1.0}	PM _{2.5}	PM _{5.0}	PM ₁₀
8:00am-1:30pm	112.52%	116.45%	114.27%		
1:30pm-6:00pm	87.06%	84.17%	16.64%		
8:00am-10:00am				100%	71.68%
10:00am-6:00pm				106.39%	114.08%

a)

Time	Size of				
	PM _{0.5}	PM _{1.0}	PM _{2.5}	PM _{5.0}	PM ₁₀
8:00am-11:30am	130.81%	143.09%	146.70%		
3:00pm-6:00pm	130.81%	143.09%	146.70%		
11:30am-3:00pm	72.35%	67.13%	65.90%		
8:00am-11:30am				136.03%	123.62%
3:30pm-6:00pm				136.03%	123.63%
11:30am-3:30pm				73.90%	79.70%

b)

The field survey shows that PM concentrations are very high both in summer and winter 2015. From the tables (9-10), we can see the mean of PM_{2.5} concentrations (238.76 $\mu\text{g}/\text{m}^3$) collected at the twenty-three sites in winter is higher than the mean of PM_{2.5} concentrations (145.66 $\mu\text{g}/\text{m}^3$) collected in summer; the mean of PM₁₀ concentrations (466.96 $\mu\text{g}/\text{m}^3$) in winter is also higher than the mean of PM₁₀ concentrations (299.84 $\mu\text{g}/\text{m}^3$) in summer. In order to test if there is a significant difference of the data collected at the twenty-three sites in the two seasons, Student T-Test is used again (the codes of Student's T-Test in R3.4.3 were attached in Appendix B). The results show that the concentrations of PM_{0.5} and PM_{1.0} do not have significant difference between summer and winter 2015; however, the concentrations of PM_{2.5}, PM_{5.0} PM₁₀ are significant

different between summer and winter 2015.

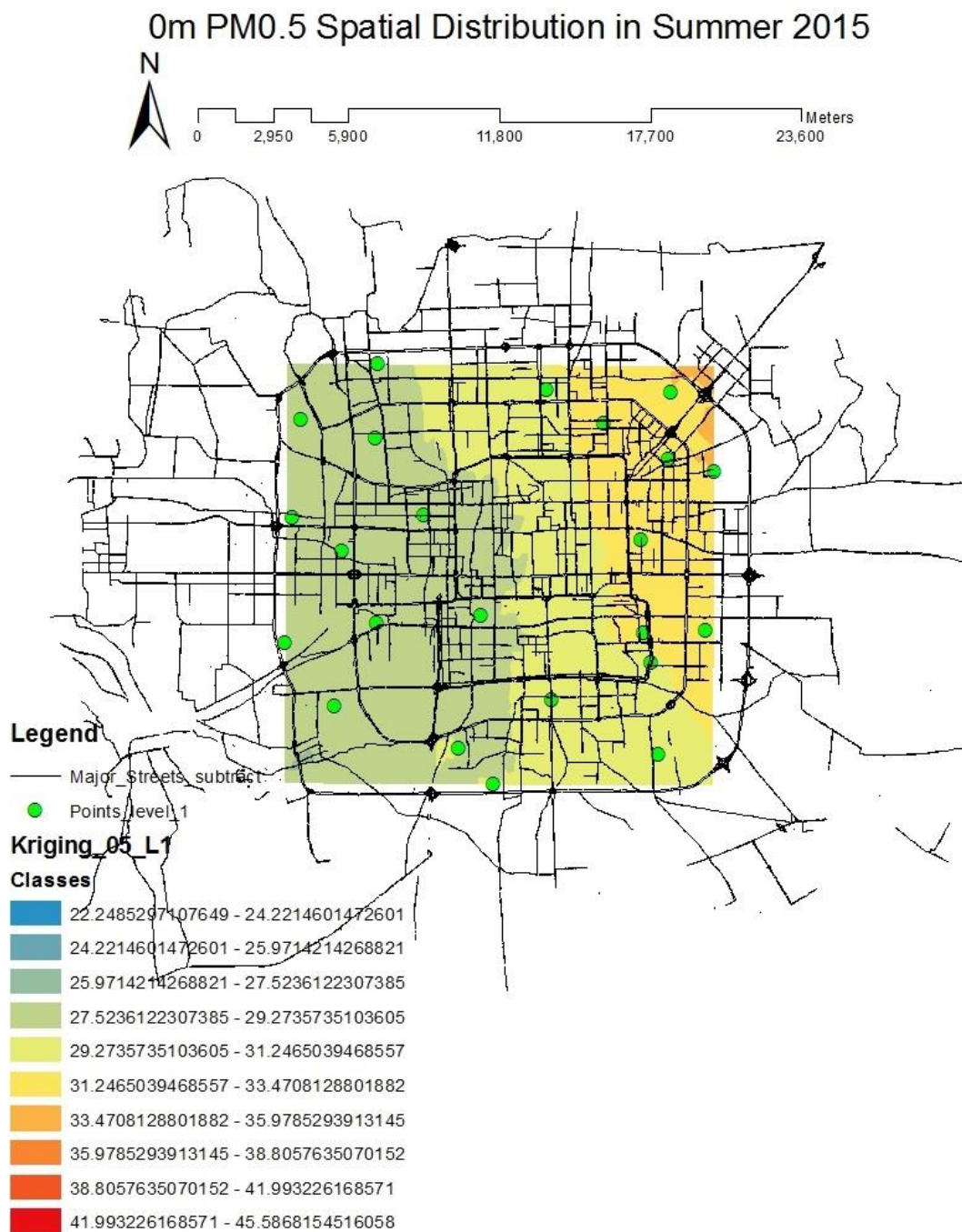
Table 9: Data of Air Particulate Pollution (summer 2015, $\mu\text{g}/\text{m}^3$)

	Size of				
	PM _{0.5}	PM _{1.0}	PM _{2.5}	PM _{5.0}	PM ₁₀
Mean	30.08	76.60	145.66	197.97	299.84
Highest Value	38.02	110.75	268.64	341.49	571.56
Lowest Value	19.17	27.34	41.01	78.05	126.01

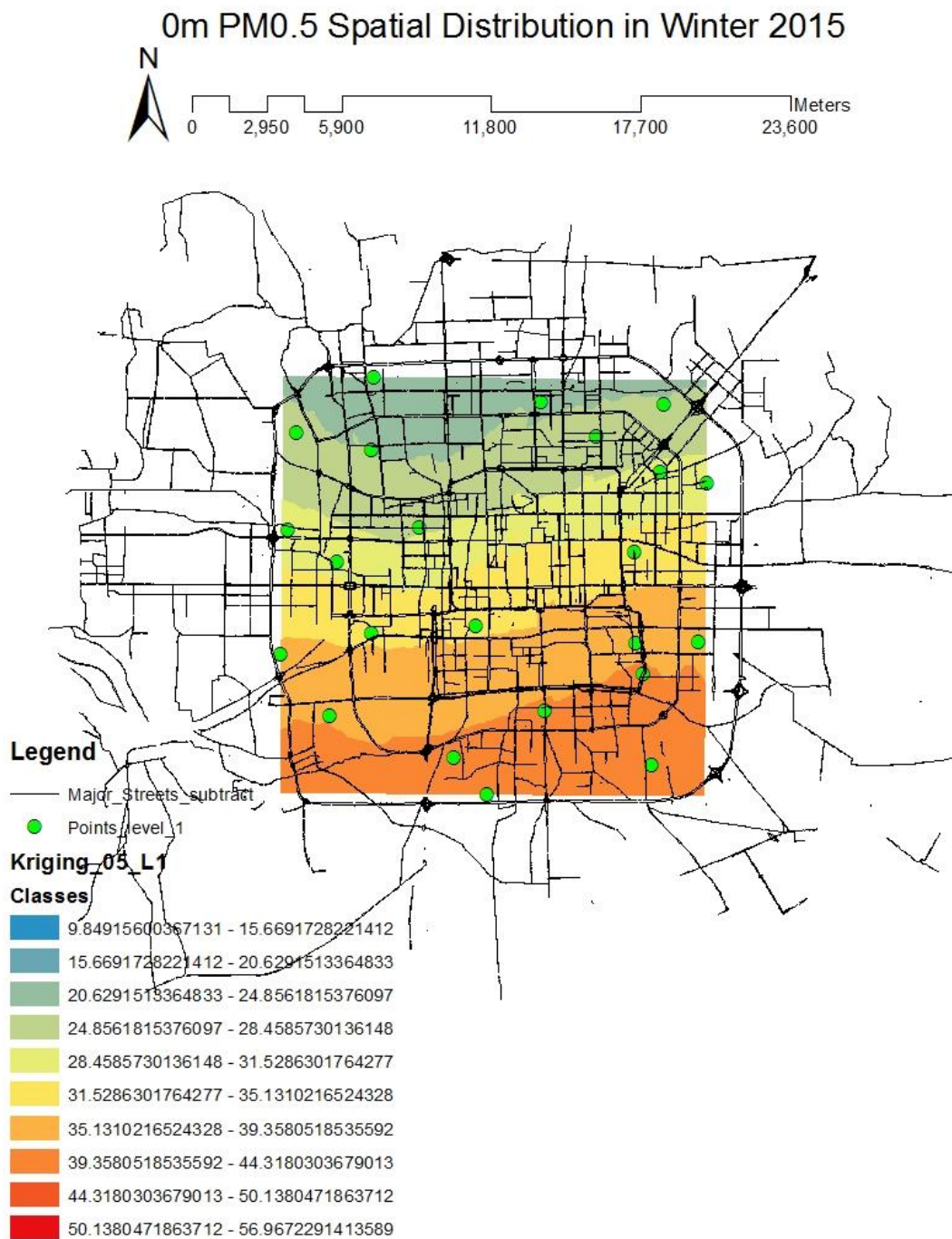
Table 10: Data of Air Particulate Pollution (winter 2015, $\mu\text{g}/\text{m}^3$)

	Size of				
	PM _{0.5}	PM _{1.0}	PM _{2.5}	PM _{5.0}	PM ₁₀
Mean	32.68	113.96	238.76	305.16	466.96
Highest Value	42.81	207.40	430.90	571.84	869.24
Lowest Value	12.88	21.59	32.69	65.78	162.85

In order to study the different spatial distributions of PM concentrations in Beijing urban area in the two seasons, spatial interpolation maps were conducted in ArcGIS environment (Figure 15-19).

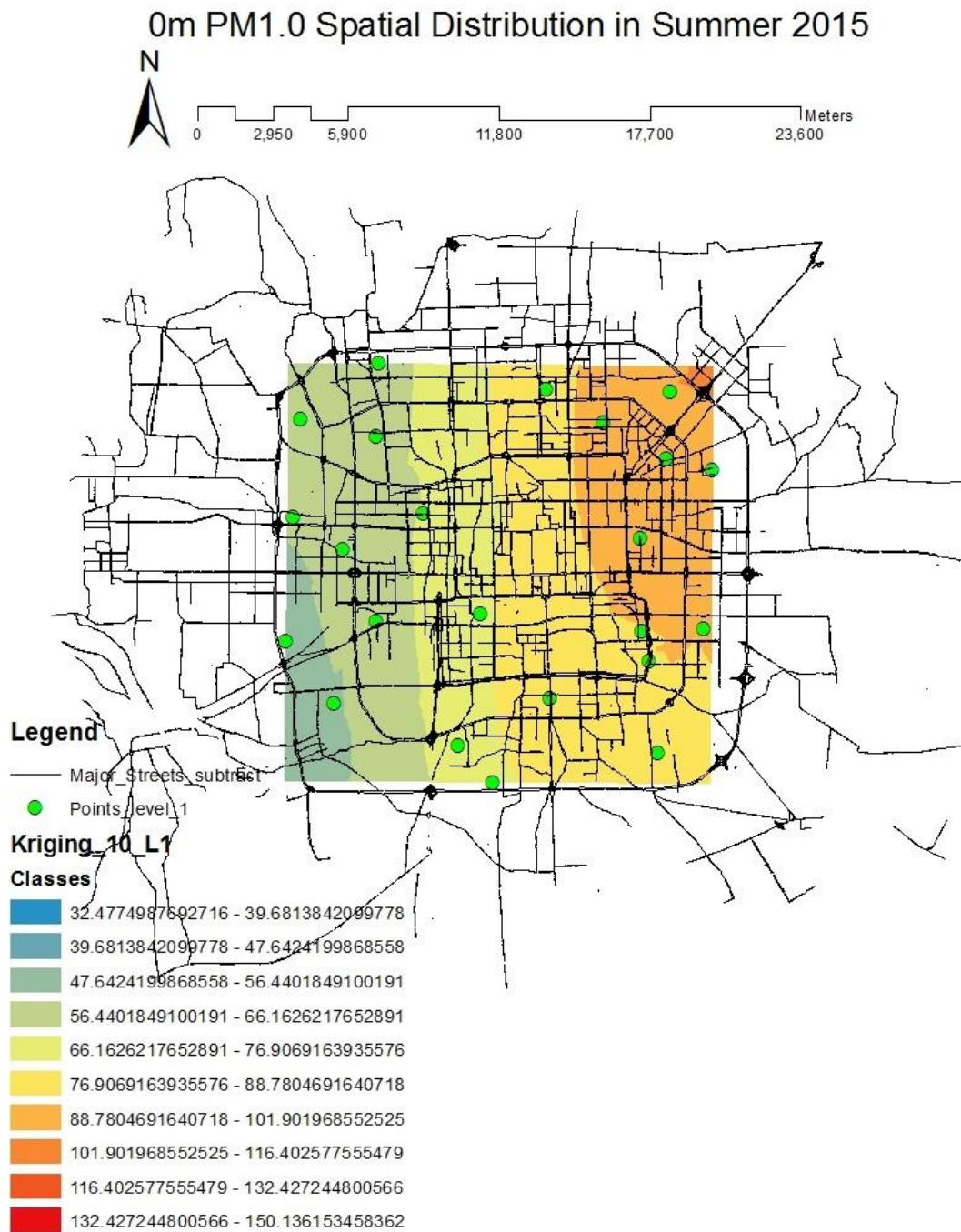


a)

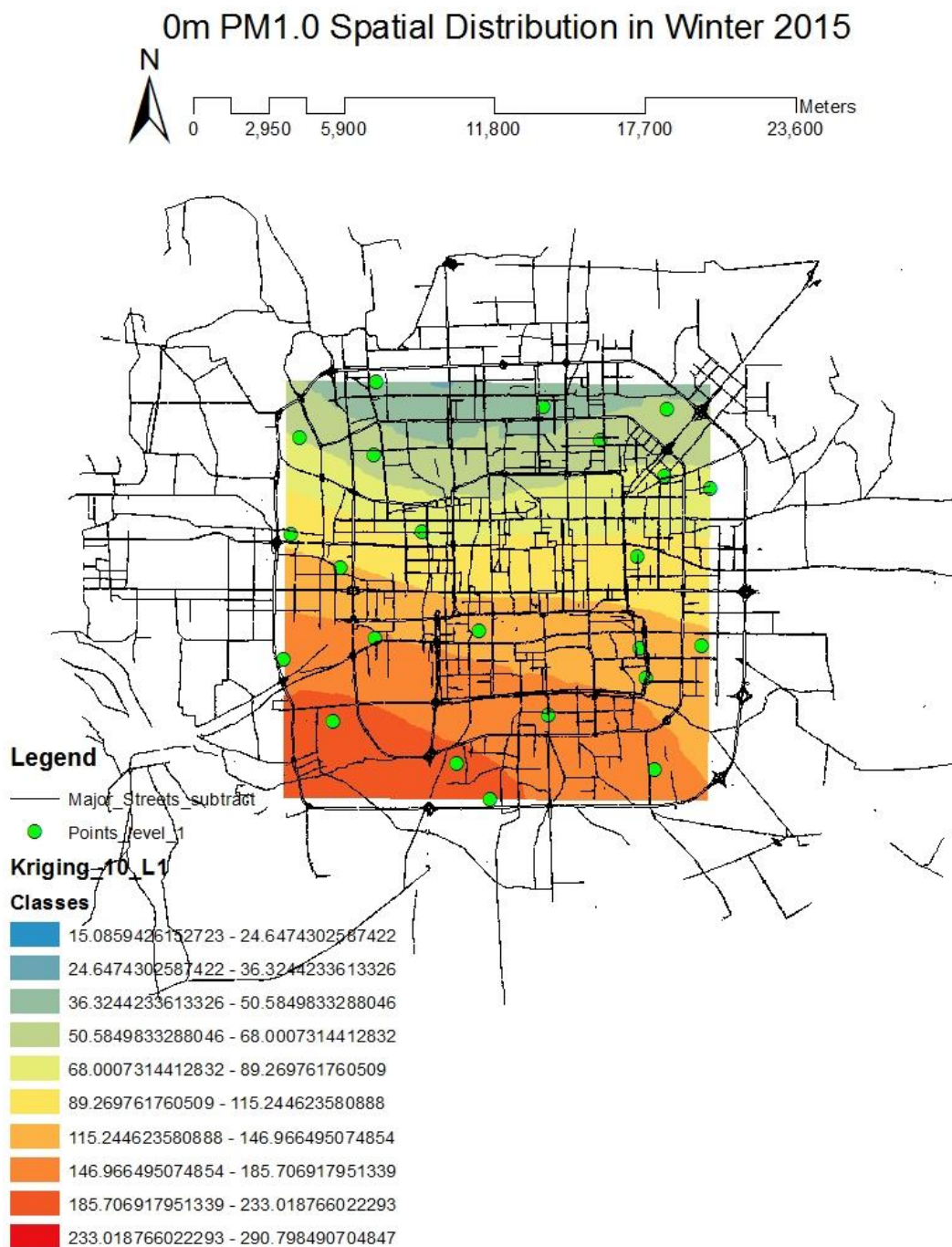


b)

Figure 15: PM_{0.5} Spatial Interpolation Map
a)summer, b)winter

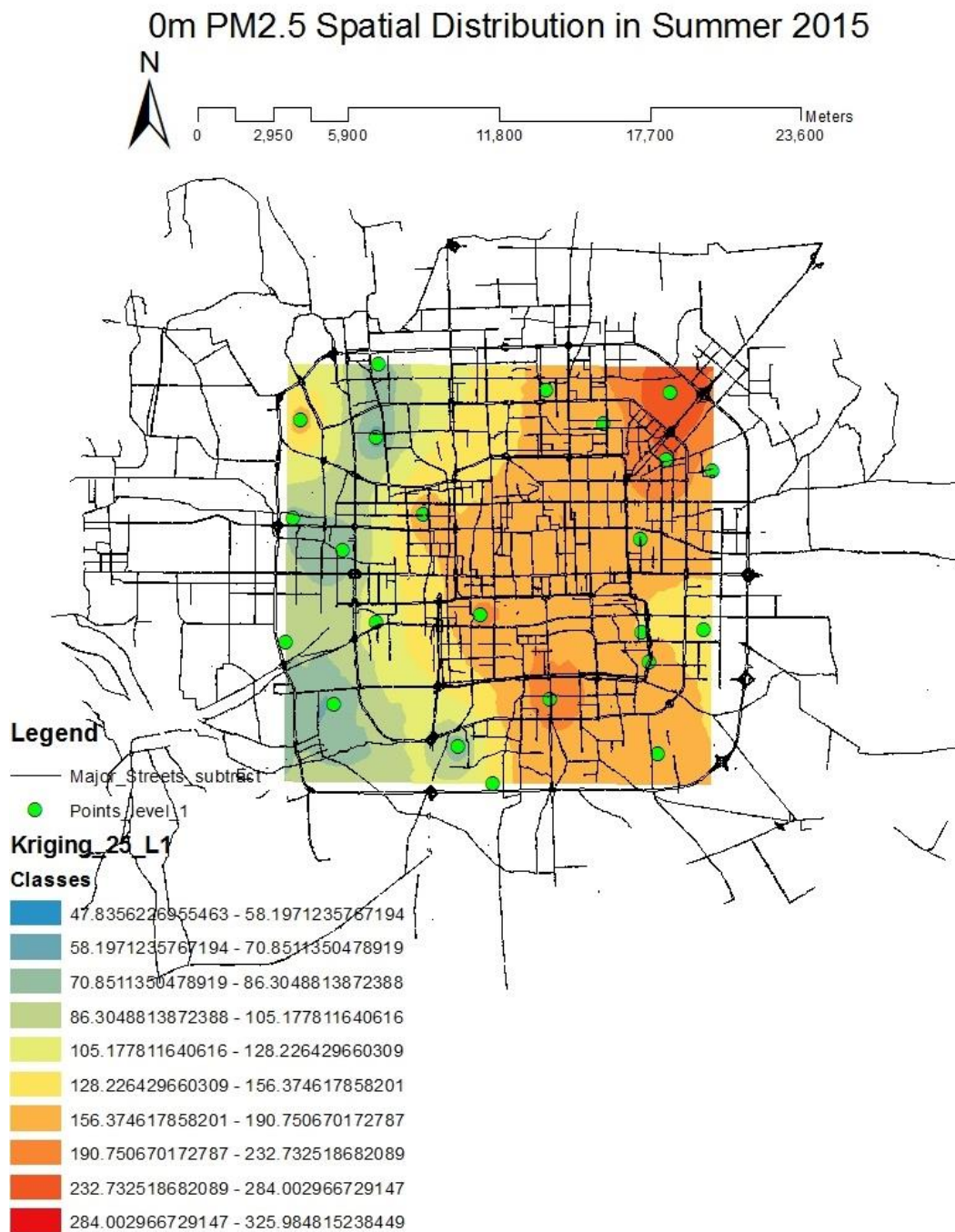


a)

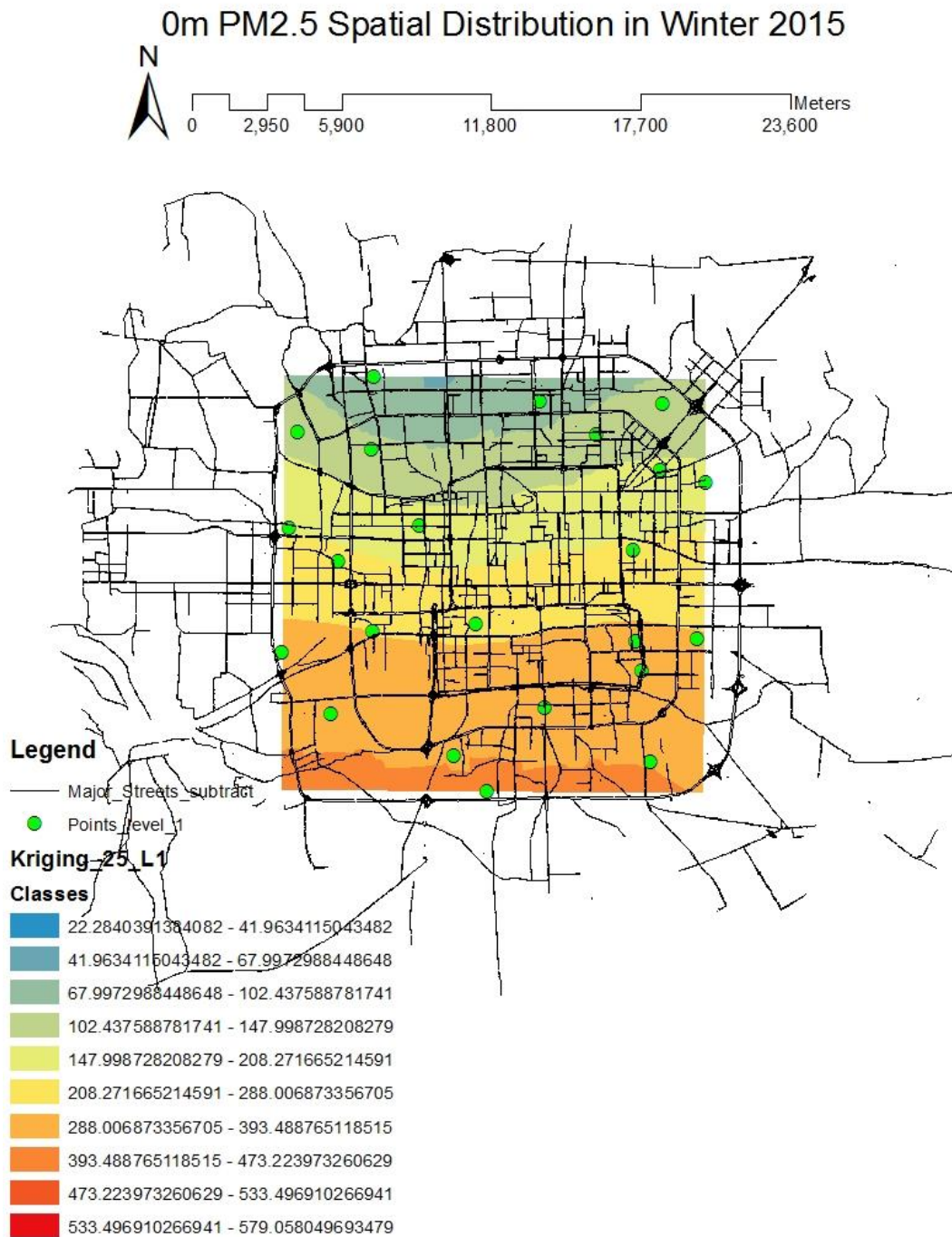


b)

Figure 16: PM_{1.0} Spatial Interpolation Map
a)summer, b)winter

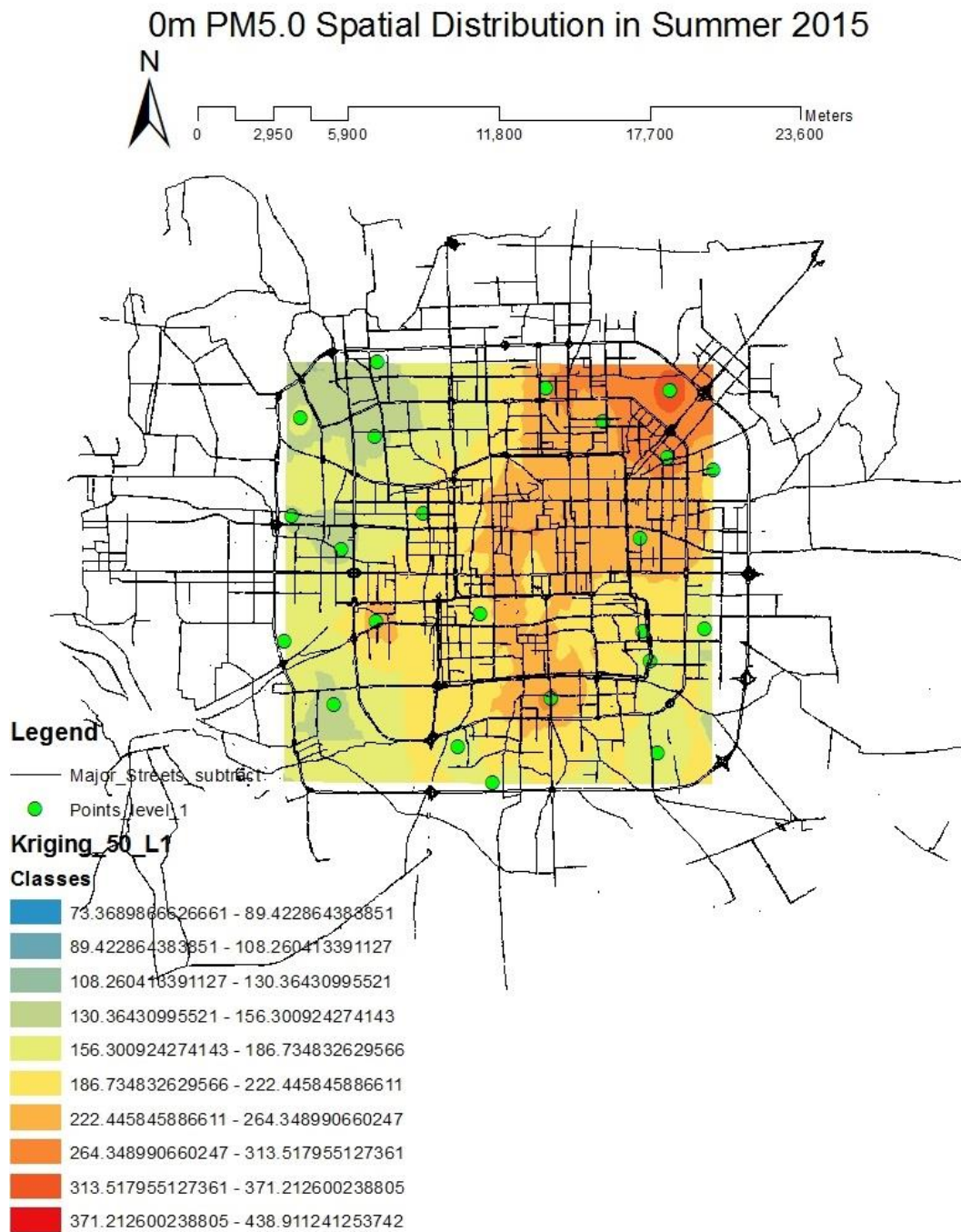


a)

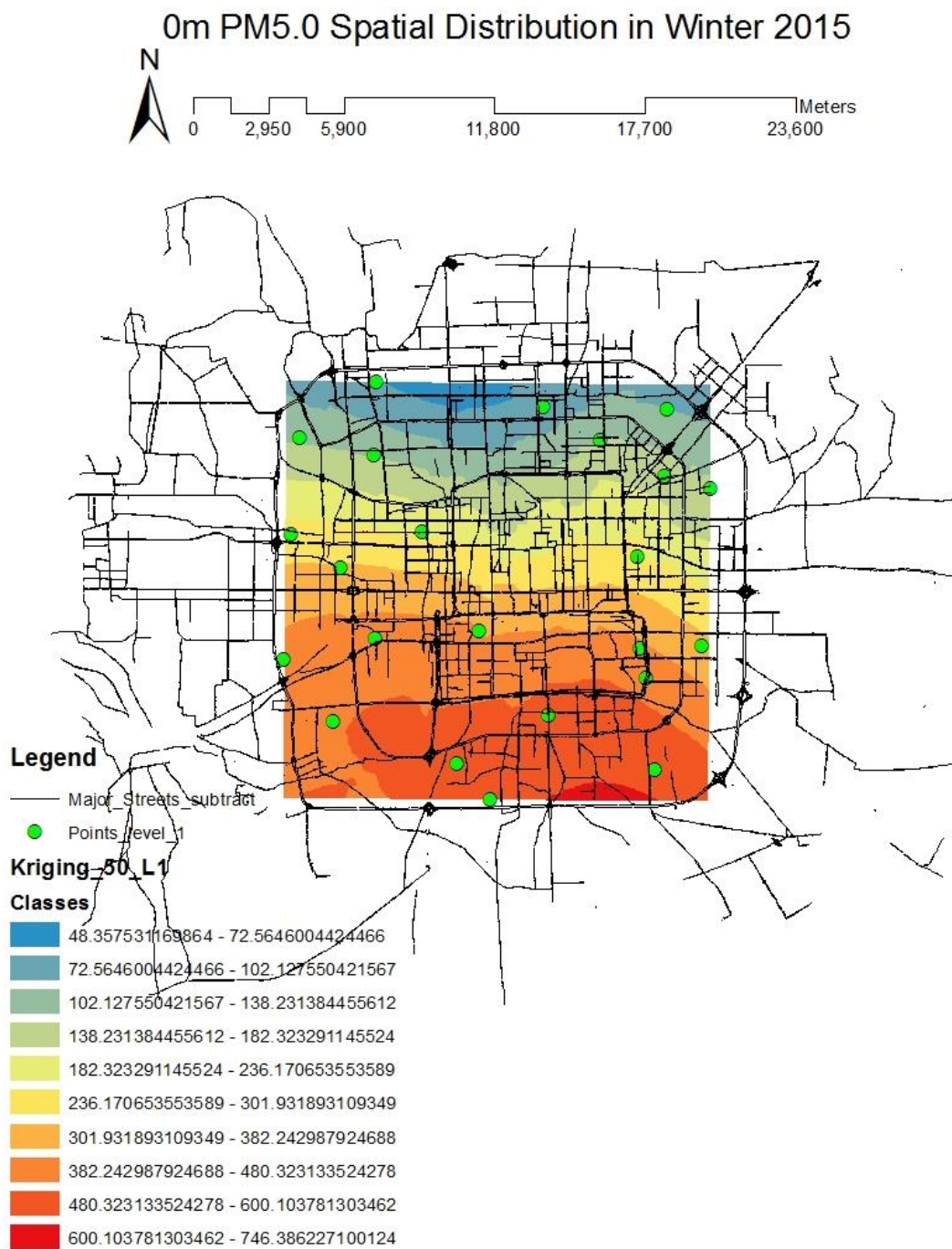


b)

Figure 17: PM_{2.5} Spatial Interpolation Map
a)summer, b)winter

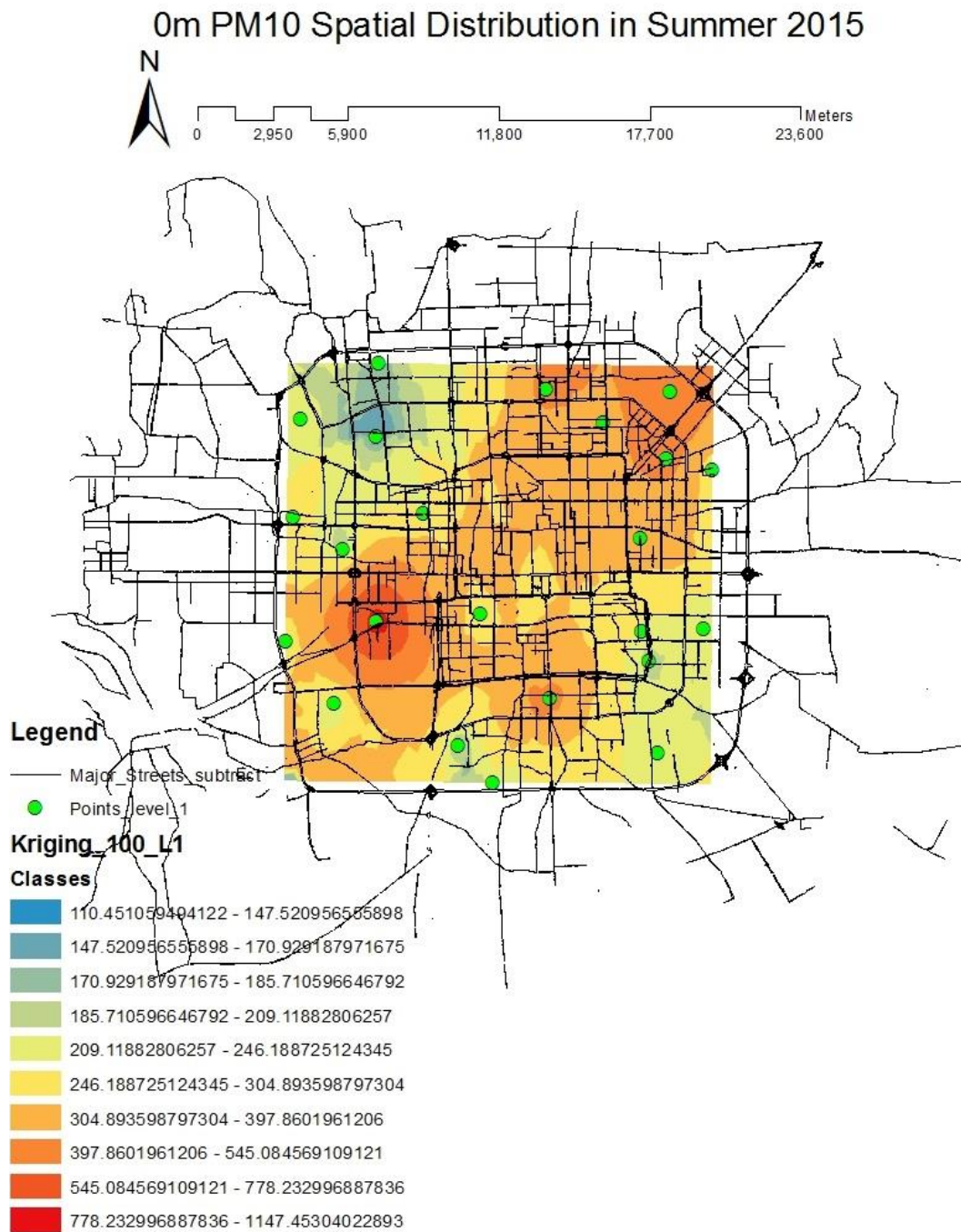


a)

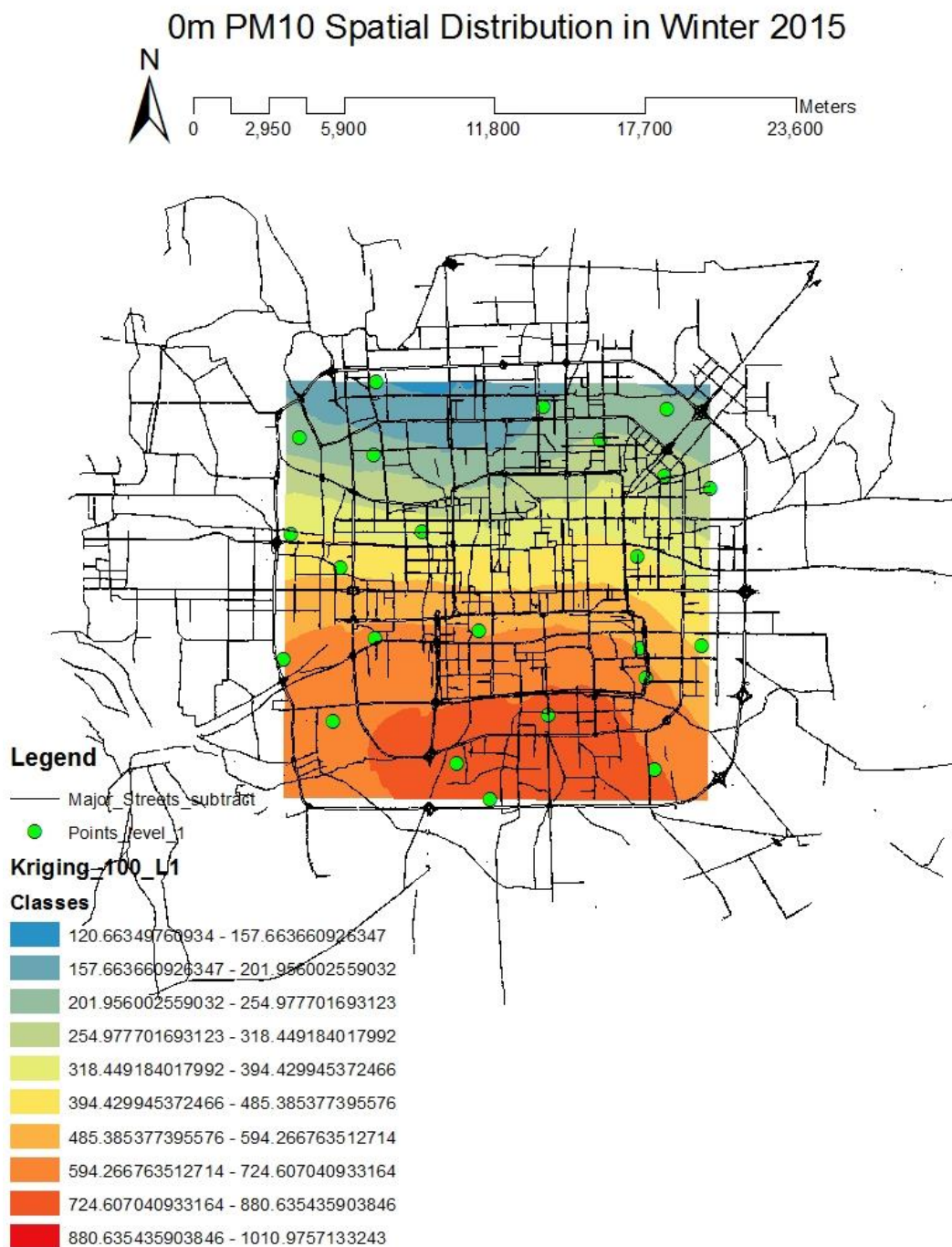


b)

Figure 18: PM_{5.0} Spatial Interpolation Map
a)summer, b)winter



a)



b)

Figure 19: PM₁₀ Spatial Interpolation Map

a)summer, b)winter

Based on the 0m spatial interpolation maps of each size PM (Figure 15-19), the spatial patterns of each size air particle concentrations distributed differently in different seasons. Generally, PM_{0.5}, PM_{1.0}, PM_{2.5} and PM_{5.0} concentrations distributed similar in summer 2015 in Beijing urban area: the concentrations in the east of Beijing was higher than the concentrations in the west of Beijing. PM₁₀ had higher concentrations in the northeastern part and southwestern part of Beijing in summer 2015. In winter 2015, all of the PM concentrations had the same spatial distribution: the concentrations of PM decreased from the south to the east of Beijing, that is to say, they may had the same sources in the southern part of Beijing.

Figure 15 shows that in summer, the PM_{0.5} concentrations in the east of Beijing were slightly higher than that were in the west of Beijing. However, the concentrations of PM_{0.5} in the south of Beijing were higher than that were in the north in winter; the trend of the PM_{0.5} concentrations in winter increased from the north to south. The spatial distribution of PM_{1.0} was similar with the spatial distribution of PM_{0.5} both in summer and winter (Figure 16). Figure 17 indicates that the highest concentration of PM_{2.5} in summer was 268.64 $\mu\text{g}/\text{m}^3$, which was located in the northeastern part of the study area; while the lowest concentration was 41.01 $\mu\text{g}/\text{m}^3$ in the southwest of Beijing. In winter, the spatial distribution of PM_{2.5} concentrations were also similar with PM_{0.5} and PM_{1.0}. The

highest concentration of $PM_{5.0}$ ($341.49\mu\text{g}/\text{m}^3$) in summer appeared in the northeastern part of Beijing and the concentrations decreased from the northeast to the west, southwest and southeast of Beijing (Figure 18). The spatial distribution of $PM_{5.0}$ concentrations in winter was similar with the spatial distributions of $PM_{0.5}$, $PM_{1.0}$ and $PM_{2.5}$. However, the distribution of PM_{10} concentrations was different from the other PM ($PM_{0.5}$, $PM_{1.0}$, $PM_{2.5}$ and $PM_{5.0}$) concentrations. According to Figure 19, the highest concentration of PM_{10} was $571.56\mu\text{g}/\text{m}^3$ which was located in the southwest of Beijing in summer; the northeastern and the southwestern parts of Beijing had high concentrations of PM_{10} in summer, while the northwestern and southeastern parts of Beijing had relative low concentrations of PM_{10} . In winter, the trend of PM_{10} concentrations decreased from south to north with the highest concentration of $869.24\mu\text{g}/\text{m}^3$ and the lowest concentration of $162.85\mu\text{g}/\text{m}^3$.

4.2.2 Three-Dimensional Spatial Distributions of Air Particulate Pollution

The mean values of each size PM concentration at each elevation (0m, 11.2m, 22.4m, 33.6m and 44.8m) of the twenty-three profiles were shown in Figure 20 and Figure 21.

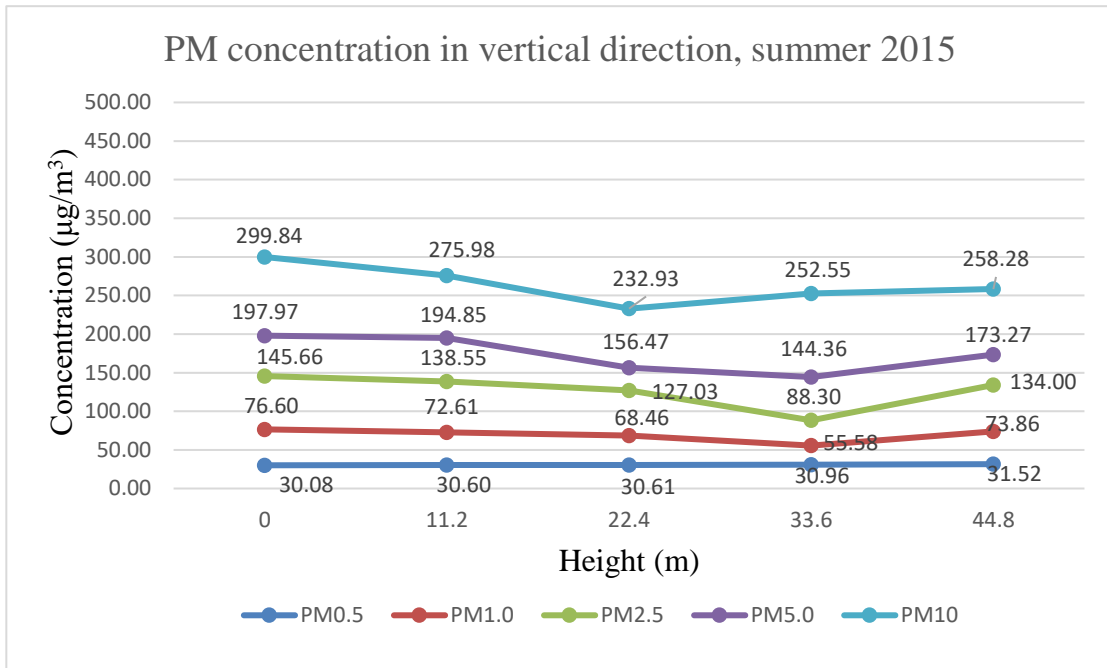


Figure 20: Change of PM Concentration in Summer 2015

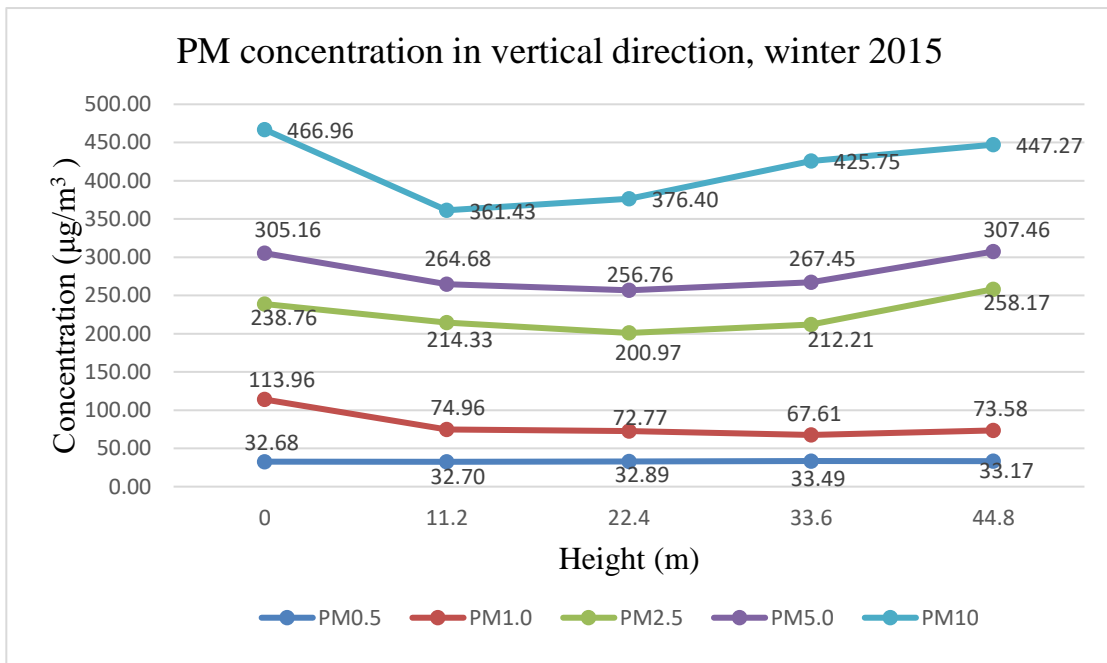
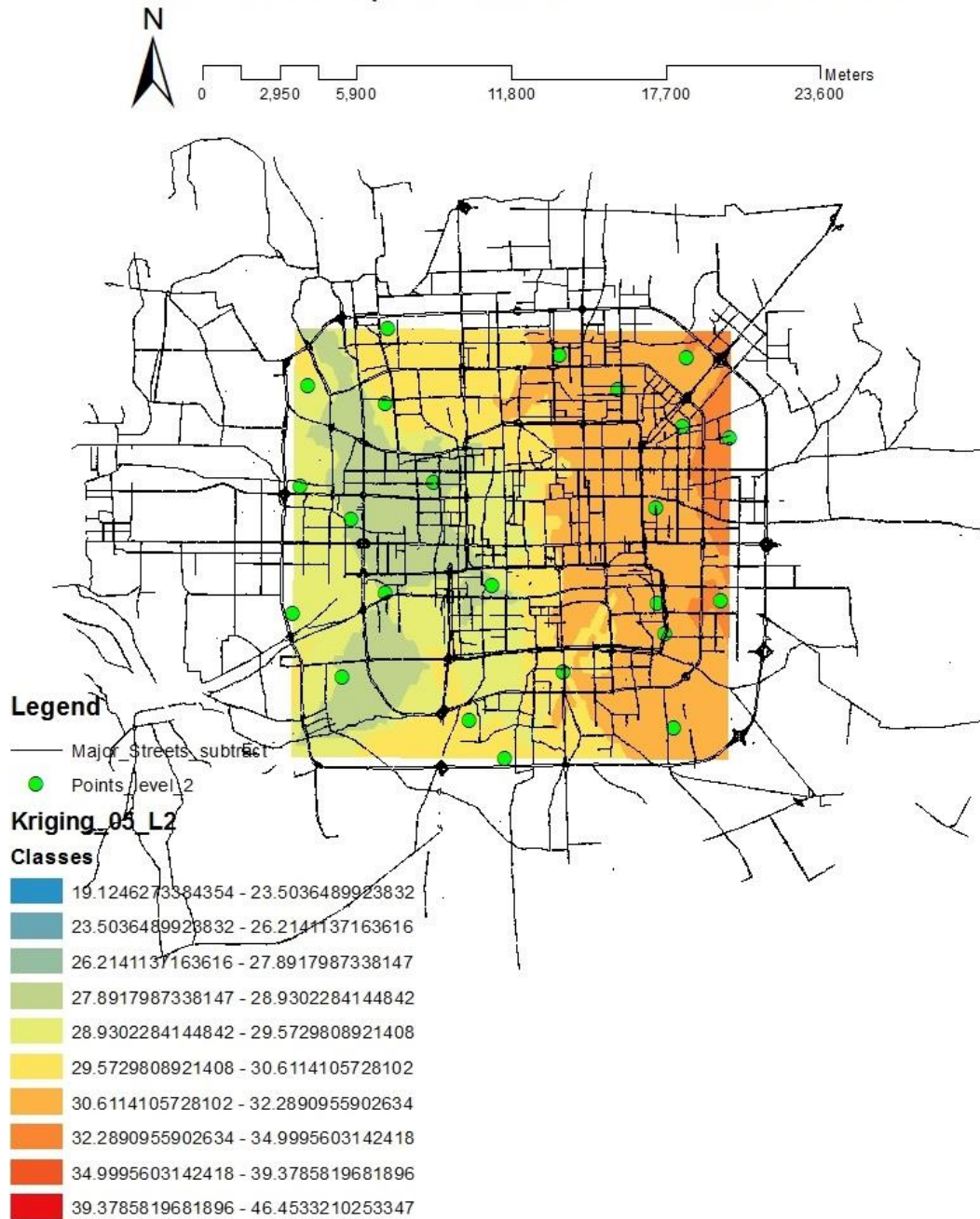


Figure 21: Change of PM Concentration in Winter 2015

As can be seen in Figure 20, in summer 2015, concentrations of $PM_{0.5}$ shew similarity with the increasing elevations; the highest concentration of $PM_{1.0}$ ($76.60\mu\text{g}/\text{m}^3$) appeared on the surface (0m), and the concentrations of $PM_{1.0}$ decreased from surface to 33.6m. However, at 44.8 m, the $PM_{1.0}$ concentration increased again with the value of $73.86\mu\text{g}/\text{m}^3$. The trend of $PM_{2.5}$ and $PM_{5.0}$ concentrations in vertical direction displayed similarity with the trend of $PM_{1.0}$ concentrations in vertical direction; the highest concentration of PM_{10} ($299.84\mu\text{g}/\text{m}^3$) also appeared on the surface, while the lowest concentration ($232.93\mu\text{g}/\text{m}^3$) of PM_{10} appeared at 22.4m, that is to say, the total PM_{10} concentrations decreased from the surface to 22.4m and then increased from 22.4m to 44.8m. In winter 2015, the concentrations of $PM_{0.5}$ also show similarity with the increasing elevations; the vertical distribution of $PM_{1.0}$ concentration in winter 2015 were same as the vertical distribution of $PM_{1.0}$ concentration in summer: the highest concentration of $PM_{1.0}$ ($113.96\mu\text{g}/\text{m}^3$) appeared on the surface (0m), and they decreased from surface to 33.6m. At 44.8 m, the $PM_{1.0}$ concentration increased again with the value of $73.58\mu\text{g}/\text{m}^3$. The trend of $PM_{2.5}$ and $PM_{5.0}$ concentrations in vertical direction displayed similarity: they decreased from the surface to 22.4m and then increased from 22.4m to 44.8m. However, the highest concentration of PM_{10} ($466.96\mu\text{g}/\text{m}^3$) appeared on the surface, while the lowest concentration ($361.43\mu\text{g}/\text{m}^3$) of PM_{10} appeared at 11.2m, PM_{10} concentration increased from 11.2m to 44.8m in winter 2015 (Figure 21).

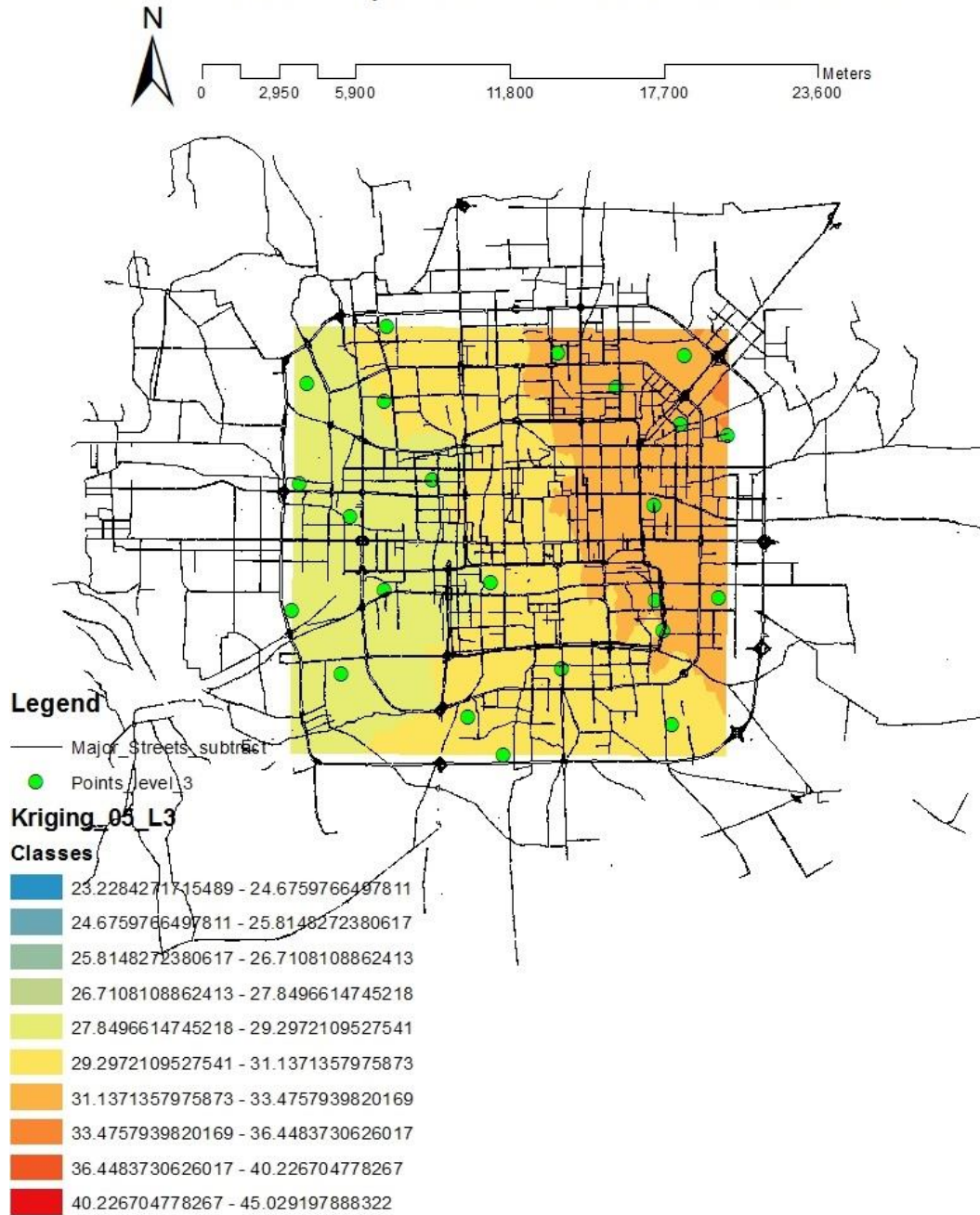
In order to visualize and compare the different spatial patterns of air particulate pollution at different levels of elevations, the PM concentrations spatial distribution maps from surface (0m) to 44.8m (0m, 11.2m, 22.4m, 33.6m and 44.8m) were conducted in ArcGIS environment (Figures 15-19 and Figure 22-31).

11.2m PM0.5 Spatial Distribution in Summer 2015



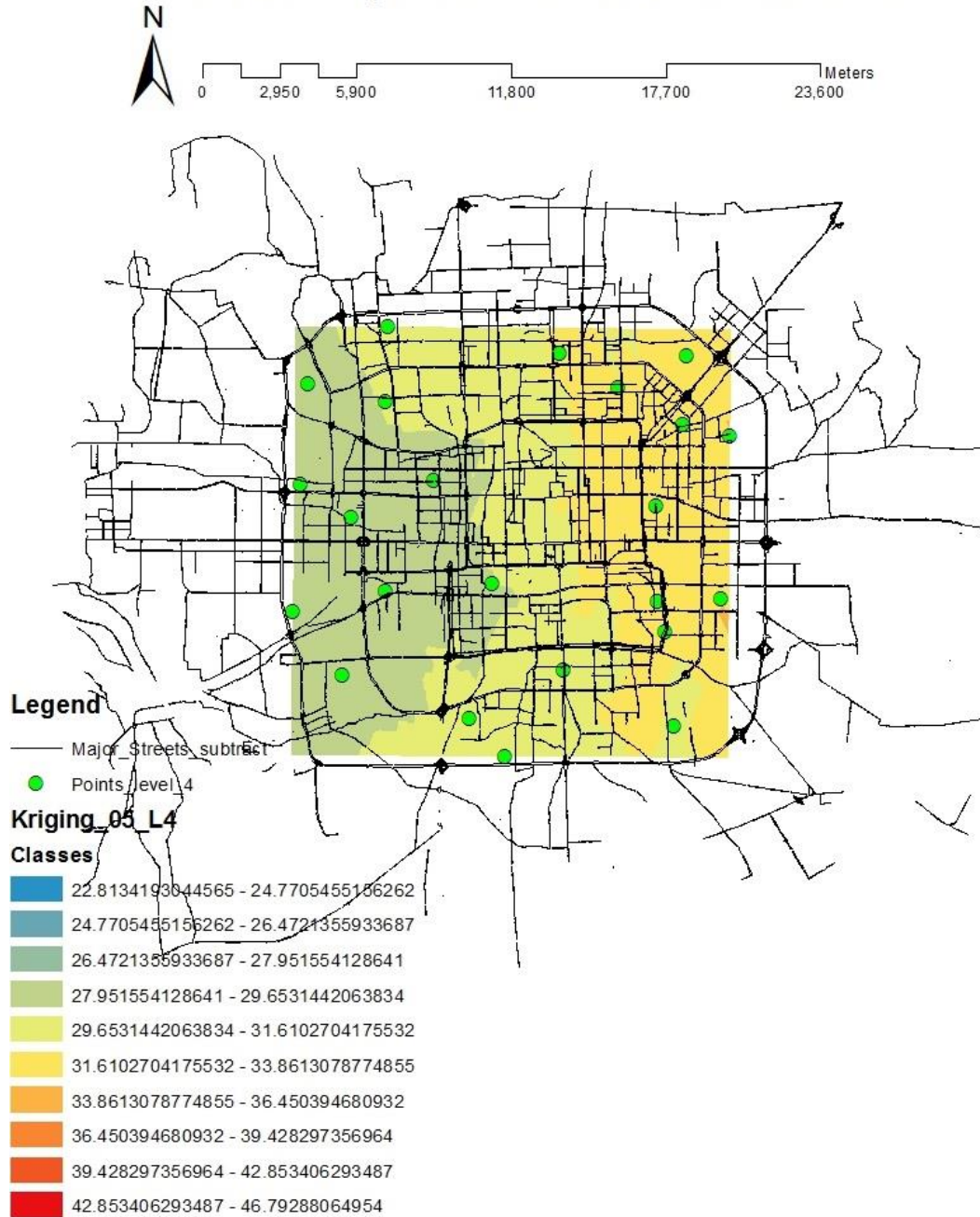
a)

22.4m PM0.5 Spatial Distribution in Summer 2015



b)

33.6m PM0.5 Spatial Distribution in Summer 2015



c)

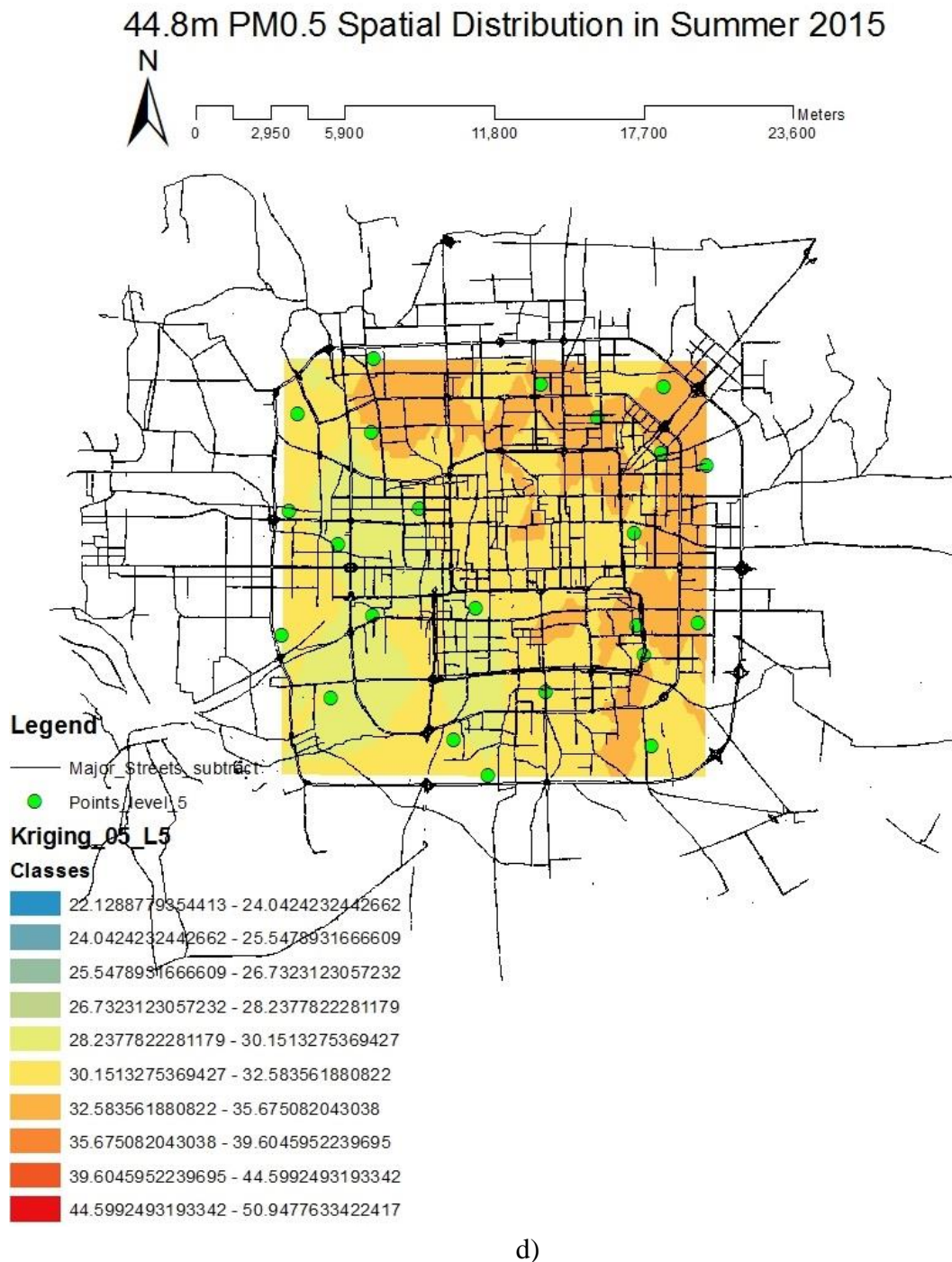
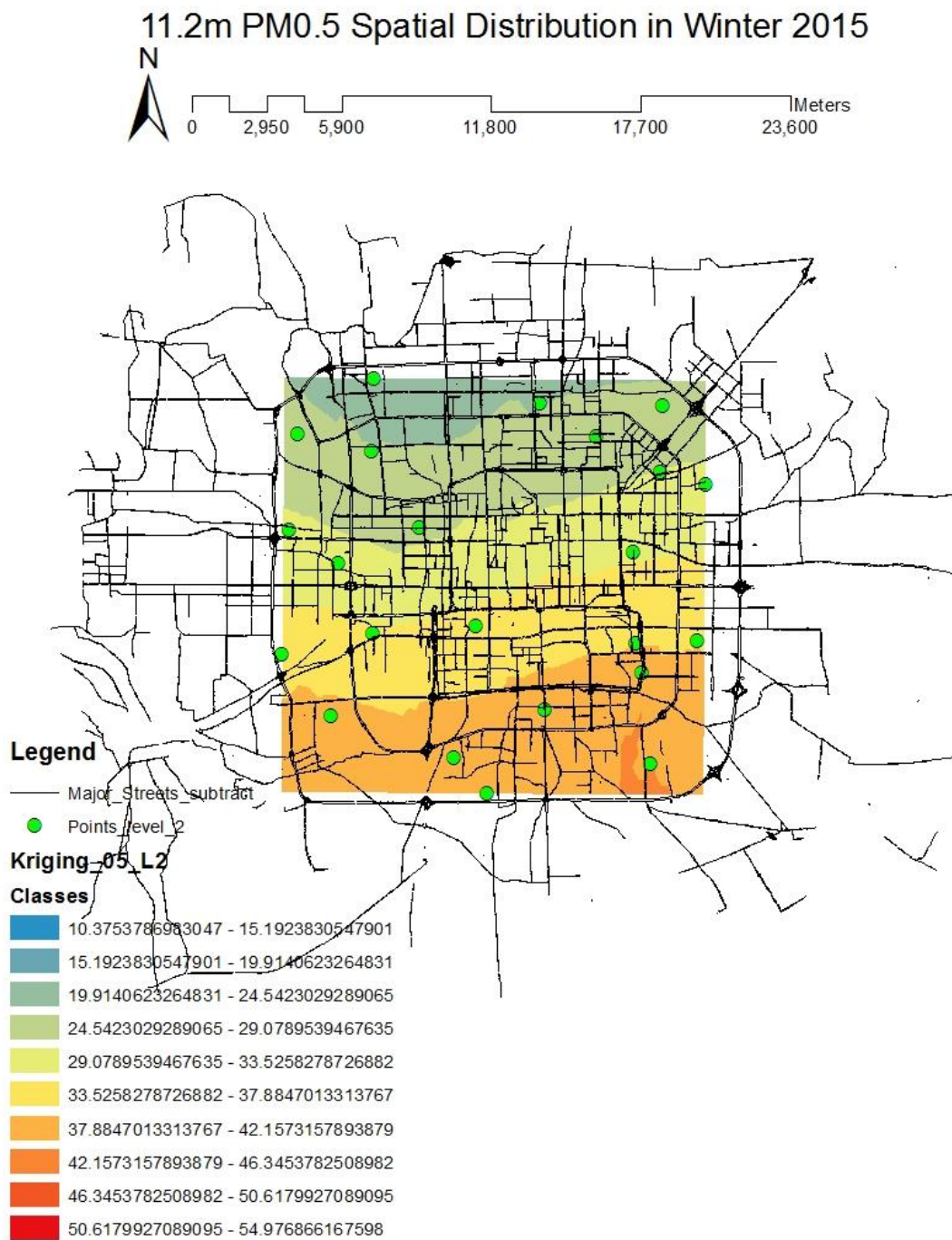
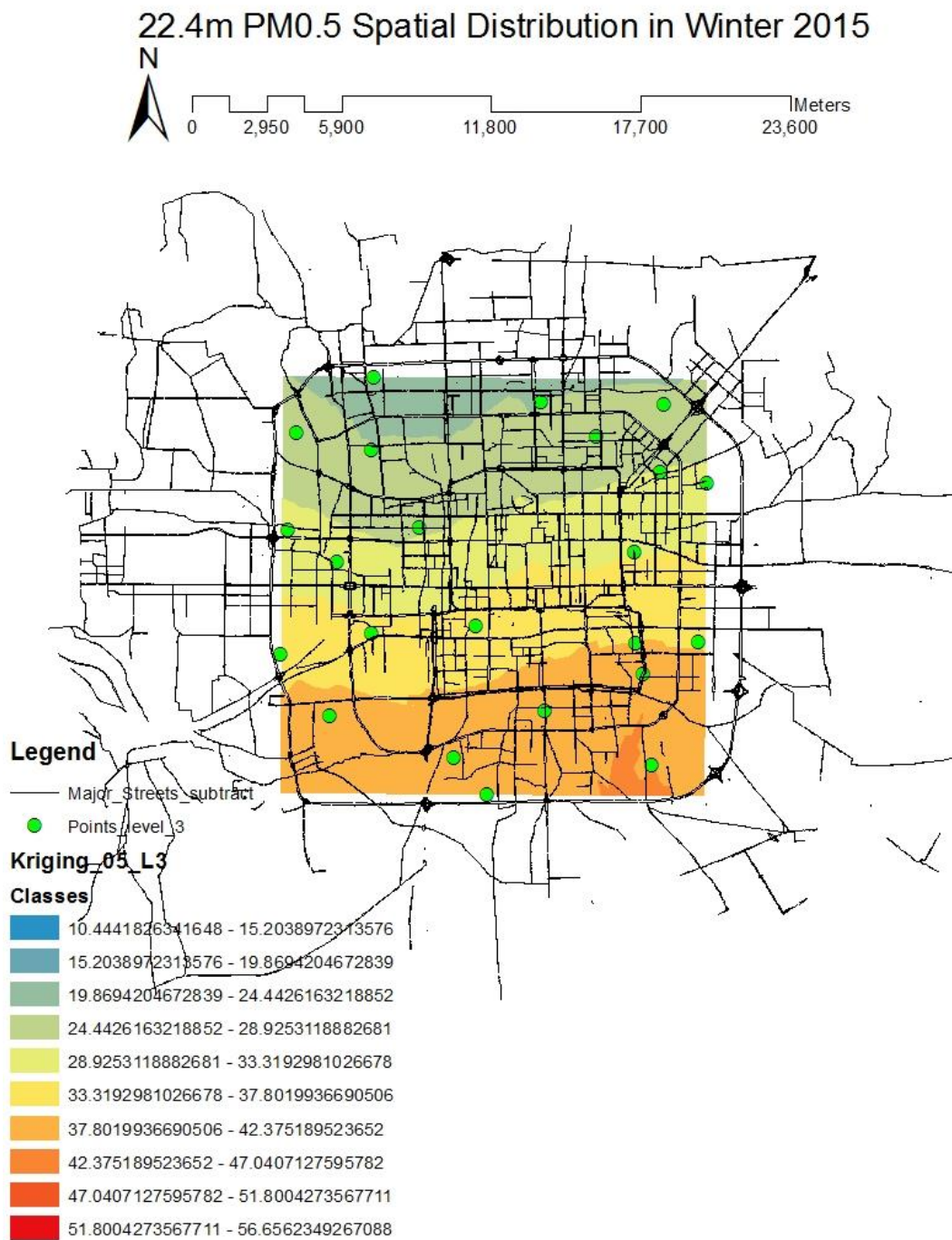


Figure 22: PM_{0.5} Spatial Distribution Map in Summer
a)11.2m; b)22.4m; c)33.6m; d)44.8m

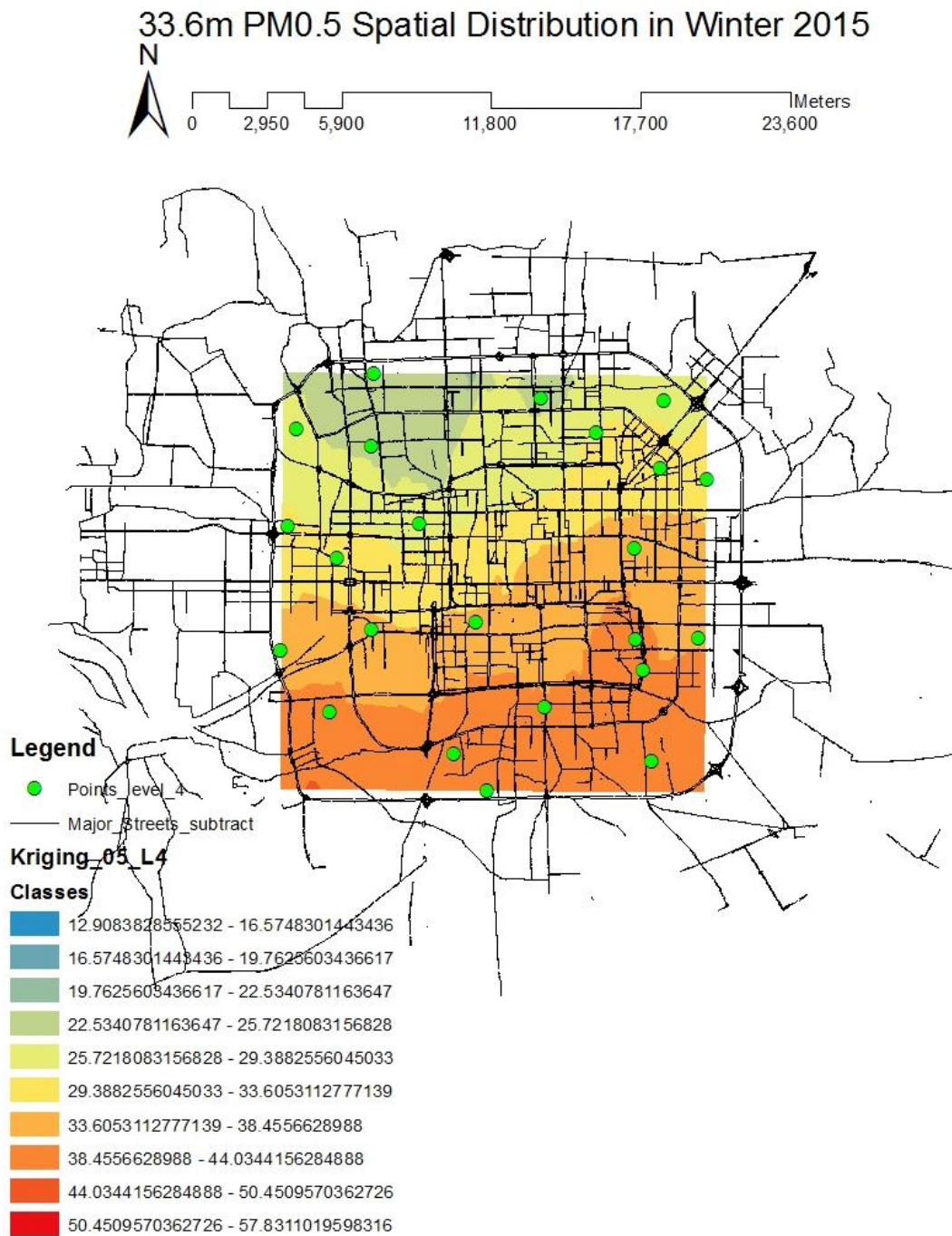
According to Figure 15a and Figure 22, the spatial distributions of $PM_{0.5}$ concentrations at 11.2m, 22.4m, 33.6m and 44.8m were similar with the spatial distribution of $PM_{0.5}$ concentration on the ground (0m), that is to say, the concentrations $PM_{0.5}$ increased from the west to the east of Beijing at the five levels of elevations in summer 2015.



a)



b)



c)

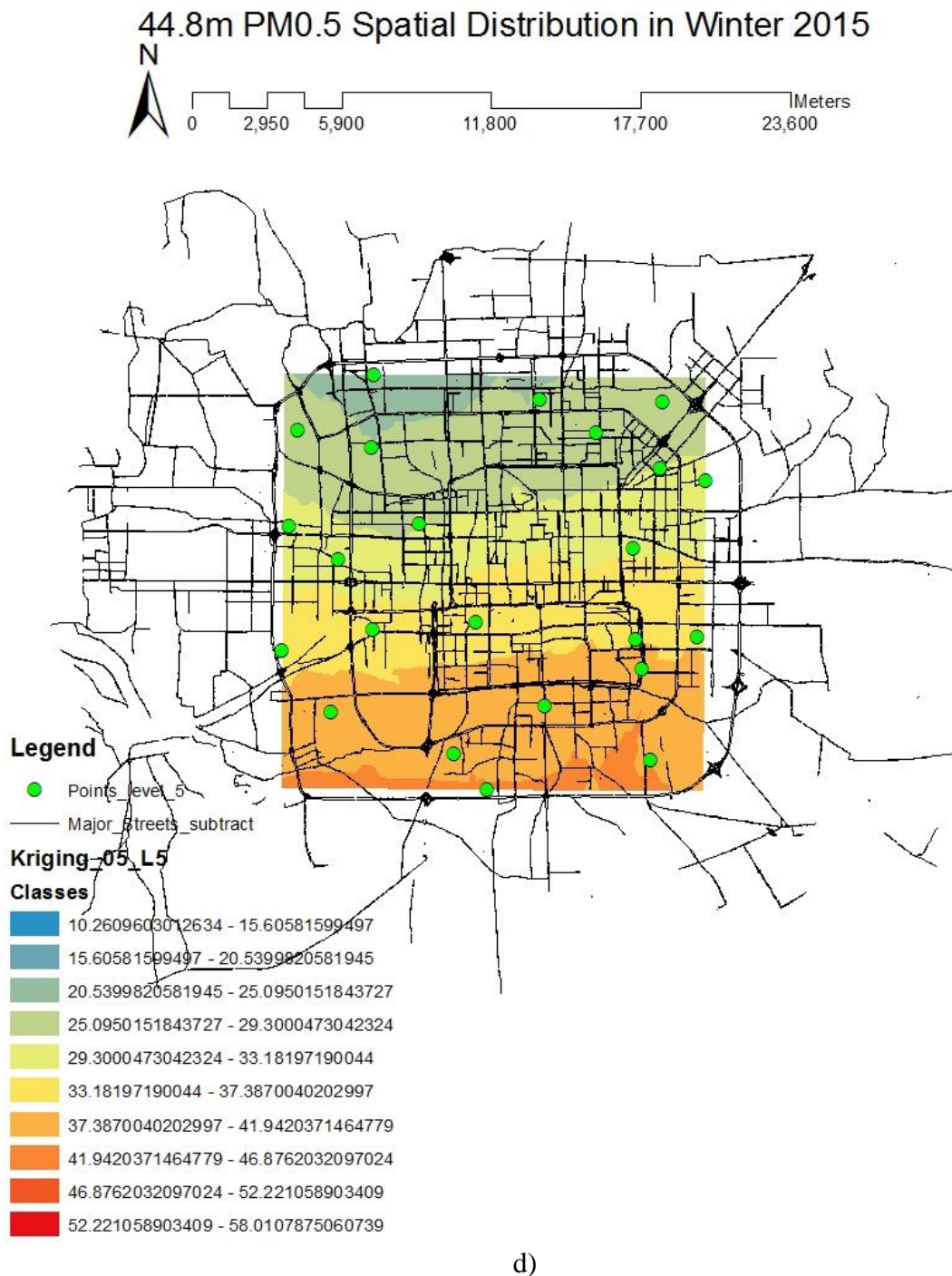
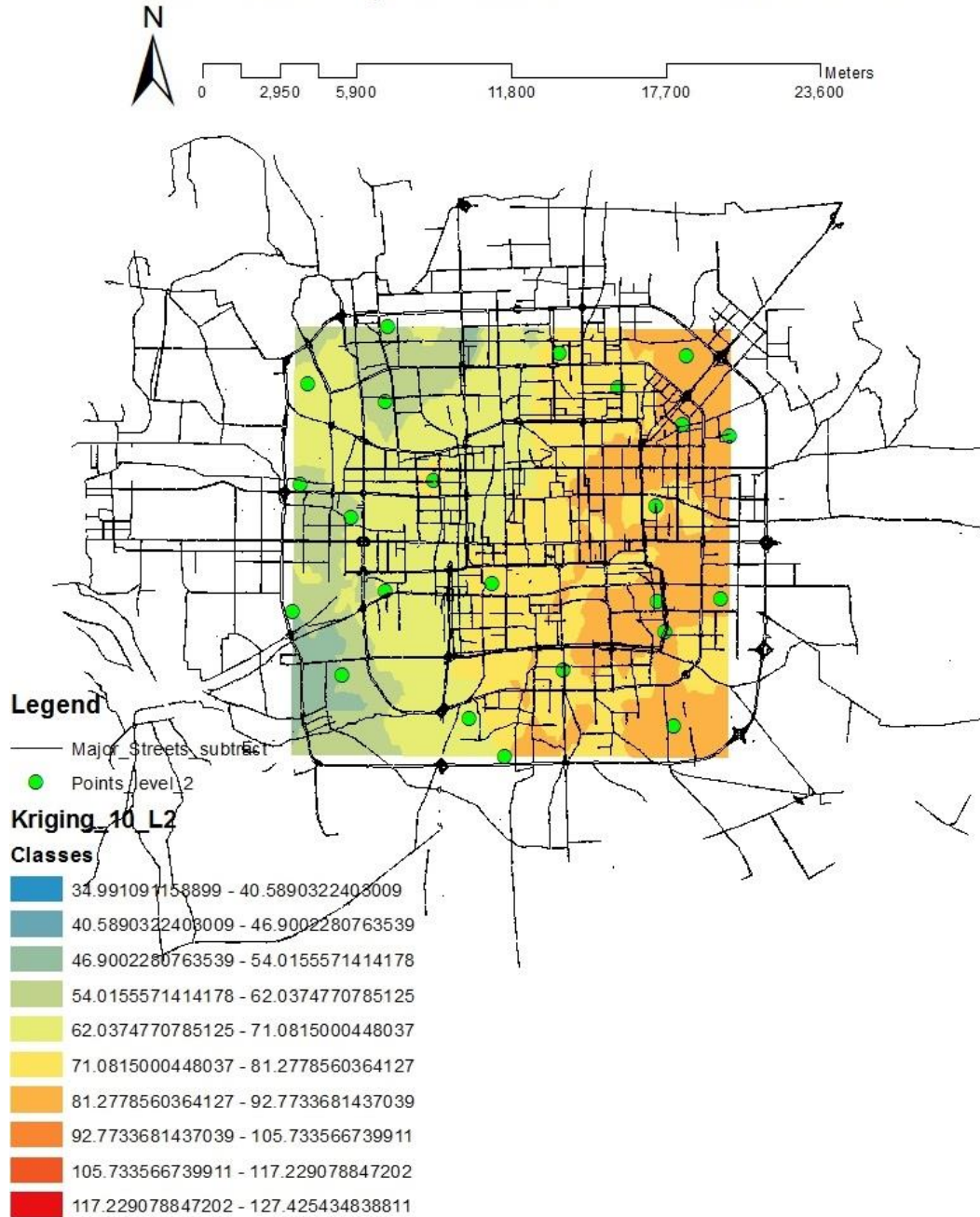


Figure 23: PM_{0.5} Spatial Distribution Map in Winter
a)11.2m; b)22.4m; c)33.6m; d)44.8m

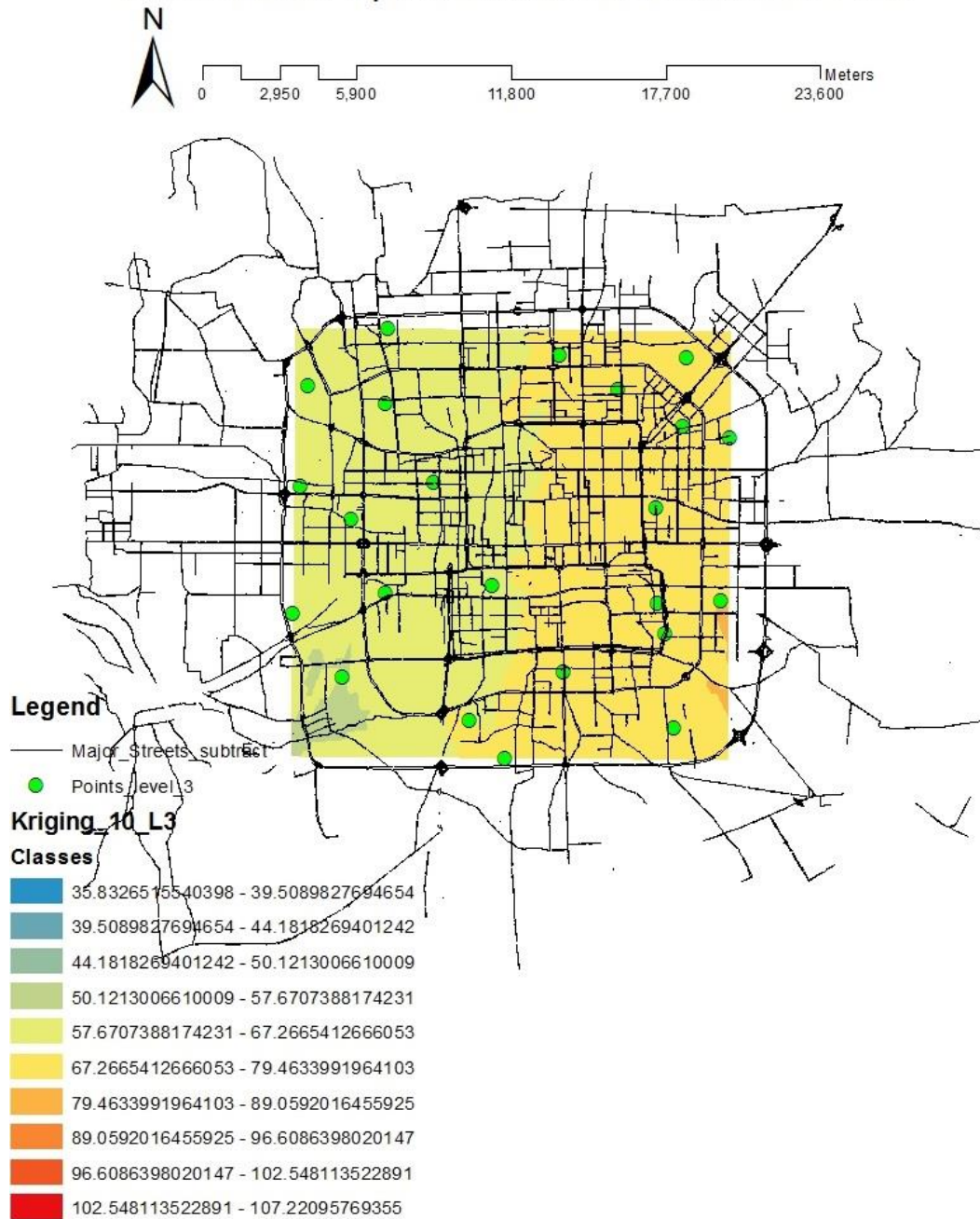
Based on Figure 15b and Figure 23, the spatial distributions of $PM_{0.5}$ concentrations at 11.2m, 22.4m, 33.6m and 44.8m were also the same as the spatial distribution of $PM_{0.5}$ concentration on the ground (0m). The trend of $PM_{0.5}$ concentrations increased from the southern part to the northern part of Beijing in vertical direction in winter 2015.

11.2m PM1.0 Spatial Distribution in Summer 2015



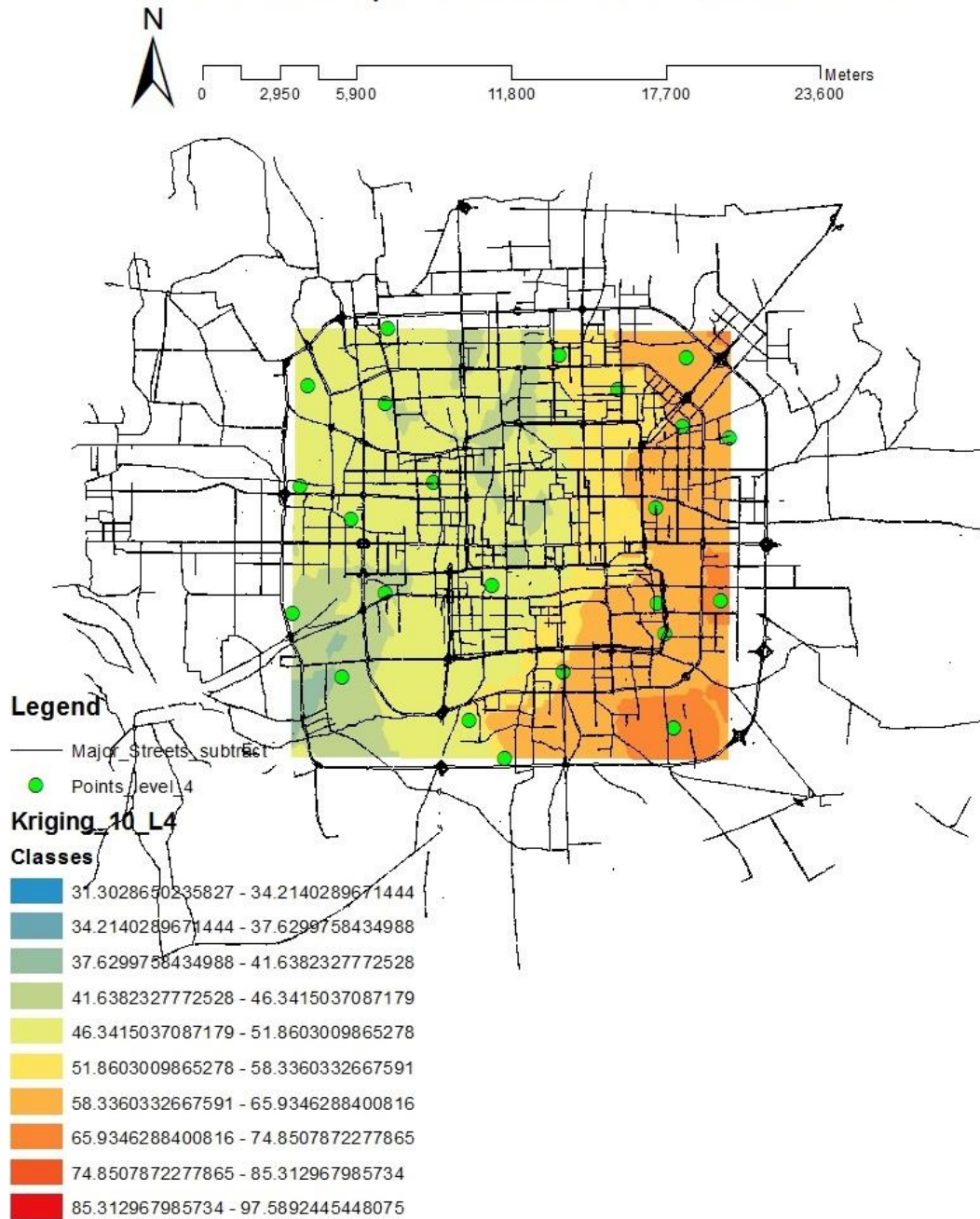
a)

22.4m PM1.0 Spatial Distribution in Summer 2015

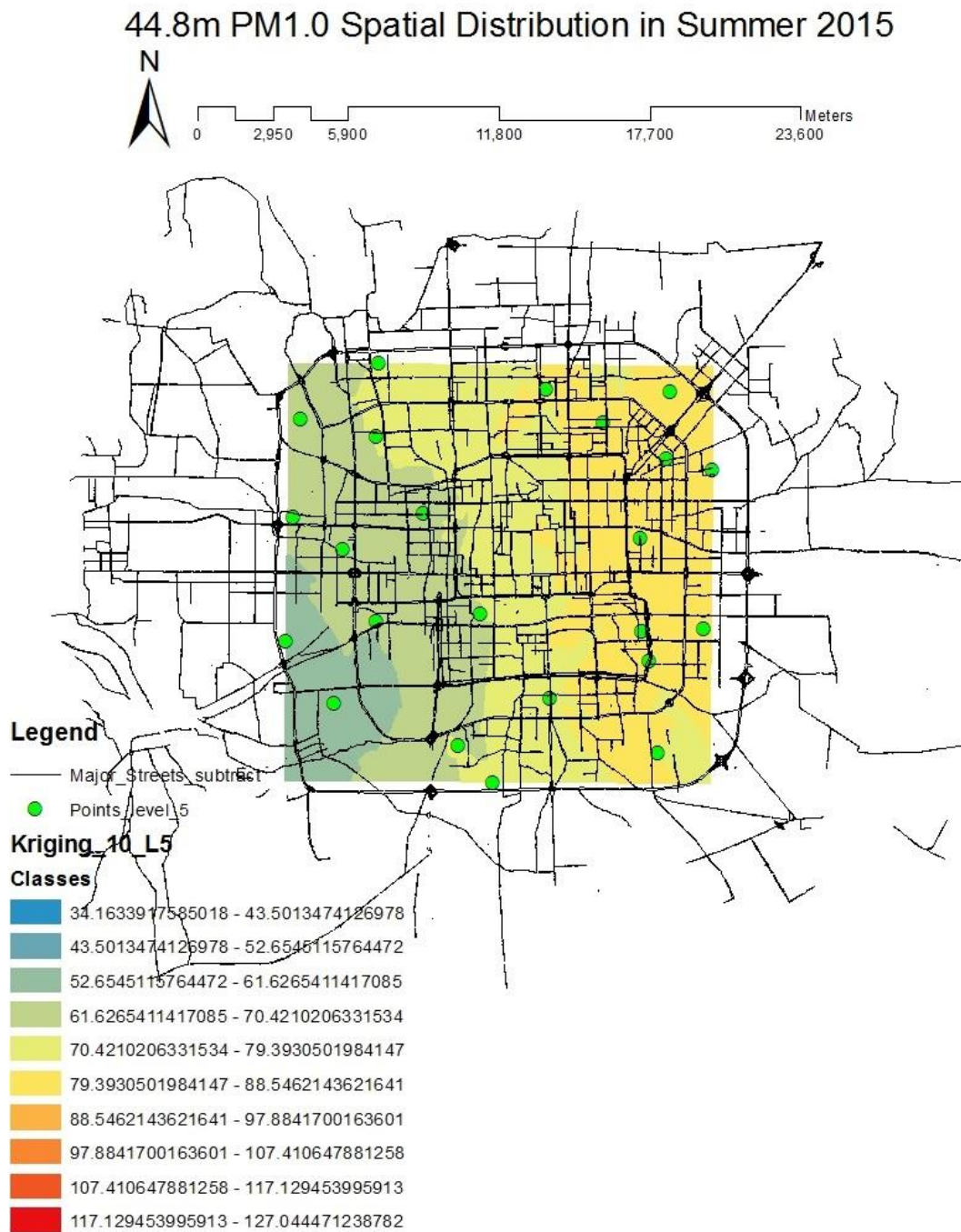


b)

33.6m PM1.0 Spatial Distribution in Summer 2015



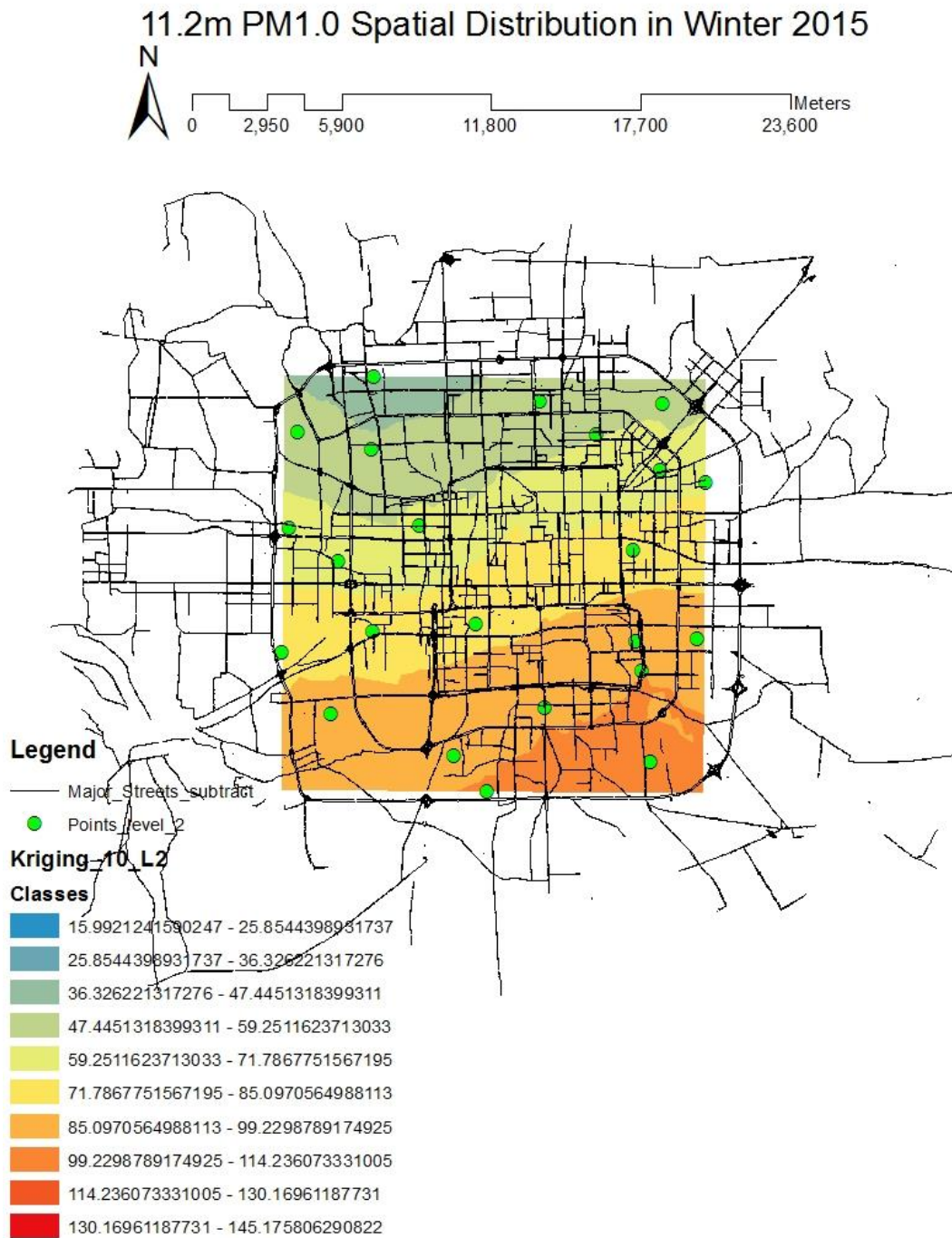
c)



d)

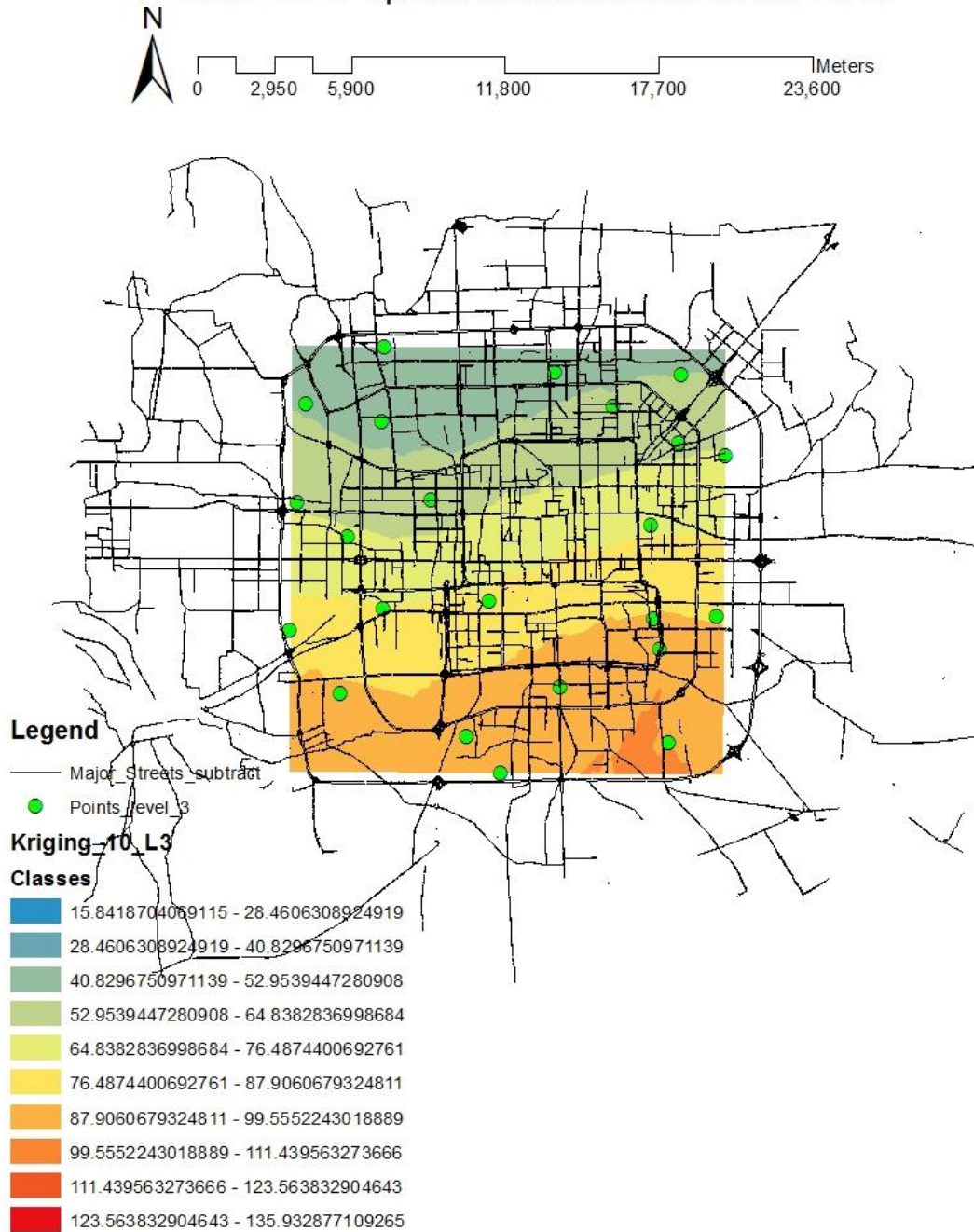
Figure 24: PM_{1.0} Spatial Distribution Map in Summer
a)11.2m; b)22.4m; c)33.6m; d)44.8m

At the altitude of 11.2m, 22.4m, 33.6m and 44.8m, the spatial distributions of PM_{1.0} concentrations were similar with the spatial distribution of PM_{1.0} concentration on the ground (Figure 16a and Figure 24). The trend of PM_{1.0} concentrations increased from the western part to the eastern part of Beijing in vertical direction in summer 2015.

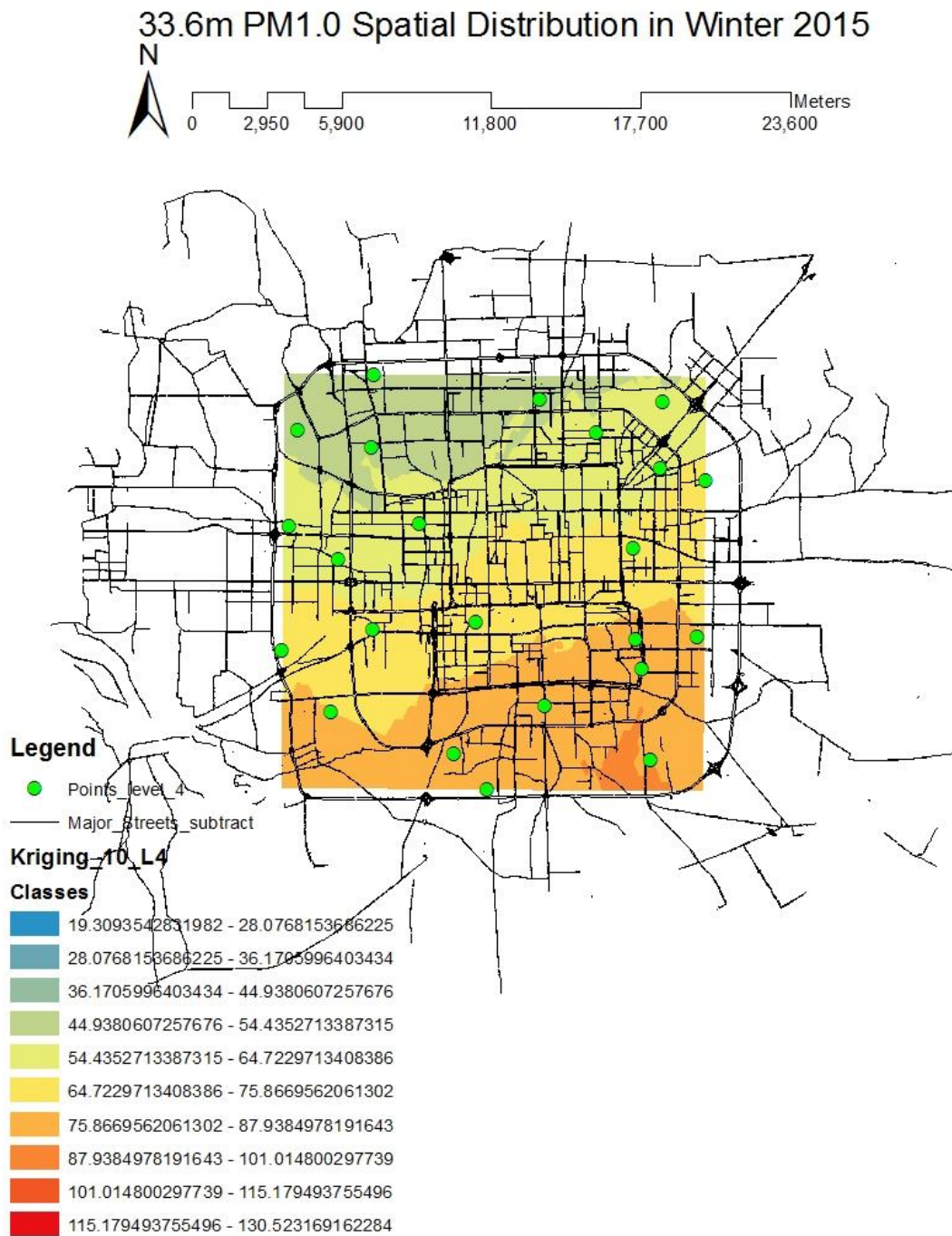


a)

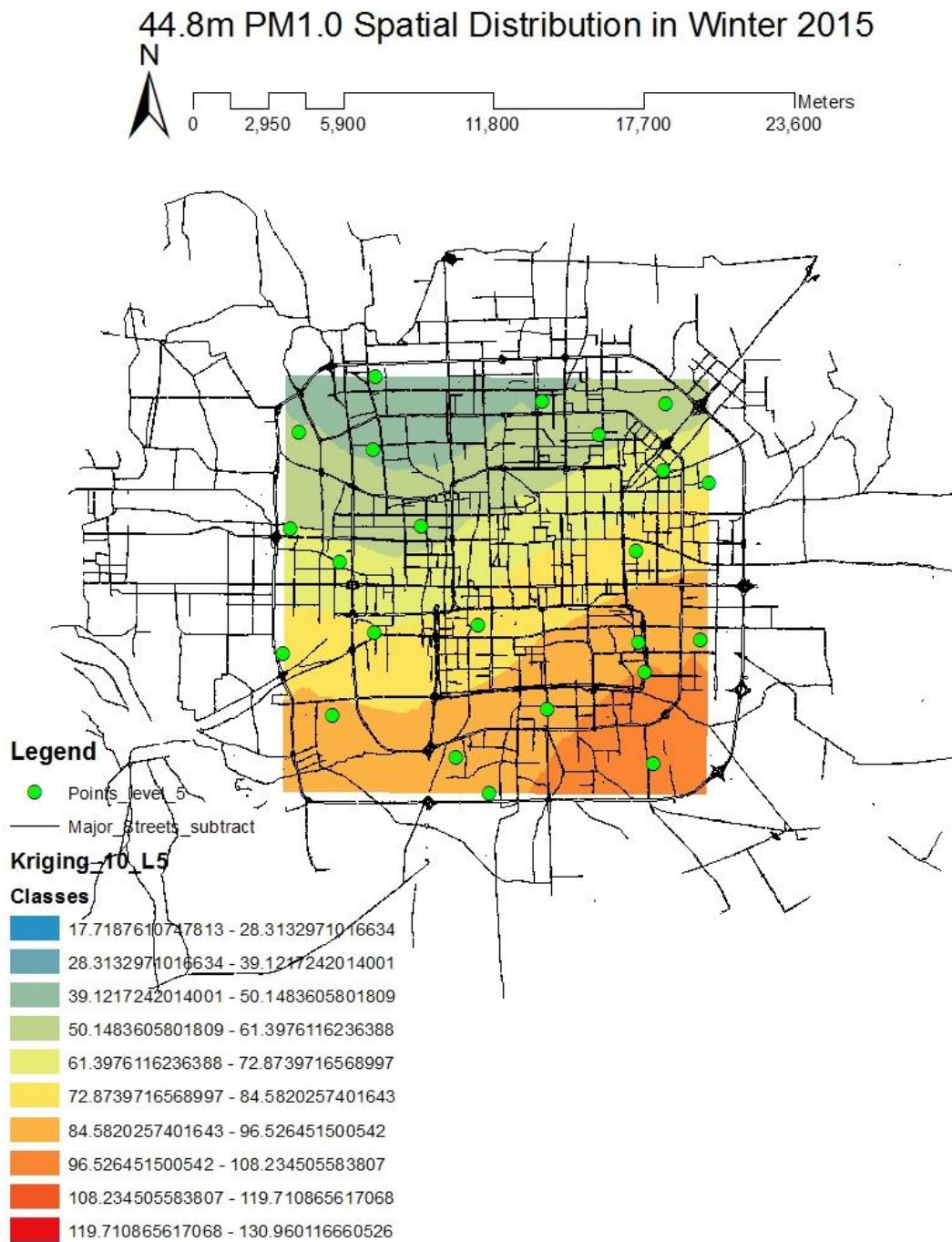
22.4m PM1.0 Spatial Distribution in Winter 2015



b)



c)



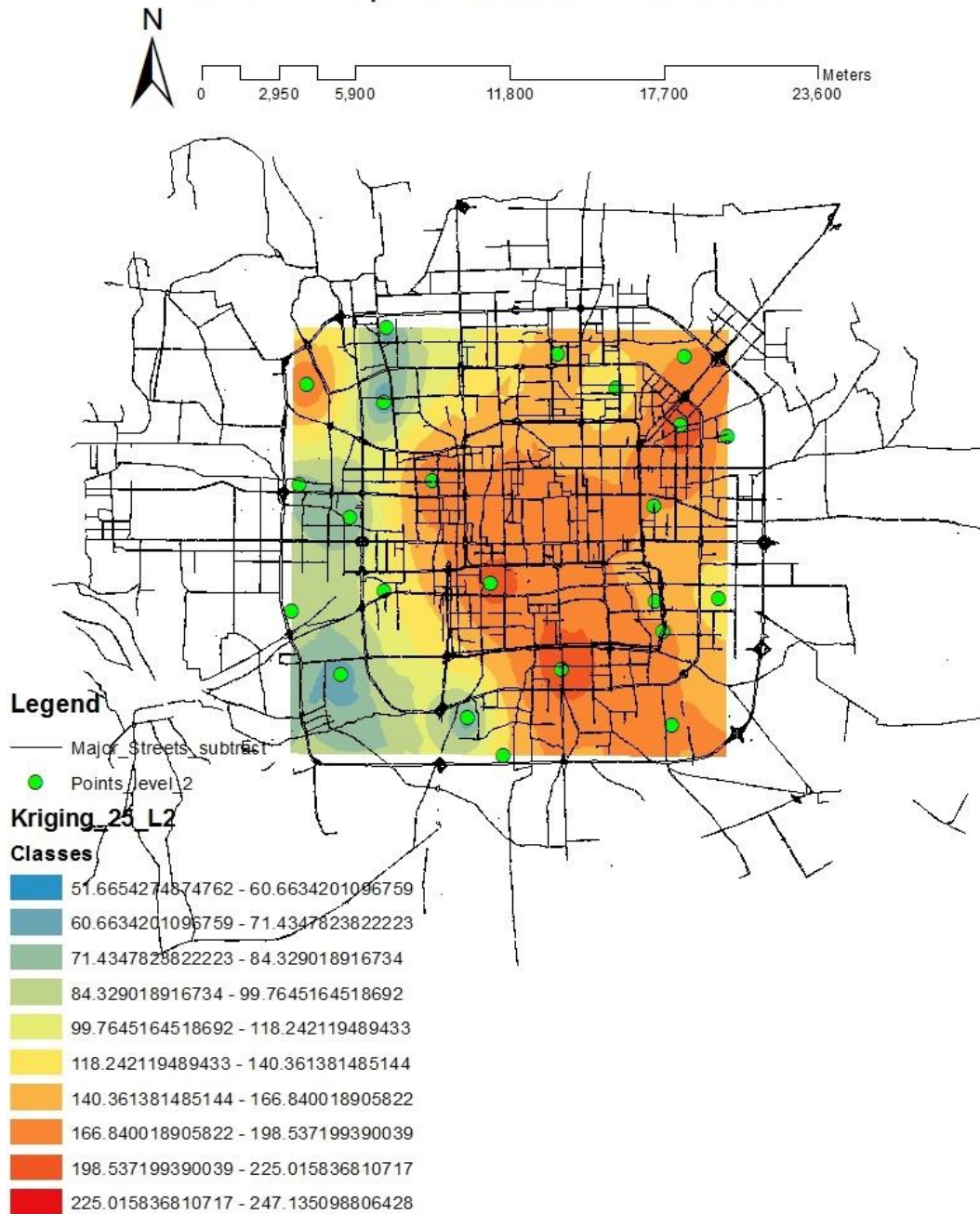
d)

Figure 25: PM_{1.0} Spatial Distribution Map in Winter
 a)11.2m; b)22.4m; c)33.6m; d)44.8m

Spatial distributions of PM_{1.0} concentrations at 11.2m, 22.4m, 33.6m and 44.8m were different from spatial distribution of PM_{1.0} concentrations at surface in winter 2015.

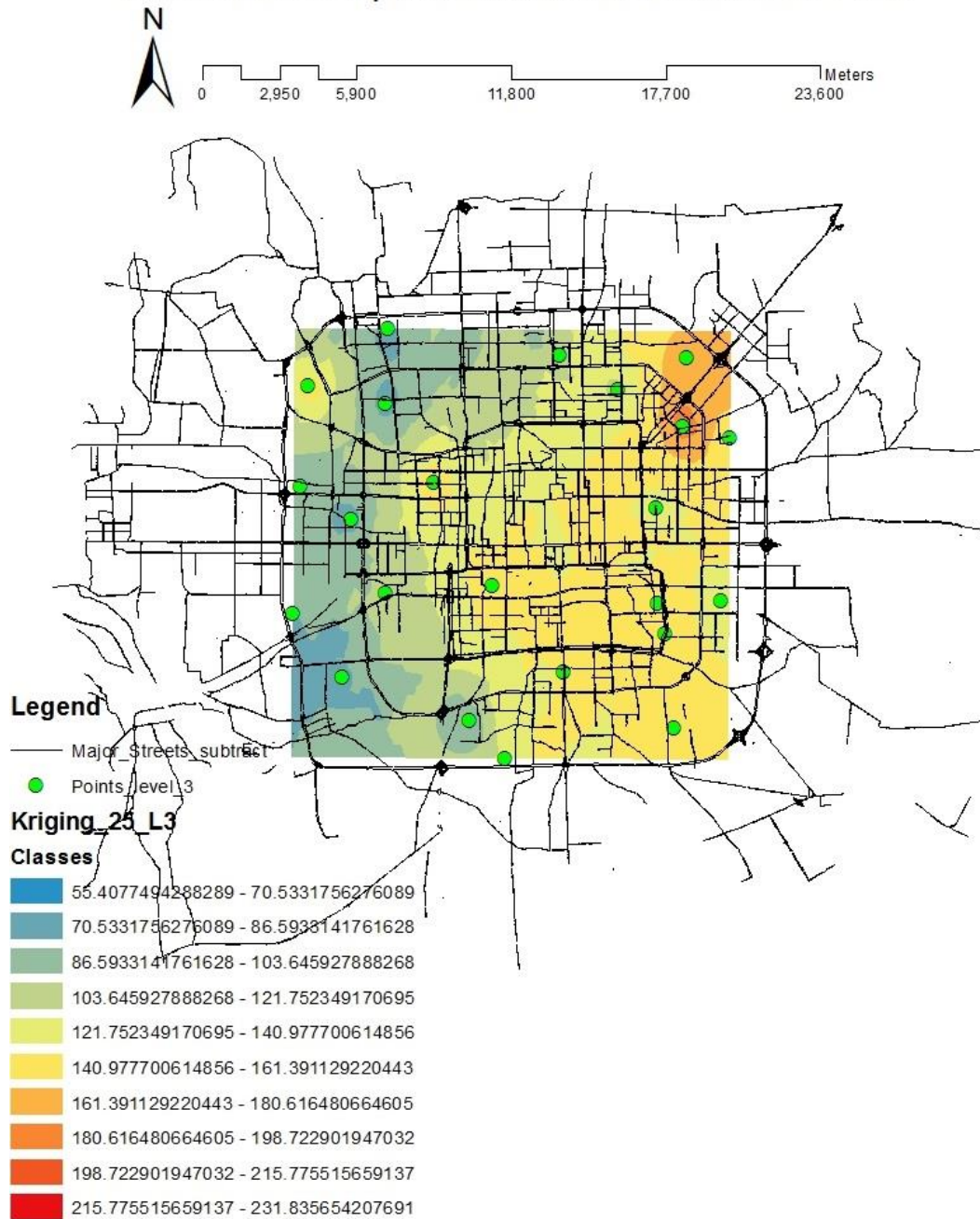
Figure 25 shows the concentrations of PM_{1.0} in winter at the four levels of elevations decreased from the southeast to the northwest of Beijing.

11.2m PM2.5 Spatial Distribution in Summer 2015



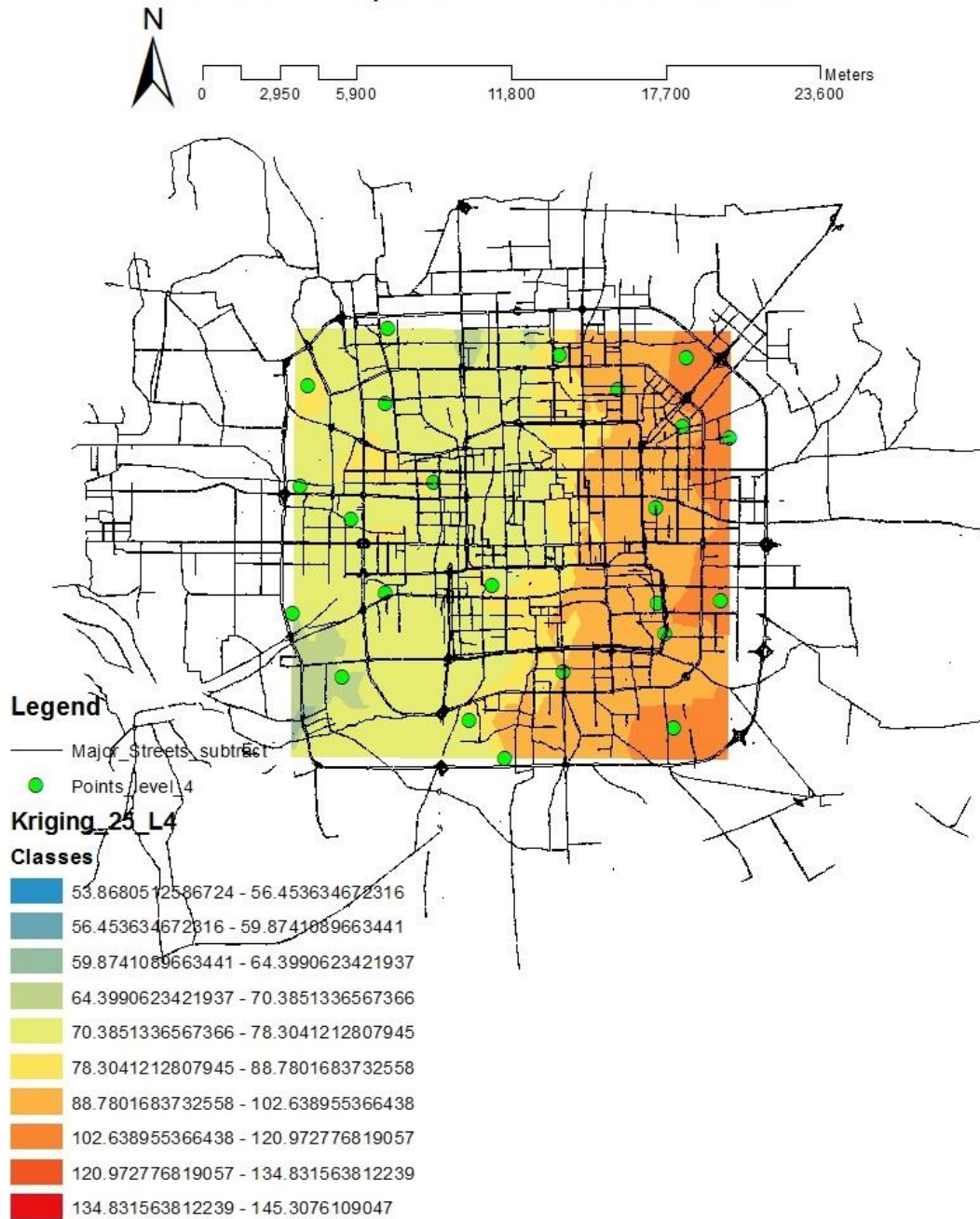
a)

22.4m PM2.5 Spatial Distribution in Summer 2015

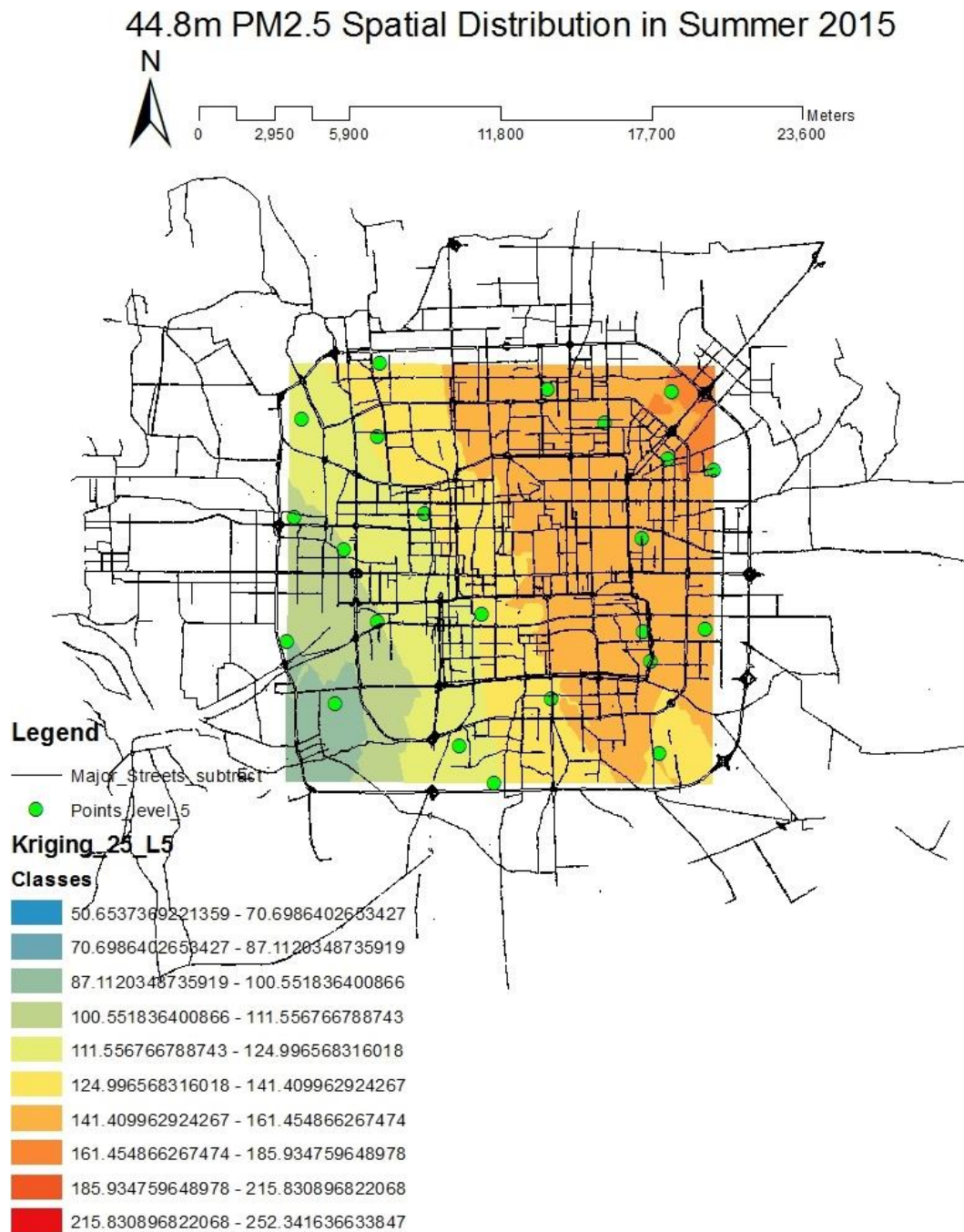


b)

33.6m PM2.5 Spatial Distribution in Summer 2015



c)

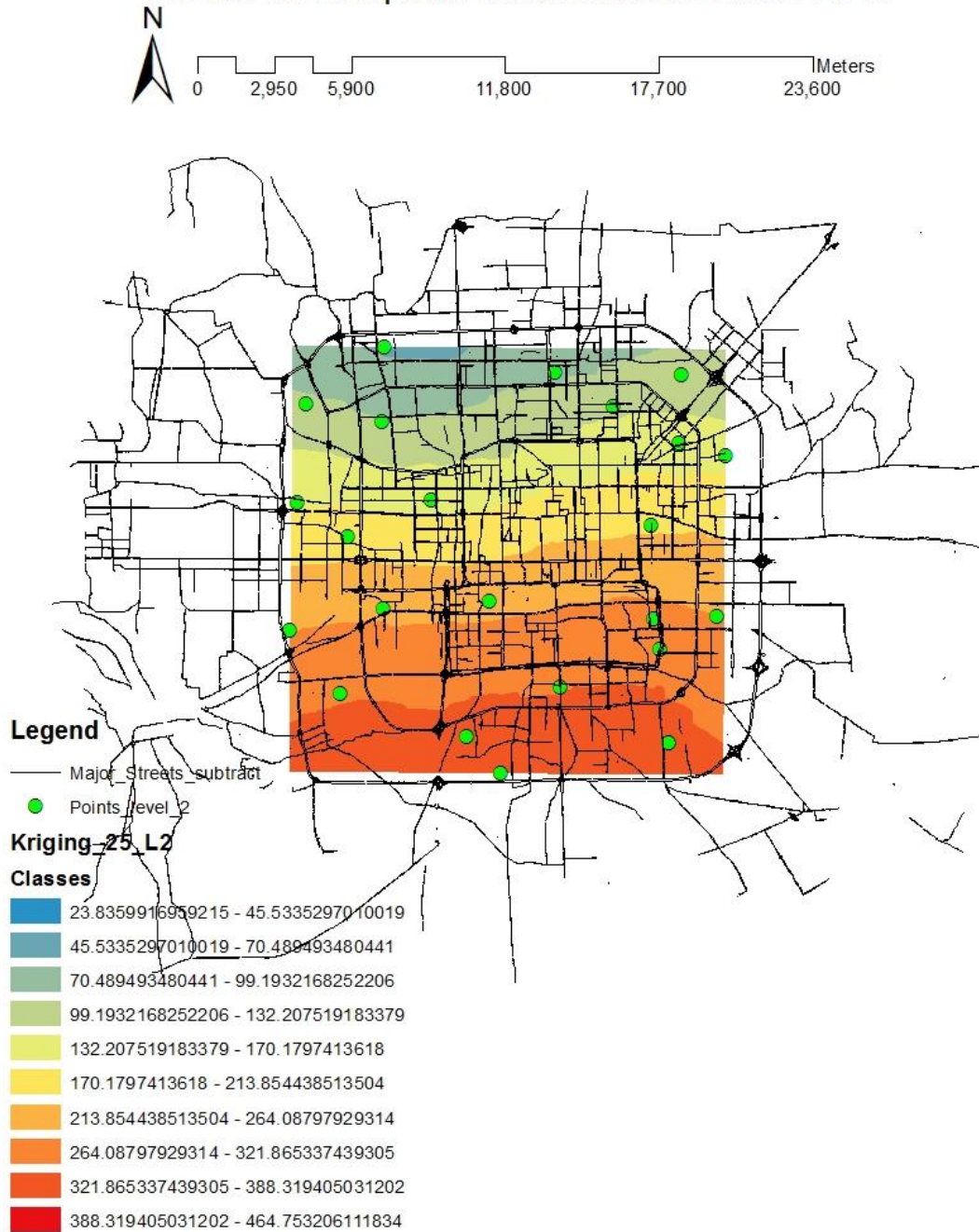


d)

Figure 26: PM_{2.5} Spatial Distribution Map in Summer
 a)11.2m; b)22.4m; c)33.6m; d)44.8m

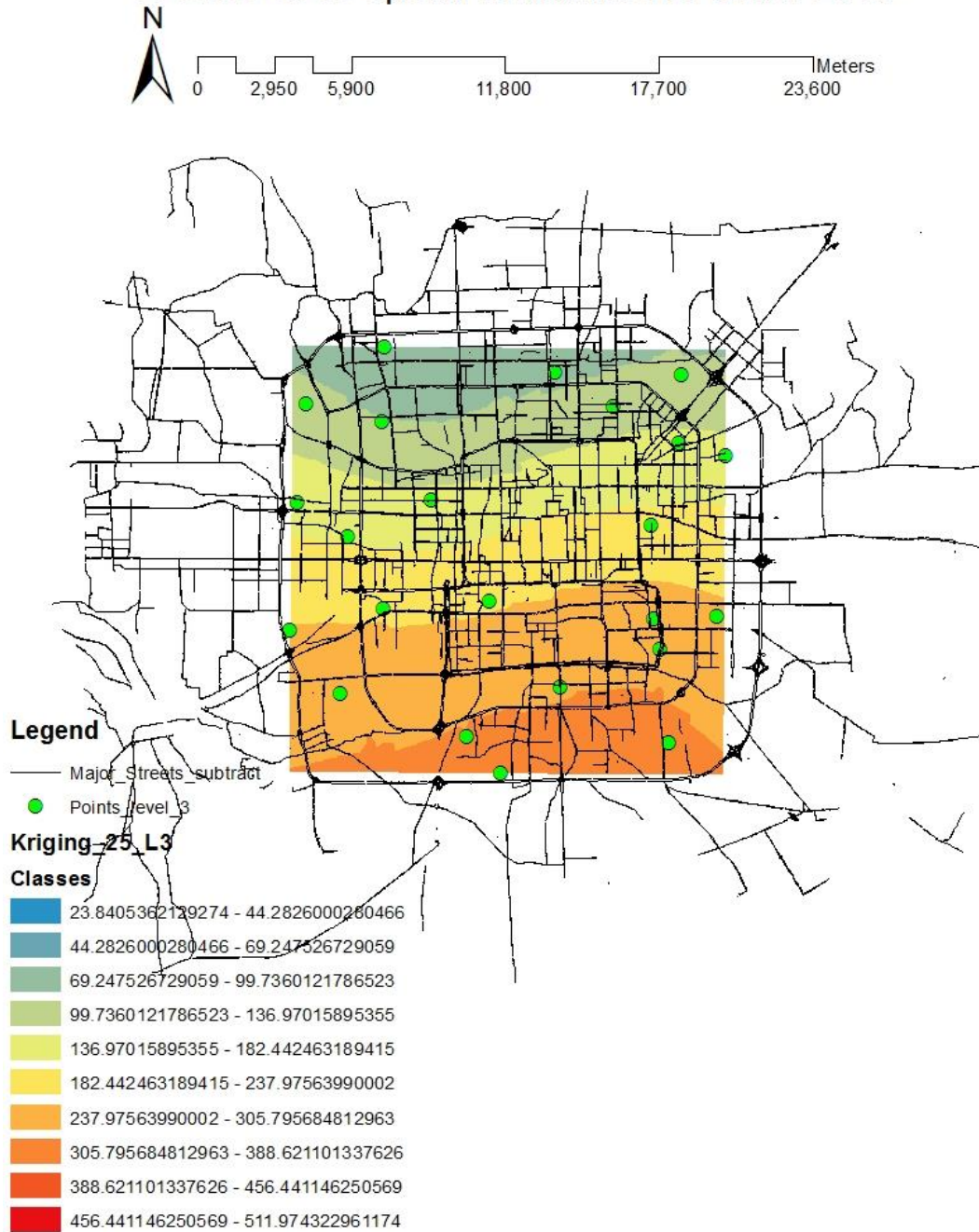
At the altitude of 11.2m and 22.4m, the spatial distributions of PM_{2.5} concentrations were similar with the spatial distribution of PM_{2.5} concentration on the ground (Figure 17a and Figure 26). However, at 33.6m, the concentrations of PM_{2.5} in the eastern part of Beijing were higher than the western part of Beijing; at 44.8m, the concentrations of PM_{2.5} decreased from the northeast to the southwest of Beijing.

11.2m PM_{2.5} Spatial Distribution in Winter 2015

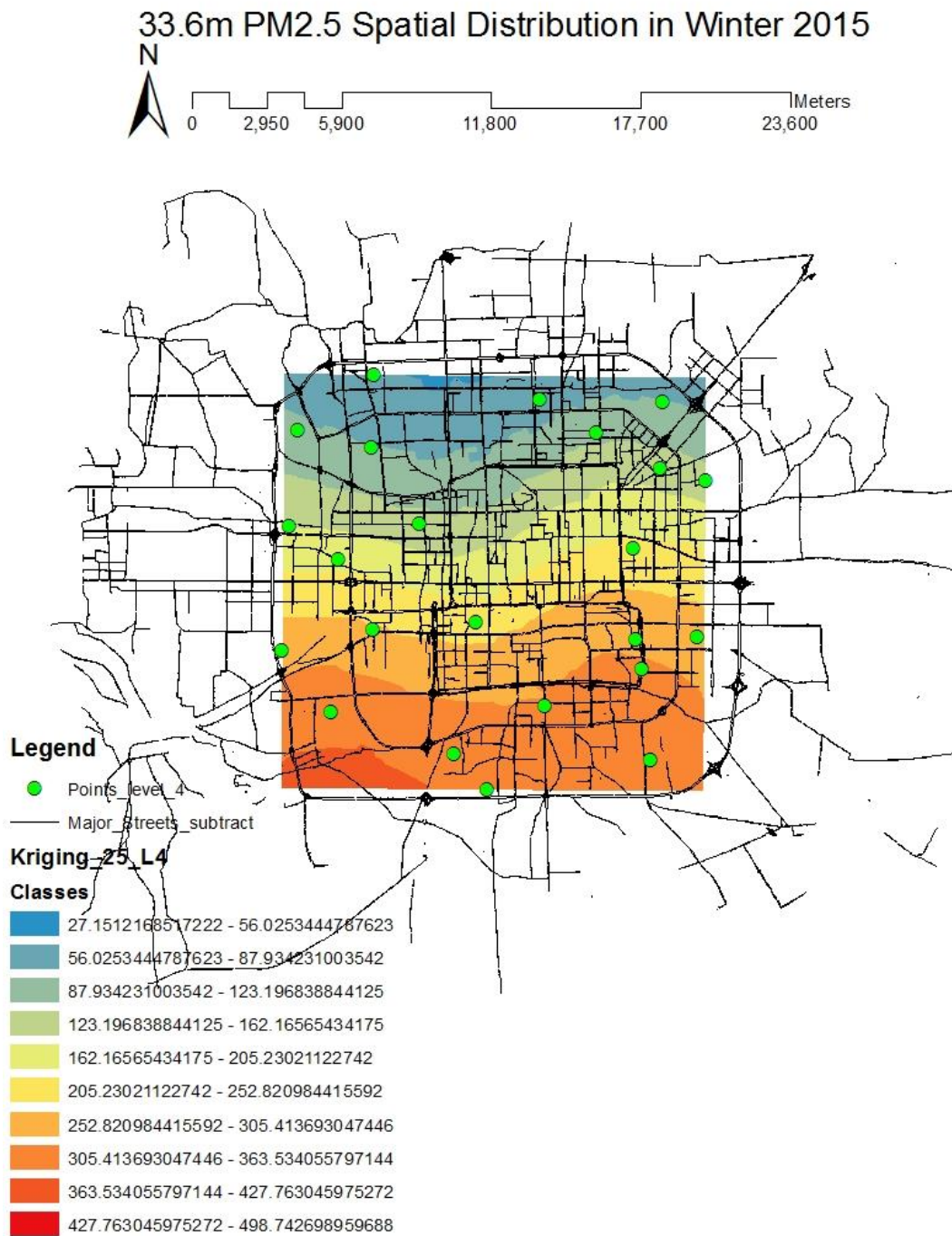


a)

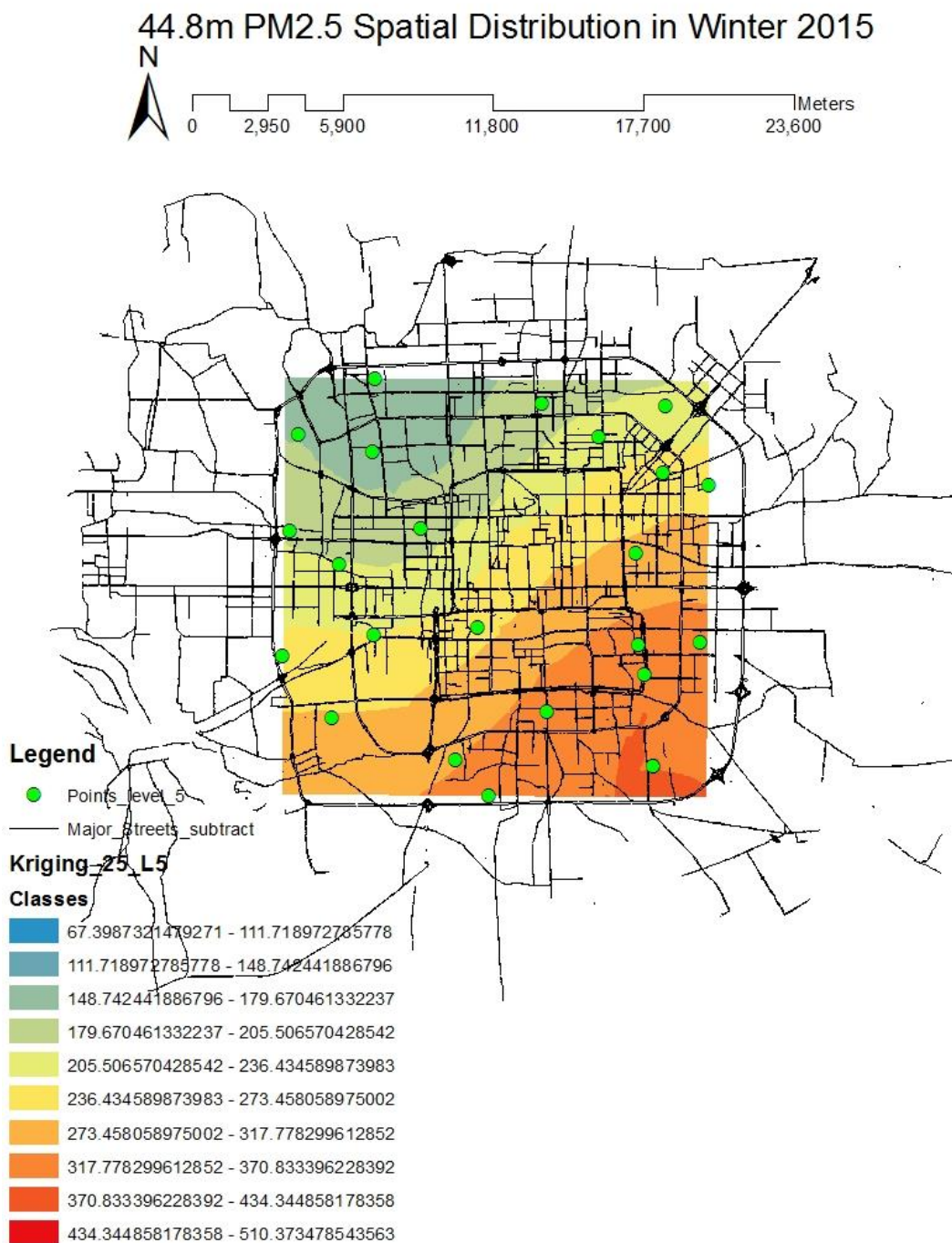
22.4m PM_{2.5} Spatial Distribution in Winter 2015



b)



c)

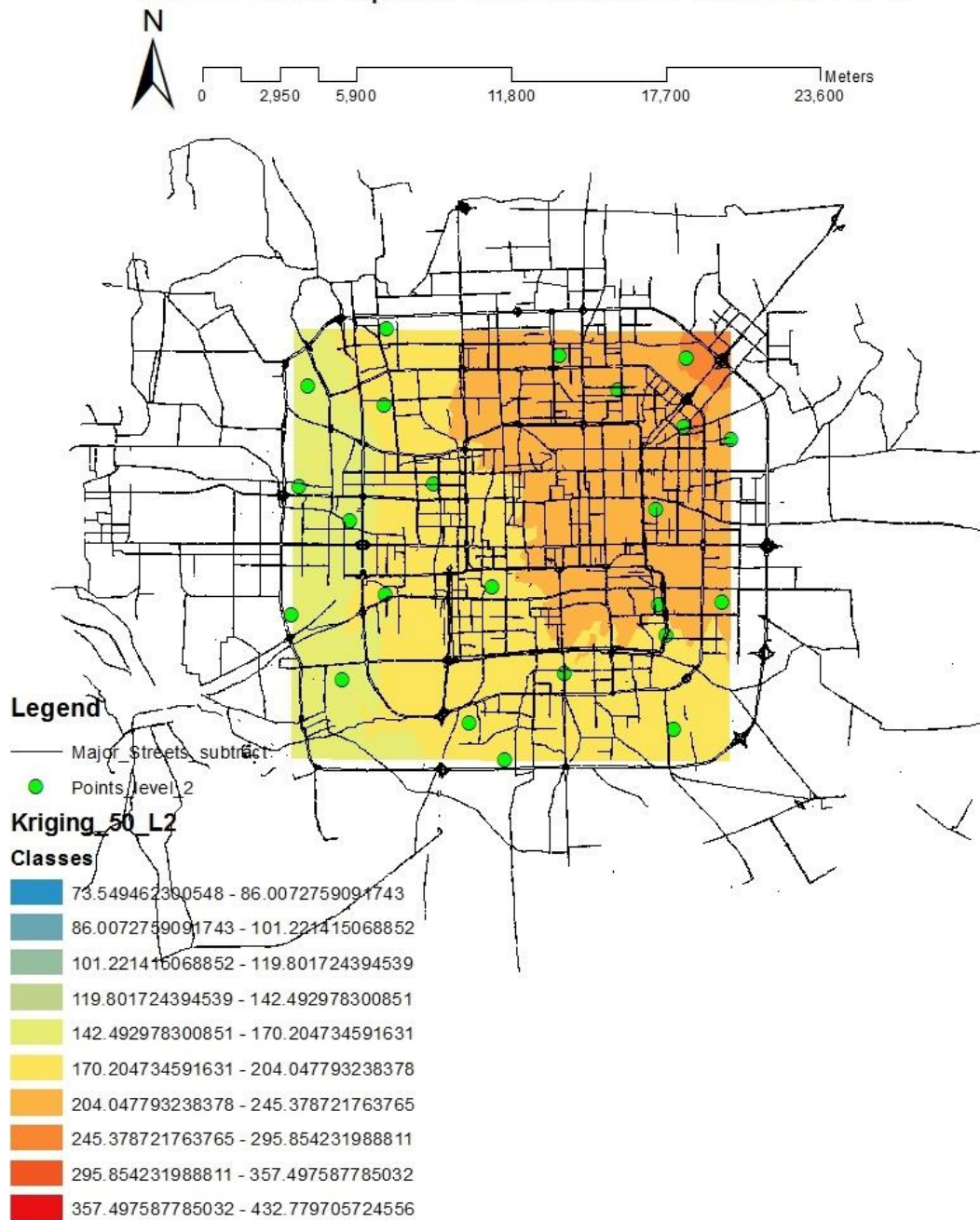


d)

Figure 27: PM_{2.5} Spatial Distribution Map in Winter
 a)11.2m; b)22.4m; c)33.6m; d)44.8m

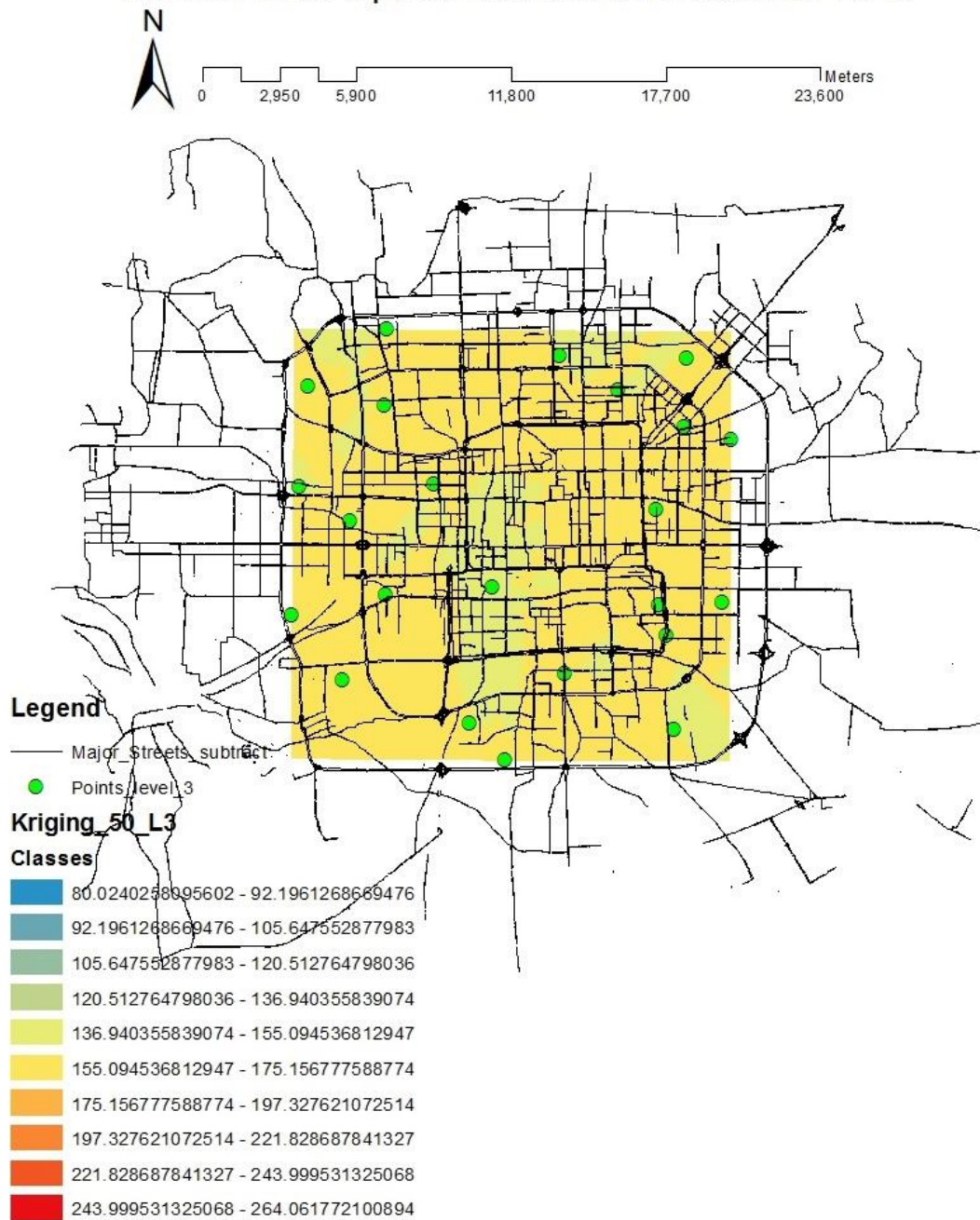
The concentrations of $PM_{2.5}$ at 11.2m, 22.4m and 33.6m distributed same as the concentrations of $PM_{2.5}$ on the ground (Figure 17b, Figure 27a, b, c), they increased from the southern part to the northern part of Beijing; while the concentrations of $PM_{2.5}$ at 44.8m increased from the northwest to the southeast of Beijing in winter 2015 (Figure 27d).

11.2m PM5.0 Spatial Distribution in Summer 2015



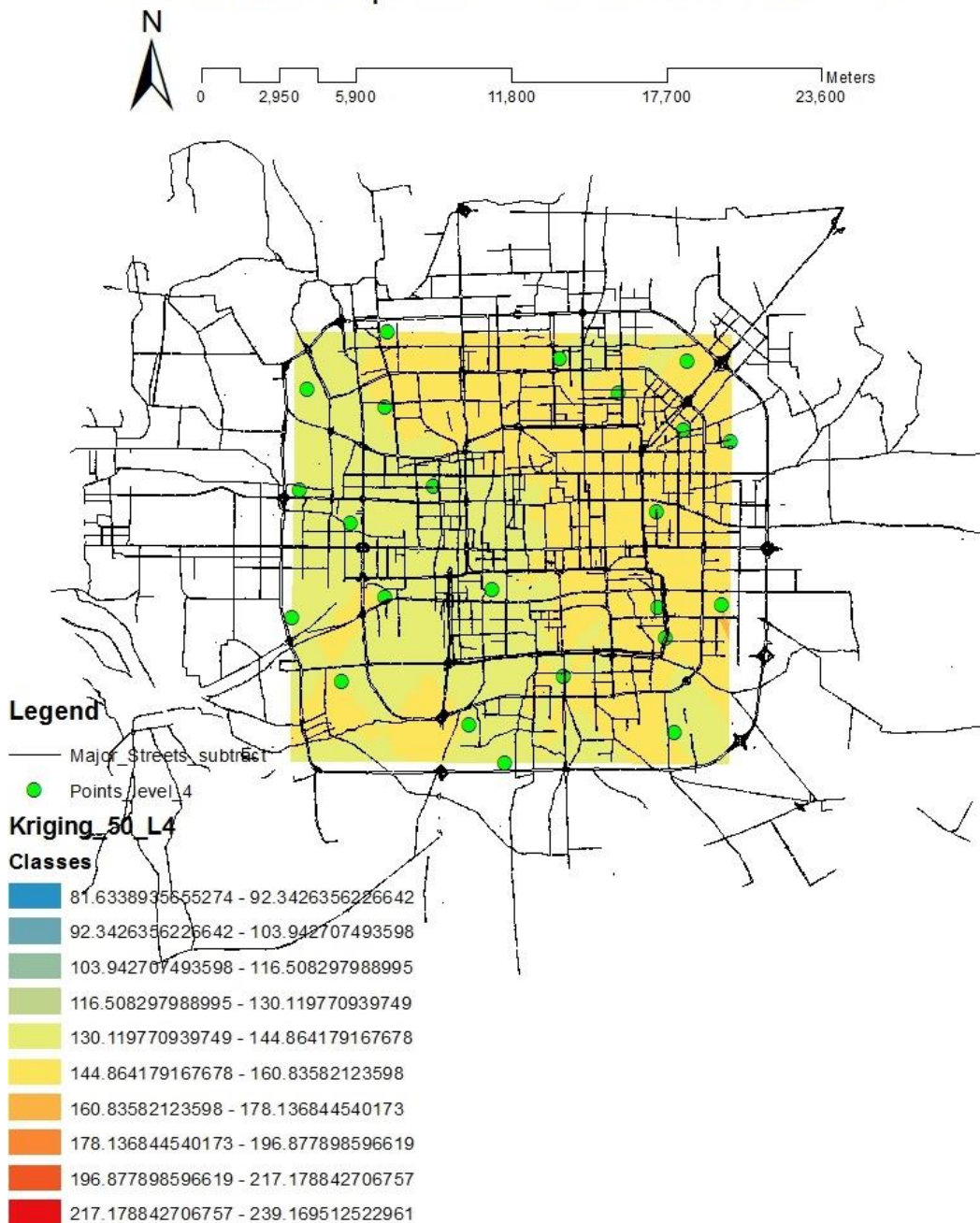
a)

22.4m PM5.0 Spatial Distribution in Summer 2015



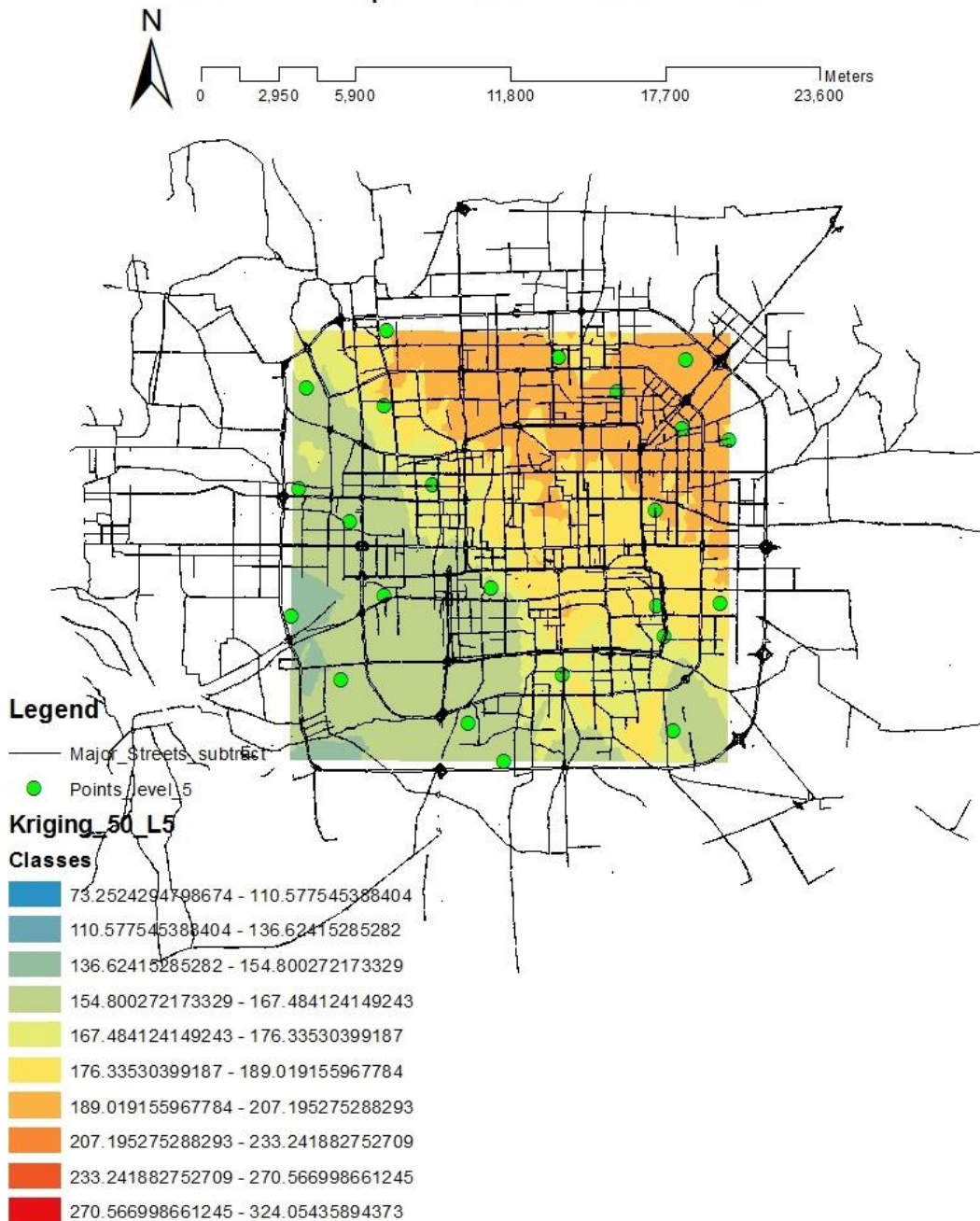
b)

33.6m PM5.0 Spatial Distribution in Summer 2015



c)

44.8m PM5.0 Spatial Distribution in Summer 2015



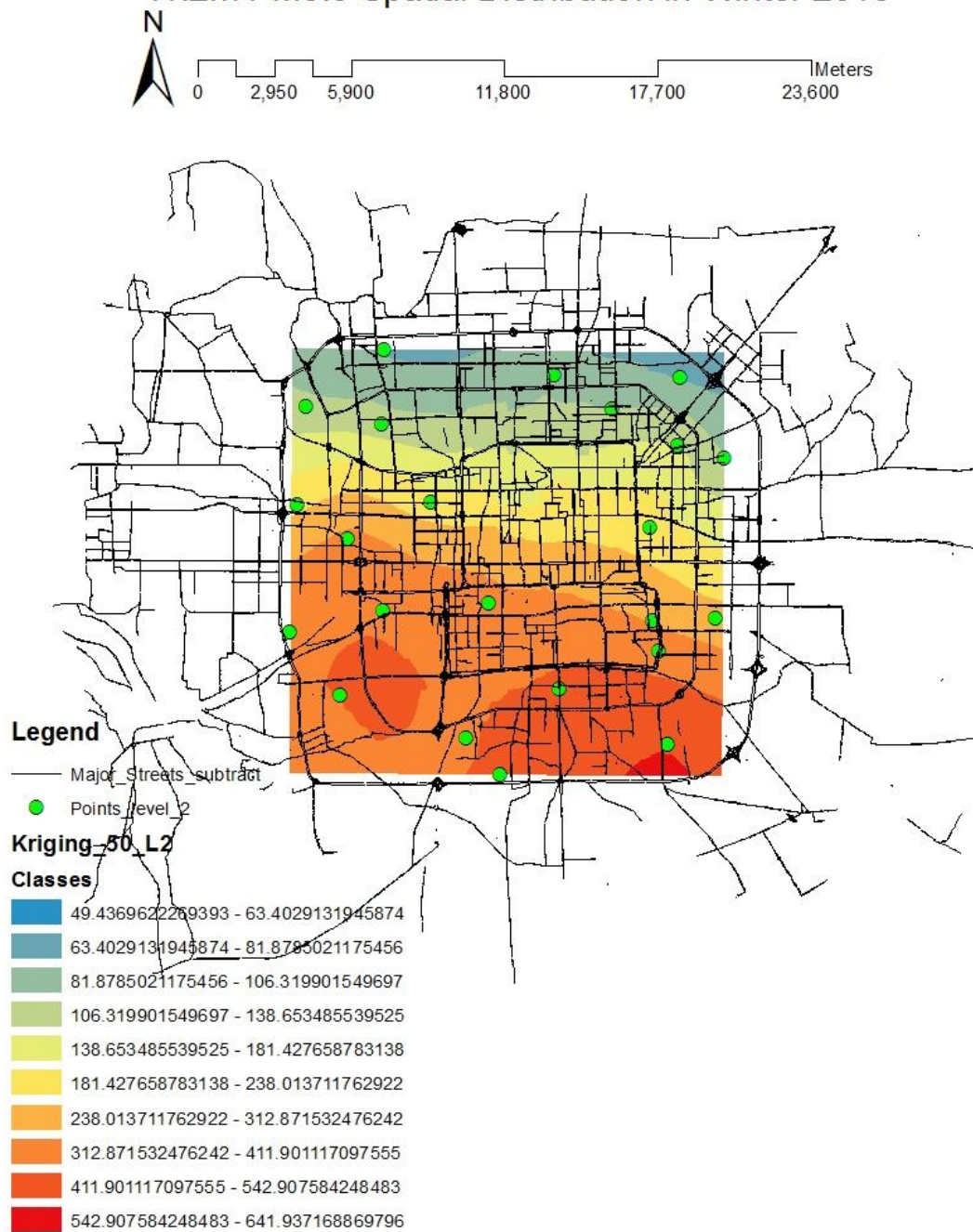
d)

Figure 28: PM_{5.0} Spatial Distribution Map in Summer
 a)11.2m; b)22.4m; c)33.6m; d)44.8m

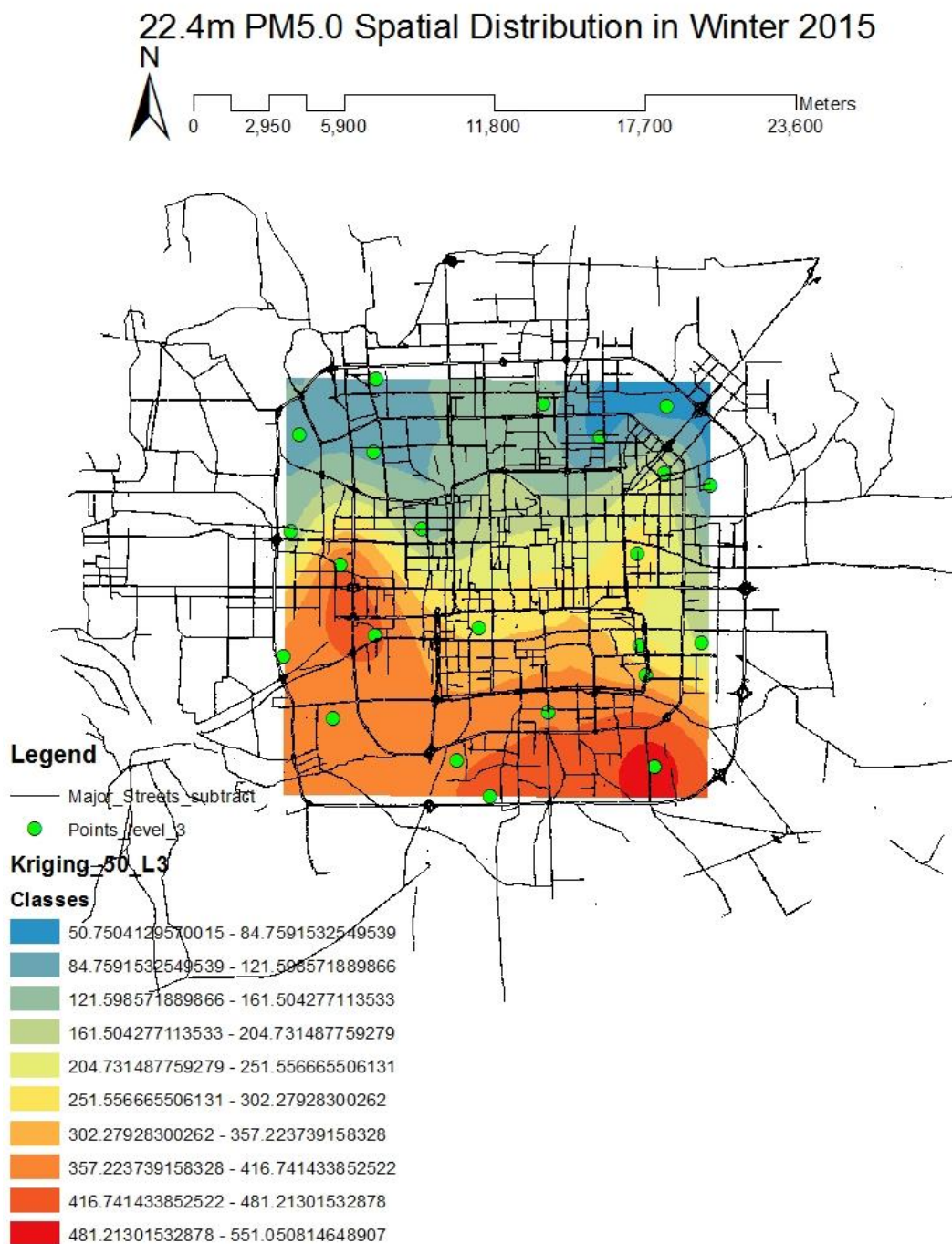
The spatial distribution of PM_{5.0} concentrations at 11.2m and 44.8m were similar with the spatial pattern of PM_{5.0} concentrations on the ground, they decreased from the northeast to the west, southwest and southeast of Beijing in summer (Figure 18a, Figure 28a, d).

The concentrations of PM_{5.0} distributed homogeneously at 22.4m and 33.6m levels.

11.2m PM5.0 Spatial Distribution in Winter 2015

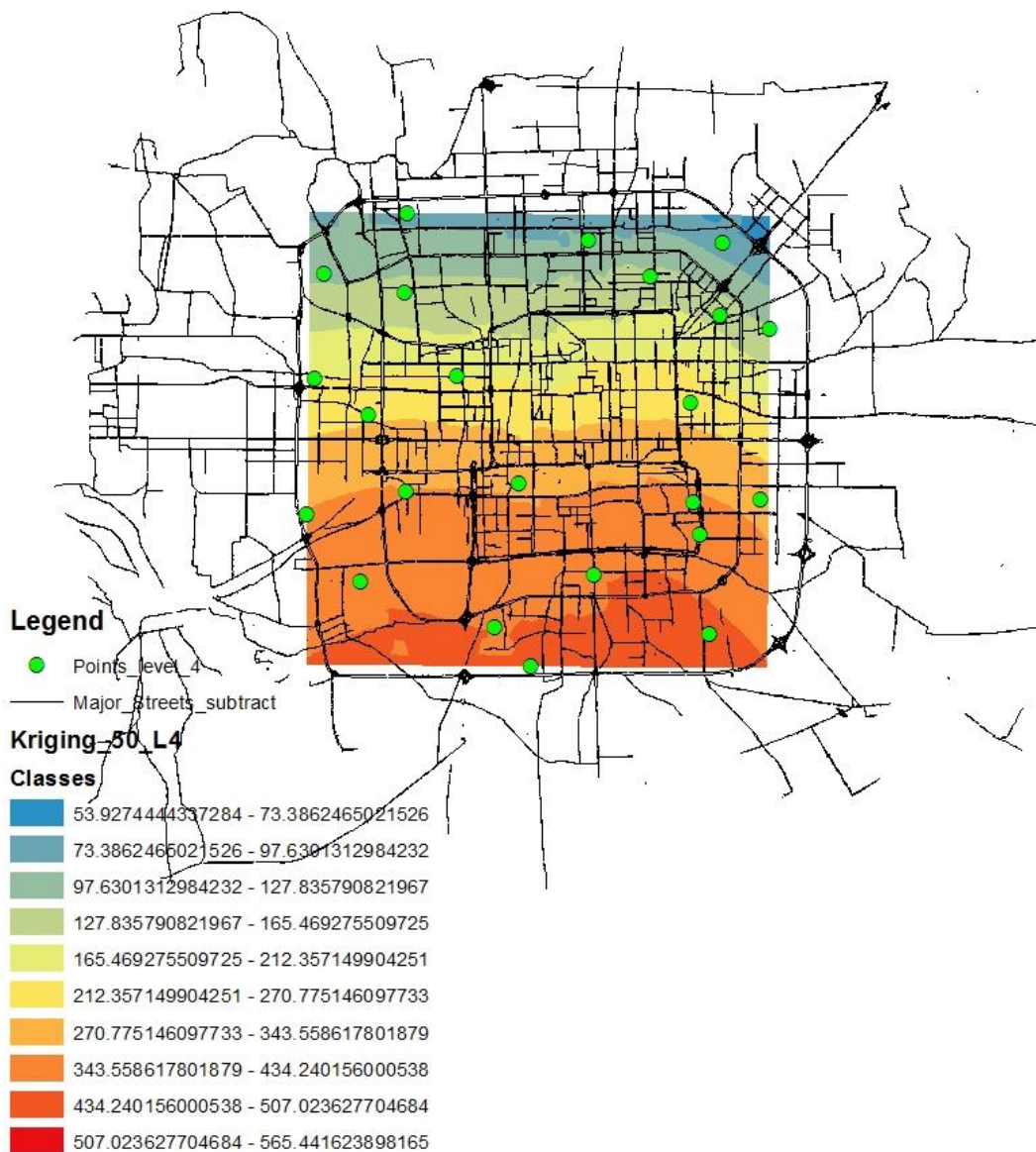
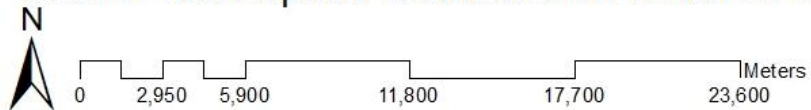


a)

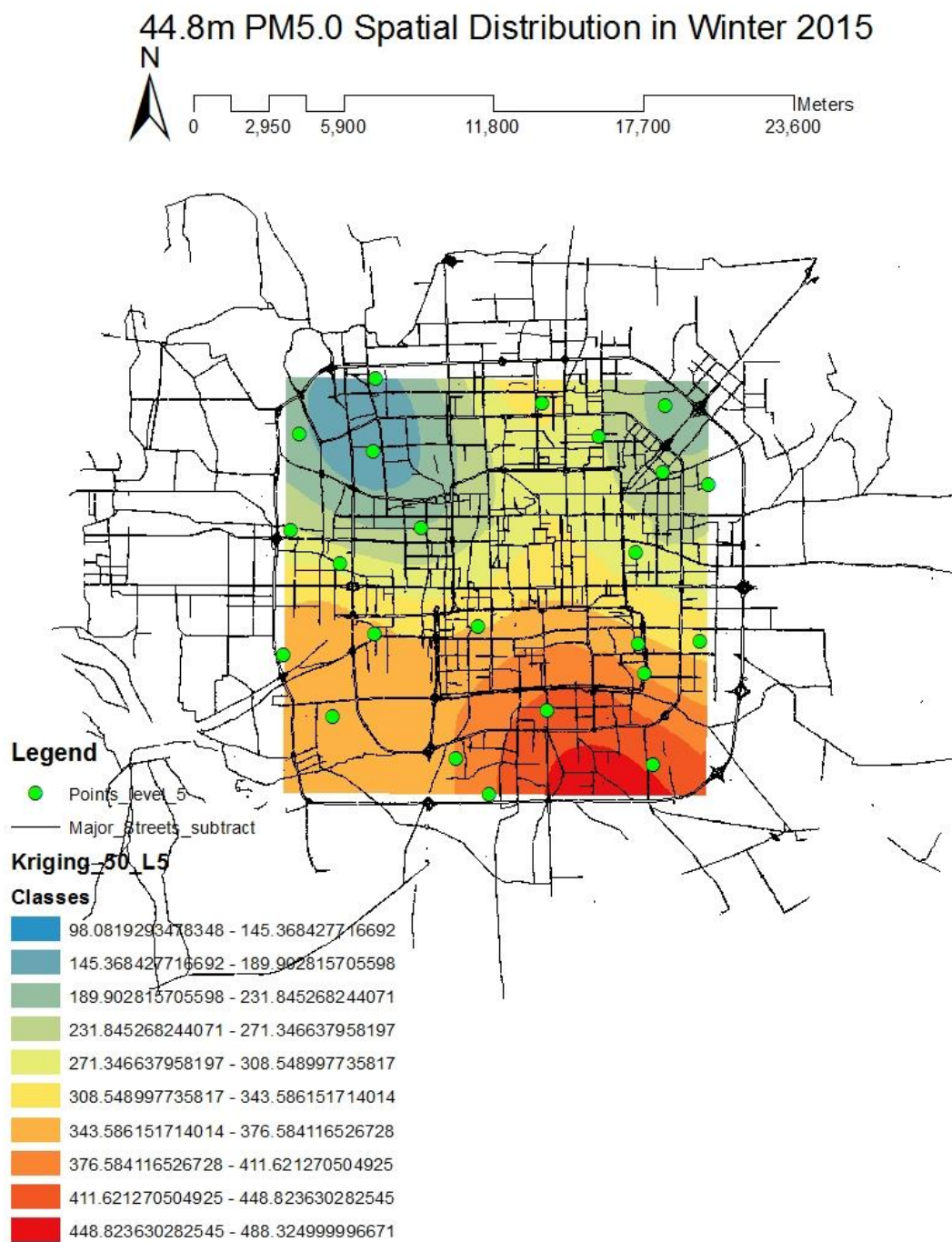


b)

33.6m PM5.0 Spatial Distribution in Winter 2015



c)

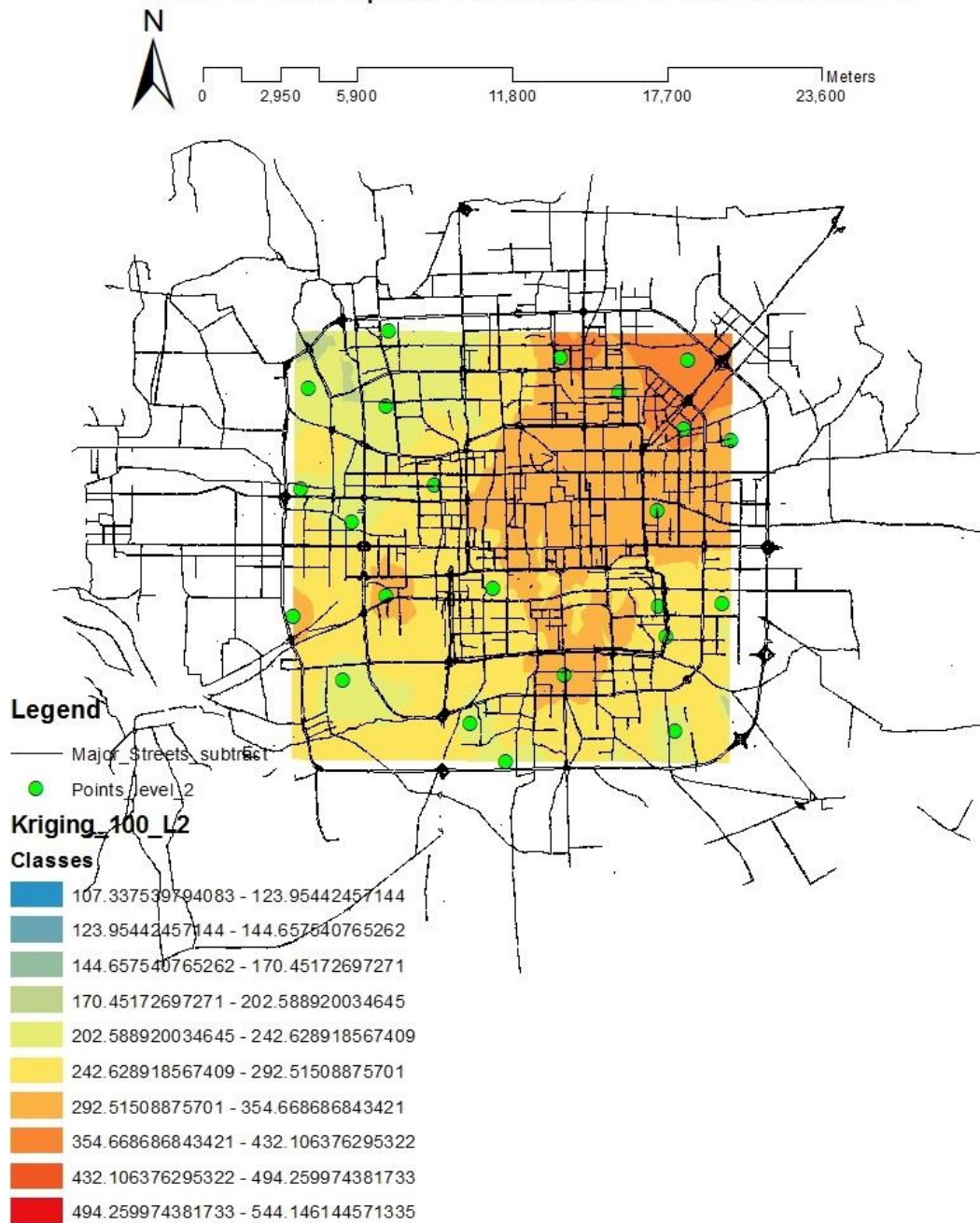


d)

Figure 29: PM_{5.0} Spatial Distribution Map in Winter
a)11.2m; b)22.4m; c)33.6m; d)44.8m

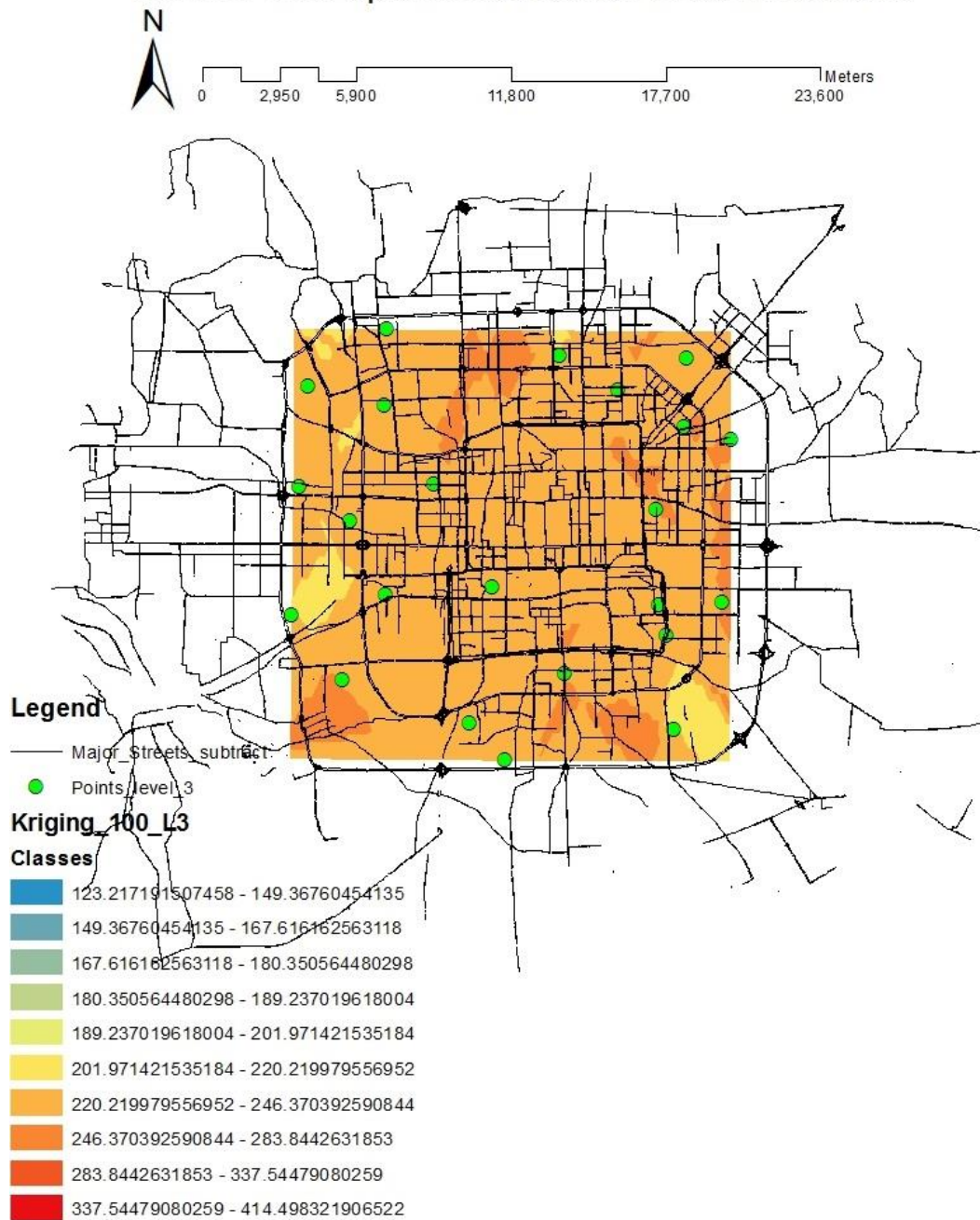
The concentrations of $PM_{5.0}$ at 33.6m distributed similarly to the concentrations of $PM_{5.0}$ at surface (Figure 18b, Figure 29c), they decreased from the south to the north in Beijing. However, the concentrations of $PM_{5.0}$ at 11.2m and 22.4m decreased from the southwest to the northeast of Beijing (Figure 29a, b). By contrast, the concentrations of $PM_{5.0}$ at 44.8 decreased from the southeastern part to the northwestern part of Beijing in winter 2015 (Figure 29d).

11.2m PM10 Spatial Distribution in Summer 2015



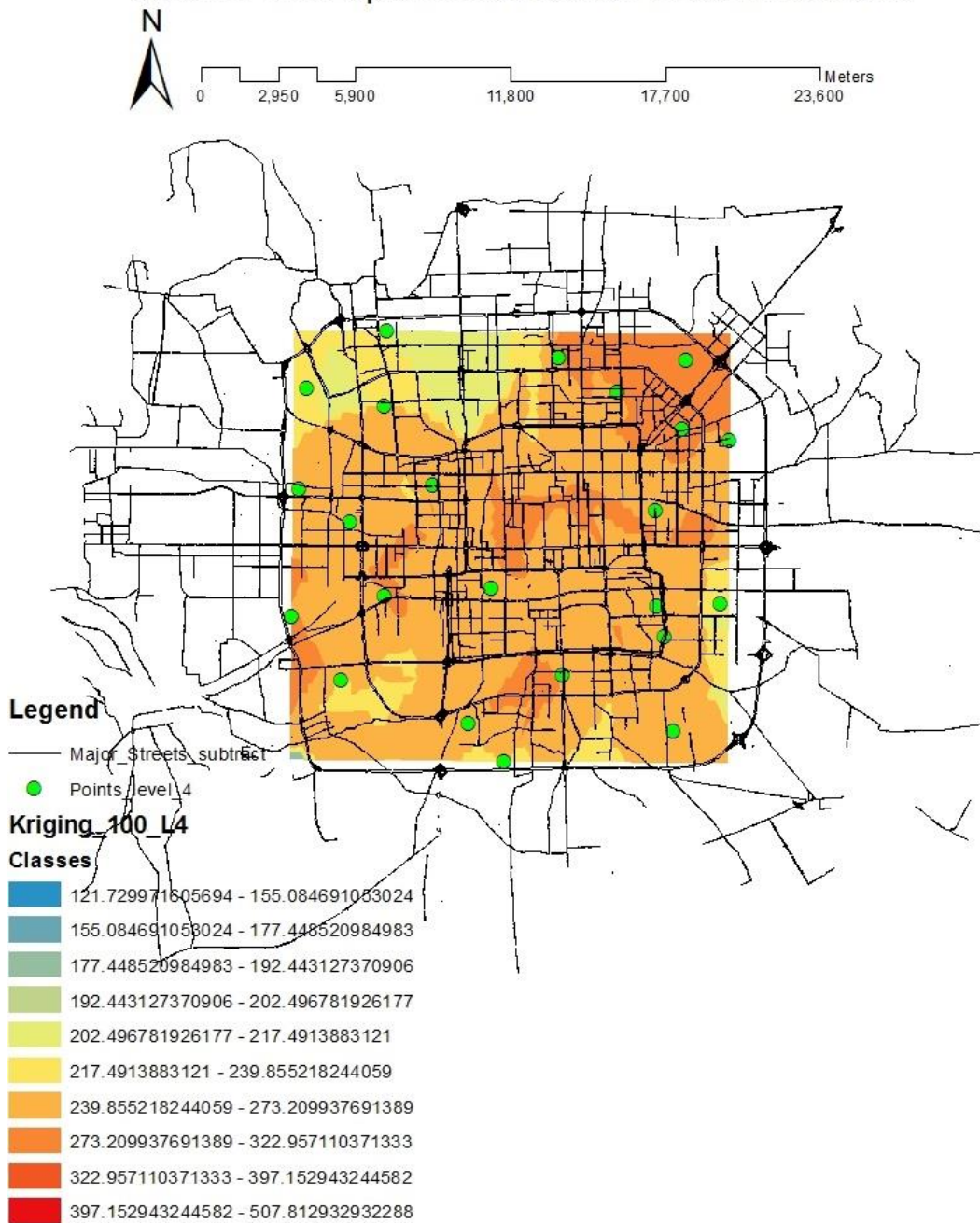
a)

22.4m PM10 Spatial Distribution in Summer 2015

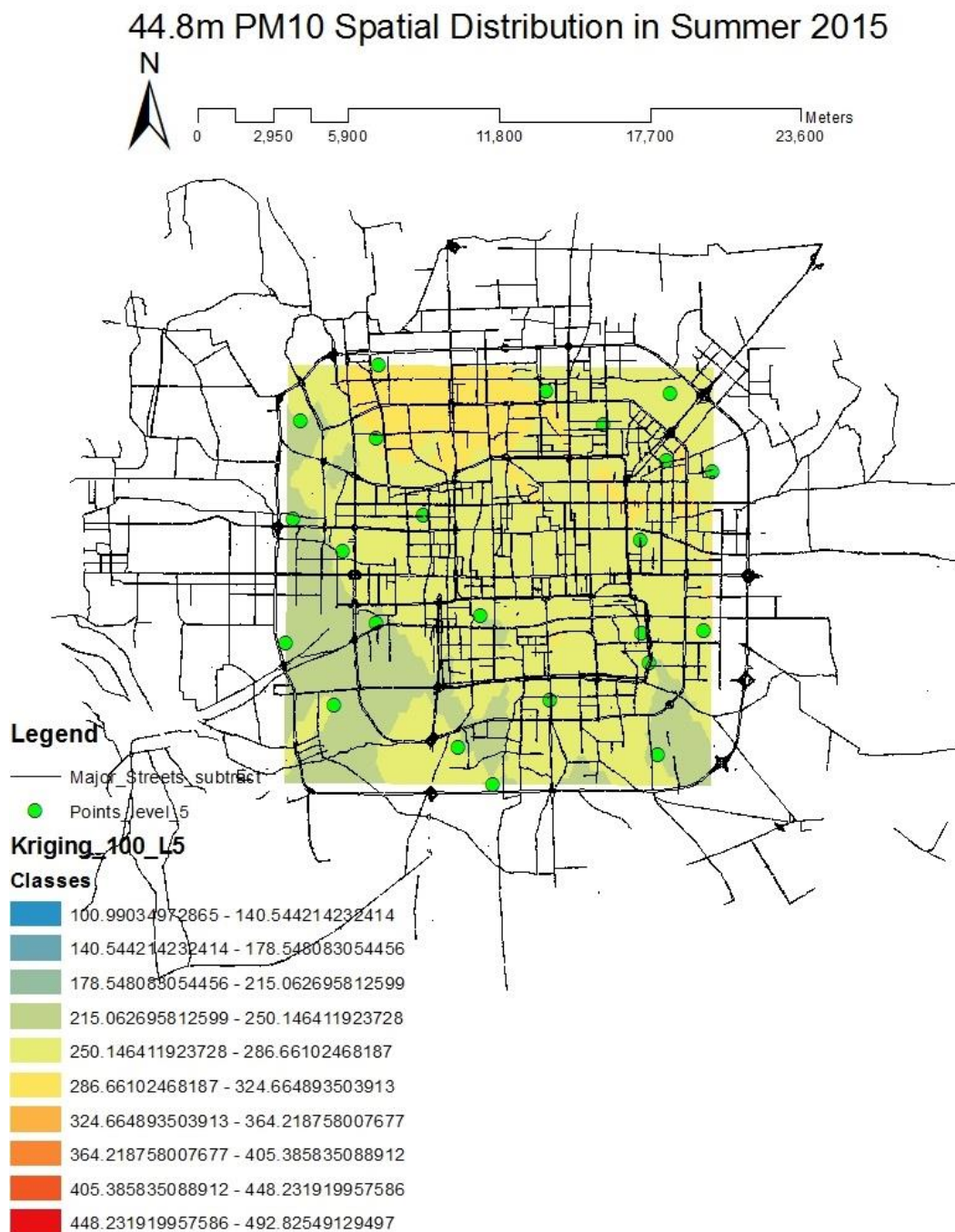


b)

33.6m PM10 Spatial Distribution in Summer 2015



c)

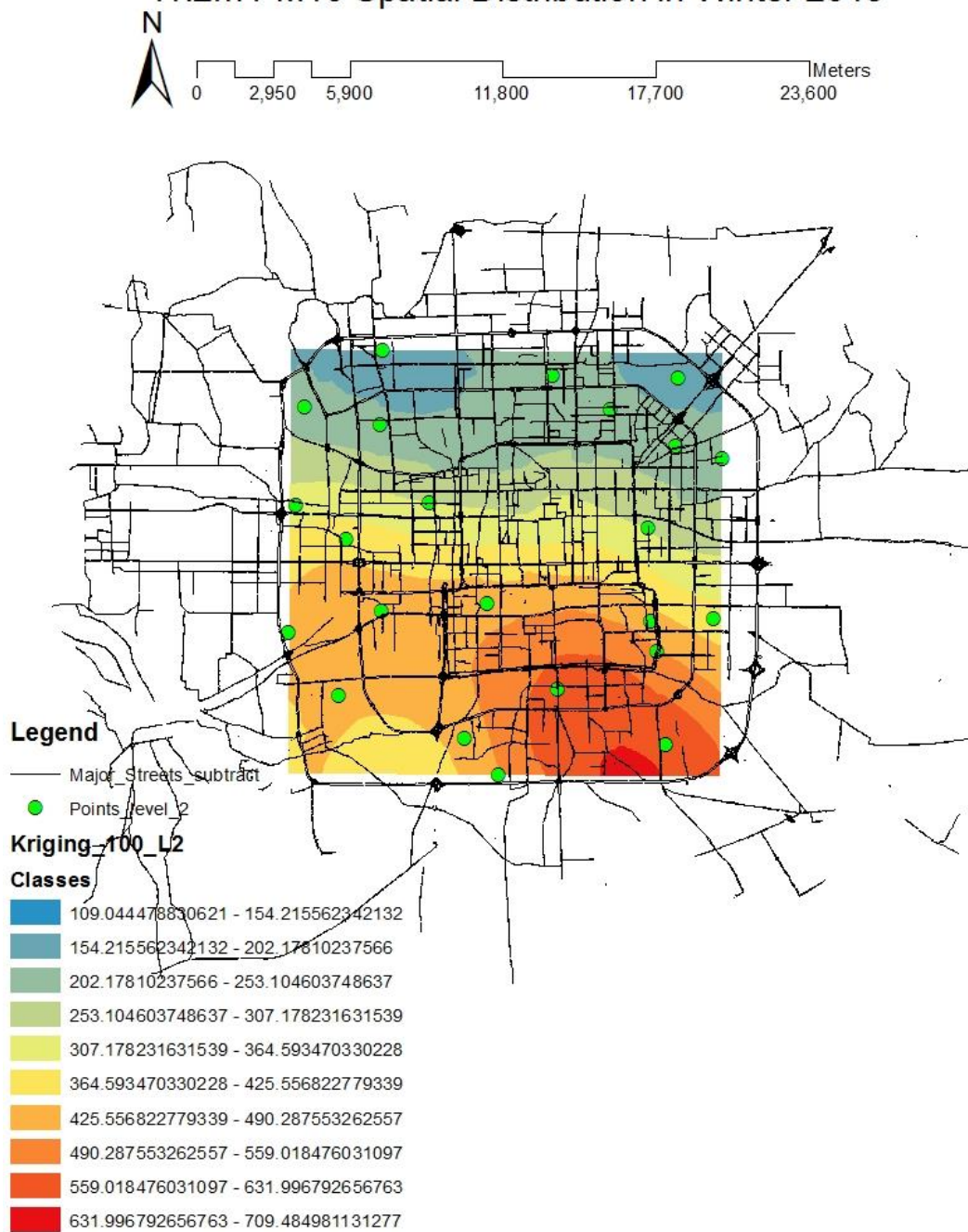


d)

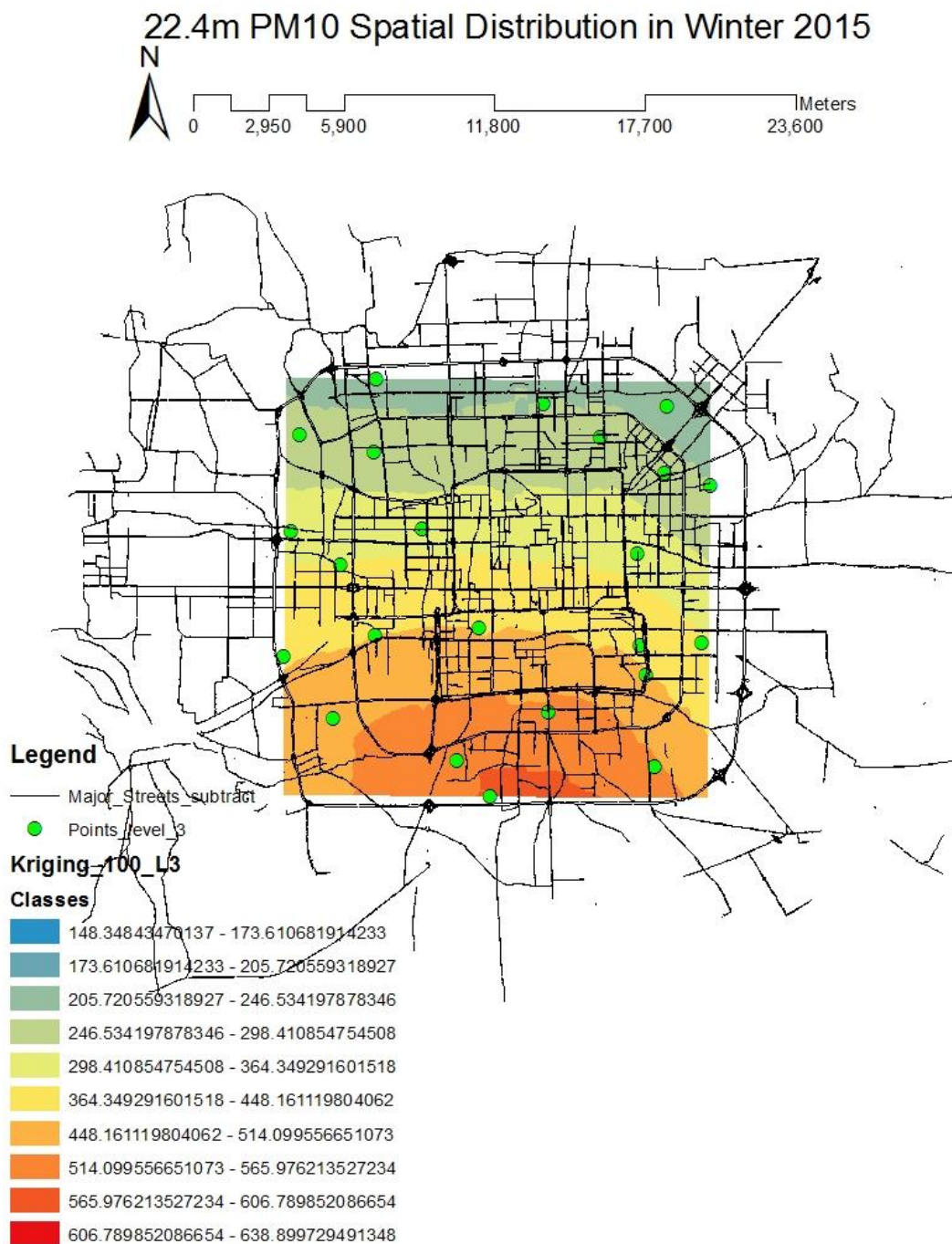
Figure 30: PM₁₀ Spatial Distribution Map in Summer
a)11.2m; b)22.4m; c)33.6m; d)44.8m

At the altitude of 11.2m, the concentrations of PM₁₀ decreased from the northeast to the west, southwest and southeast of Beijing (Figure 30a). However, the concentrations of PM₁₀ at 22.4m, 33.6m and 44.8m distributed homogeneously in summer 2015 (Figure 30b, c, d). The spatial distributions of PM₁₀ concentrations at the four levels of elevations were different from the spatial distribution of PM₁₀ concentrations on the ground.

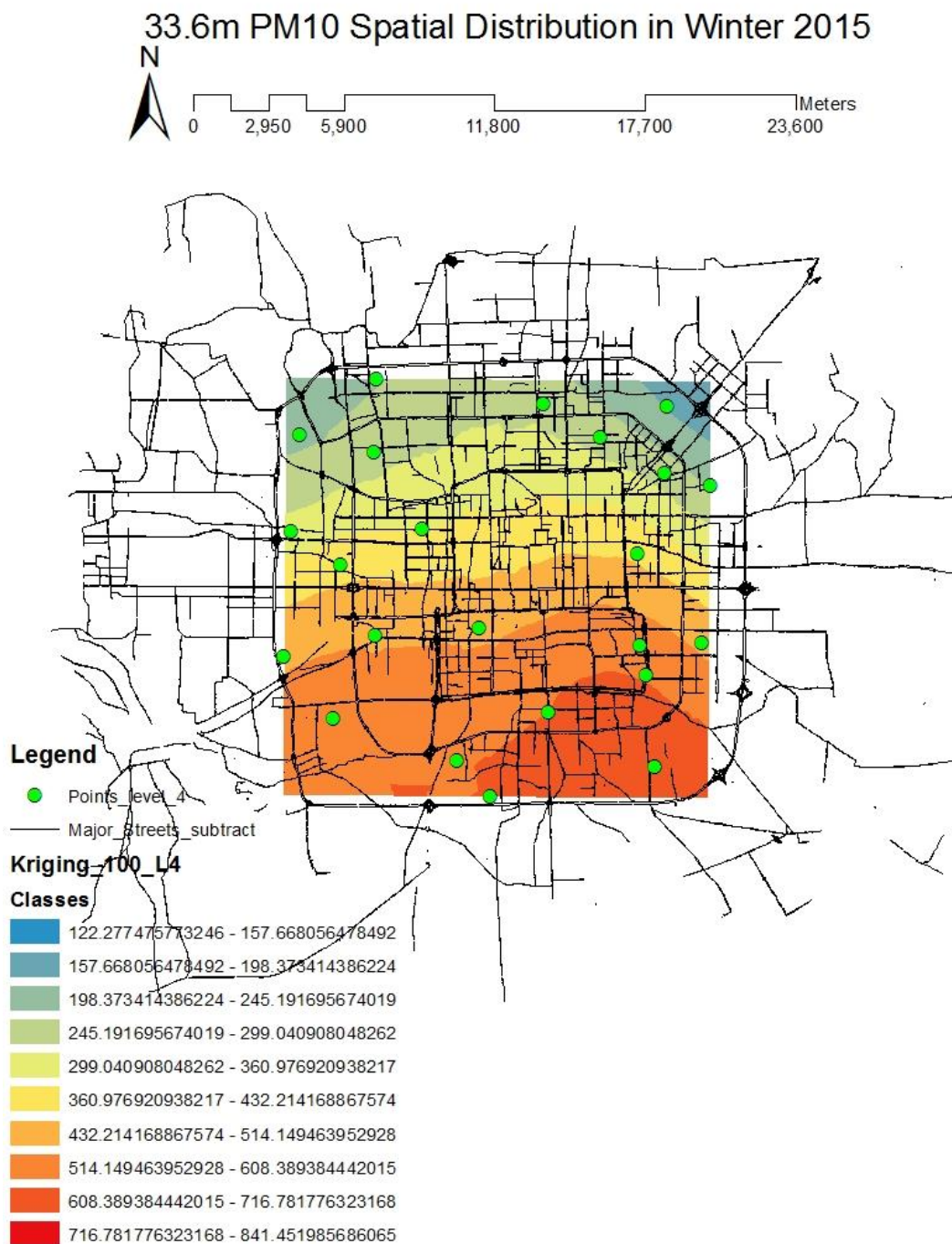
11.2m PM10 Spatial Distribution in Winter 2015



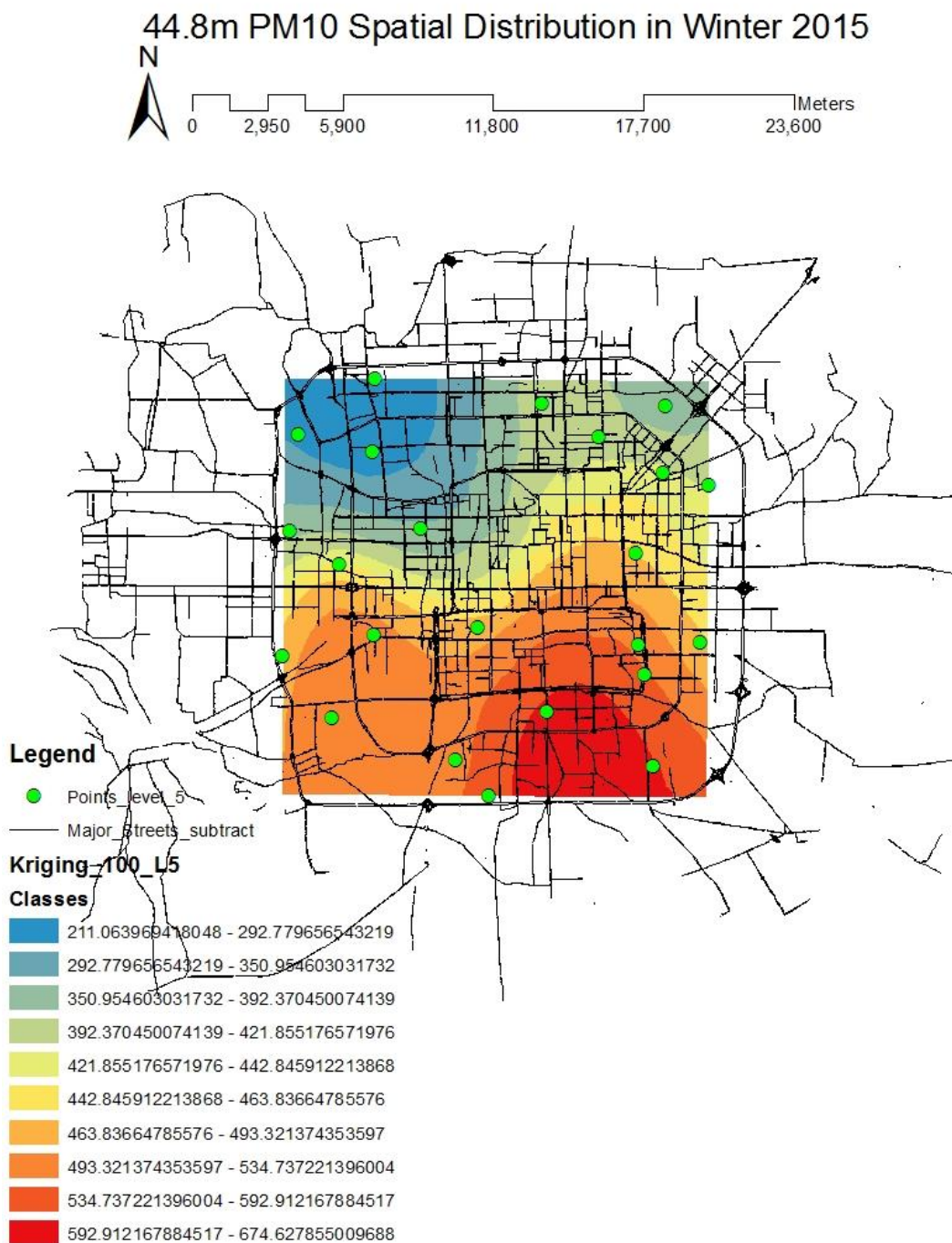
a)



b)



c)



d)

Figure 31: PM₁₀ Spatial Distribution Map in Winter
 a)11.2m; b)22.4m; c)33.6m; d)44.8m

As it is shown in Figure 19b and Figure 31b, the concentrations of PM₁₀ at 22.4m distributed the same as the concentrations of PM₁₀ on the ground. At the altitude of 11.2m, 22.4m and 44.8m, the concentrations of PM₁₀ decreased from the southeast to the northwest of Beijing.

In summary, the spatial distribution maps of each PM concentration at different altitudes show that the concentrations of different size PM had different spatial patterns in vertical direction. The spatial distributions of PM_{0.5} and PM_{1.0} concentrations were the same as their spatial distributions on the ground. However, the spatial distributions of PM_{2.5}, PM_{5.0} and PM₁₀ concentrations were different from their spatial distributions on the ground. This could be caused by the various factors, in particular, meteorological factors.

4.2.3 Spatial Distributions of Real Property Values

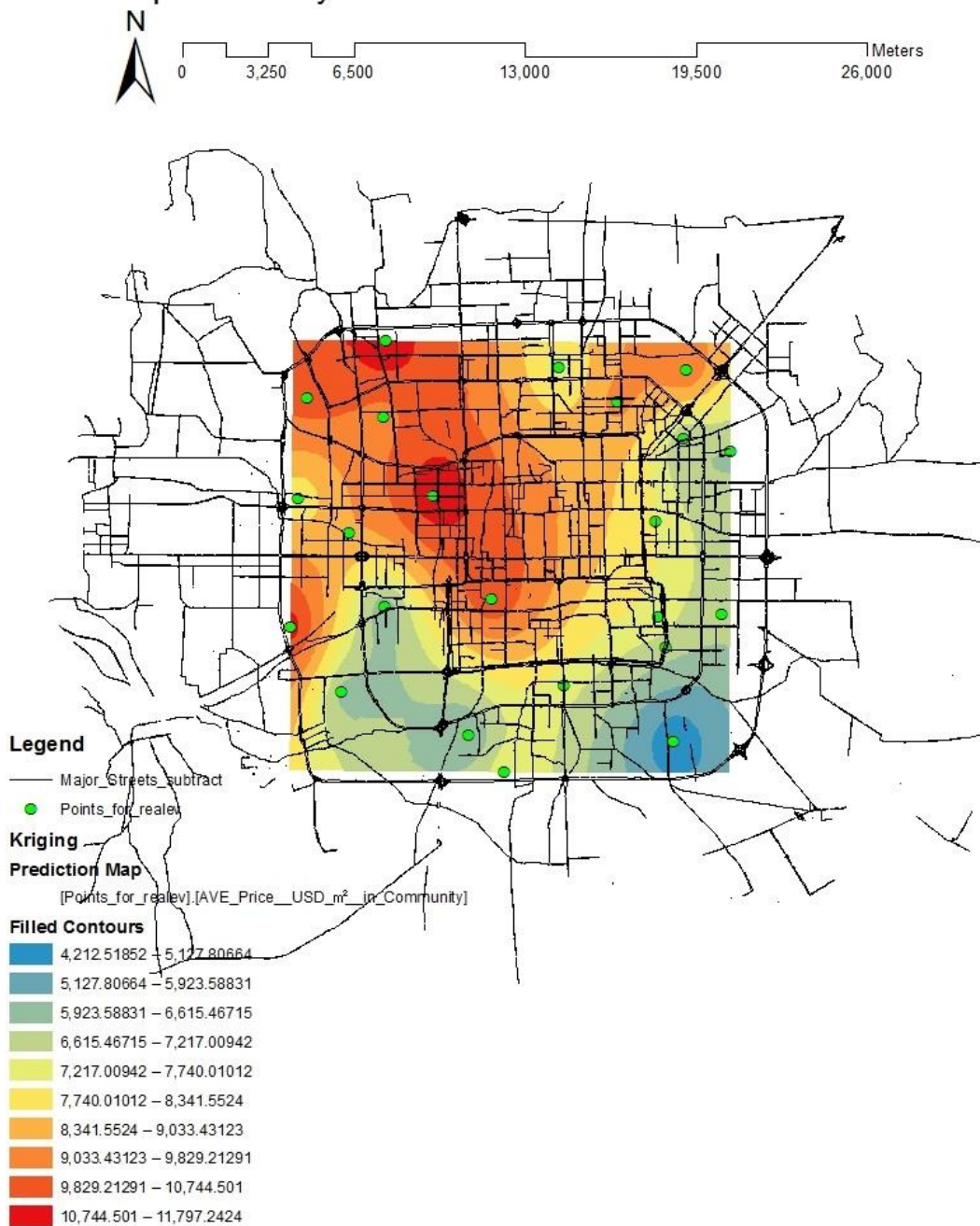
Table 11: Data of Real Property Values (USD/m²)

	June 2015	December 2015
Mean	8188.75	8778.47
Highest Value	11797.24	14442.85
Lowest Value	4212.52	4892.08

According to Table 11, the average values of real property at the twenty-three sites was 8188.75USD/m² in June 2015 and 8778.47USD/m² in December 2015. Figure 32 shows

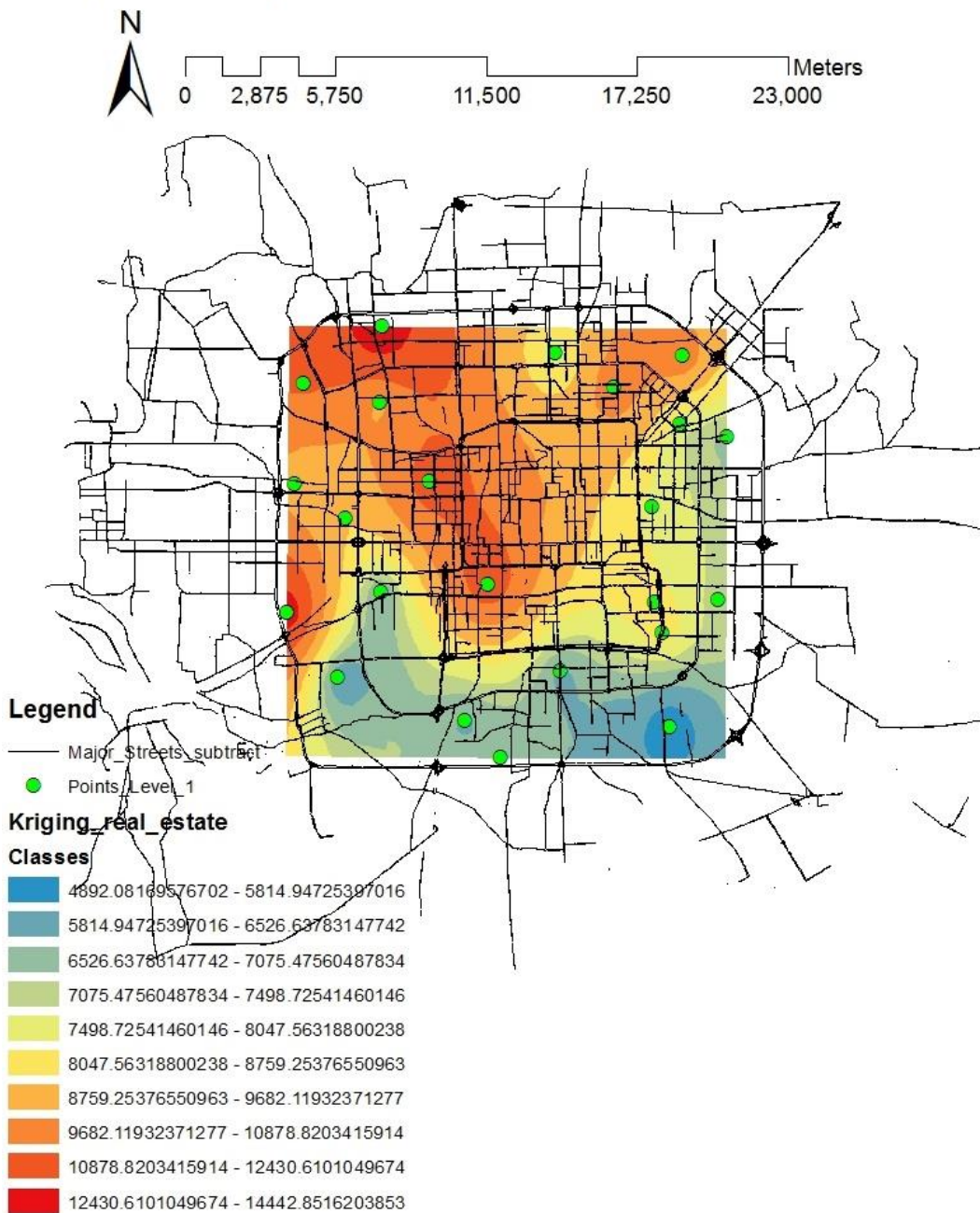
the spatial distributions of real property values in June (Figure 32a) and December (Figure 32b) 2015. Based on the figure, the spatial distribution of real property values in June 2015 were the same as the real property values in December 2015. The high values appeared in the central and northwestern part of Beijing urban area both in June and December 2015; and the real property values decreased from the northwest to the southeast of Beijing.

Spatial Analysis of Real Estate Value in June 2015



a)

Spatial Analysis of Real Estate Value in December 2015



b)

Figure 32: Spatial Distribution of Real Property Value
a)June, b)December

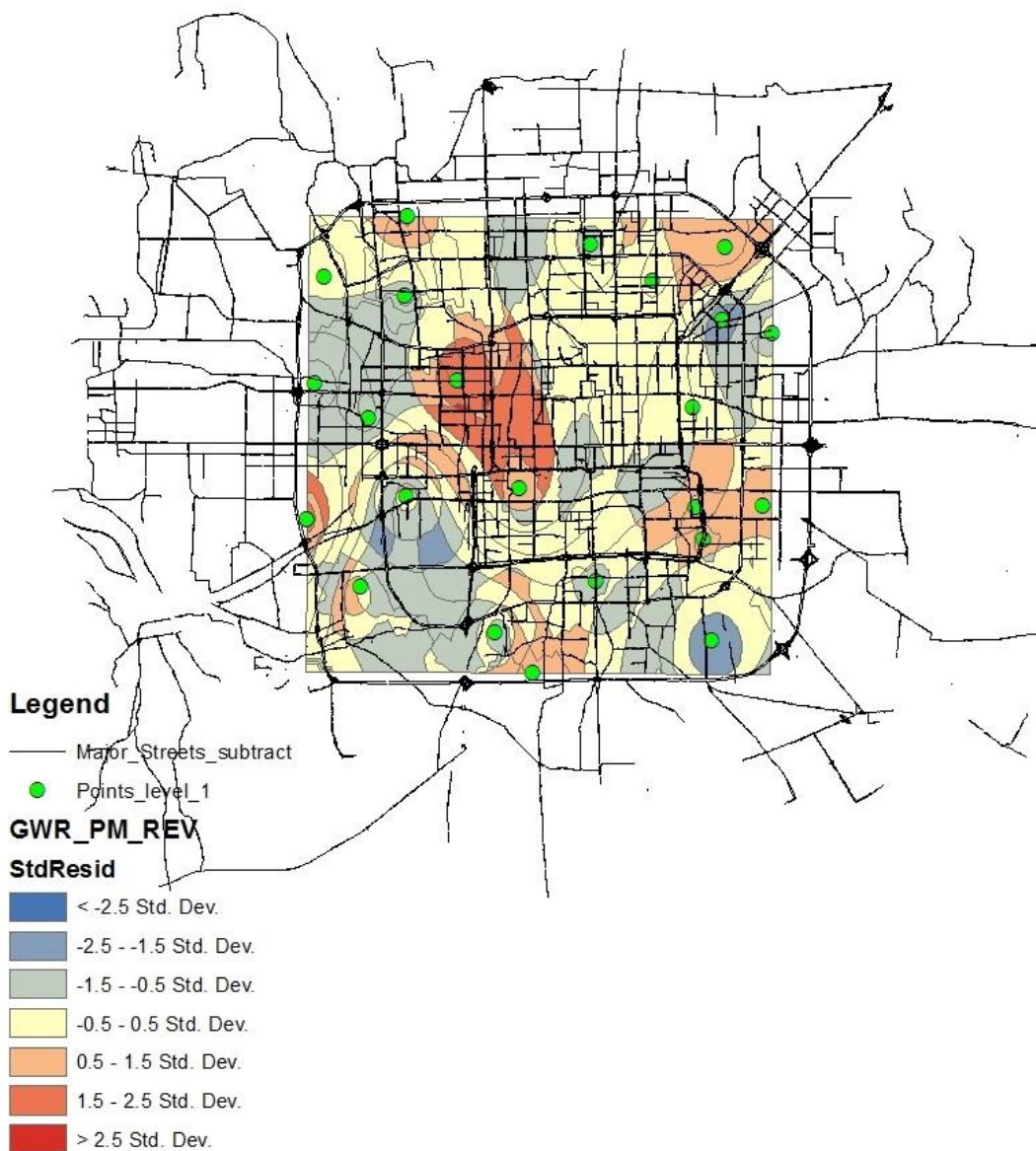
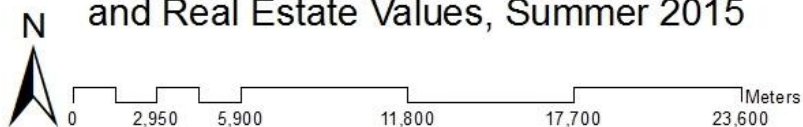
4.2.4 Spatial Relations to Distributions of Air Particulate Pollution and Real Property Values

The Geographically Weighted Regressions (GWR) for each of the five particle concentrations and the real property values in summer 2015 (Figure 33a) and winter 2015 (Figure 33b) were conducted. Condition numbers (CN) are diagnostic evaluators of local collinearity; the values of CN must be smaller than 30 in order to achieve a valid geographic regression (ArcMap, 2016).

The concentrations of PM had a small negative coefficient (-2.18) on average in summer, and they also had a relative small negative coefficient (-3.79) on average in winter in the study region with real property data (Figure 33). The coefficients represent the strength and type of relationship between the air particulate pollution and the real property values. The negative coefficients represent they had negative relationships and the small coefficients indicate these varieties had the weak relationships. The PM concentrations impose a negative impact on the real property values in the study area. The reported highest CN of total PM concentrations and real property values in summer is 7.53 and that in winter is 9.03. The results suggest that the concentrations of PM have a negative impact on real property values in the region, but they do not have causal relationship, that is to say, air particulate pollution is not a criterion of real estate choice. The mean of local

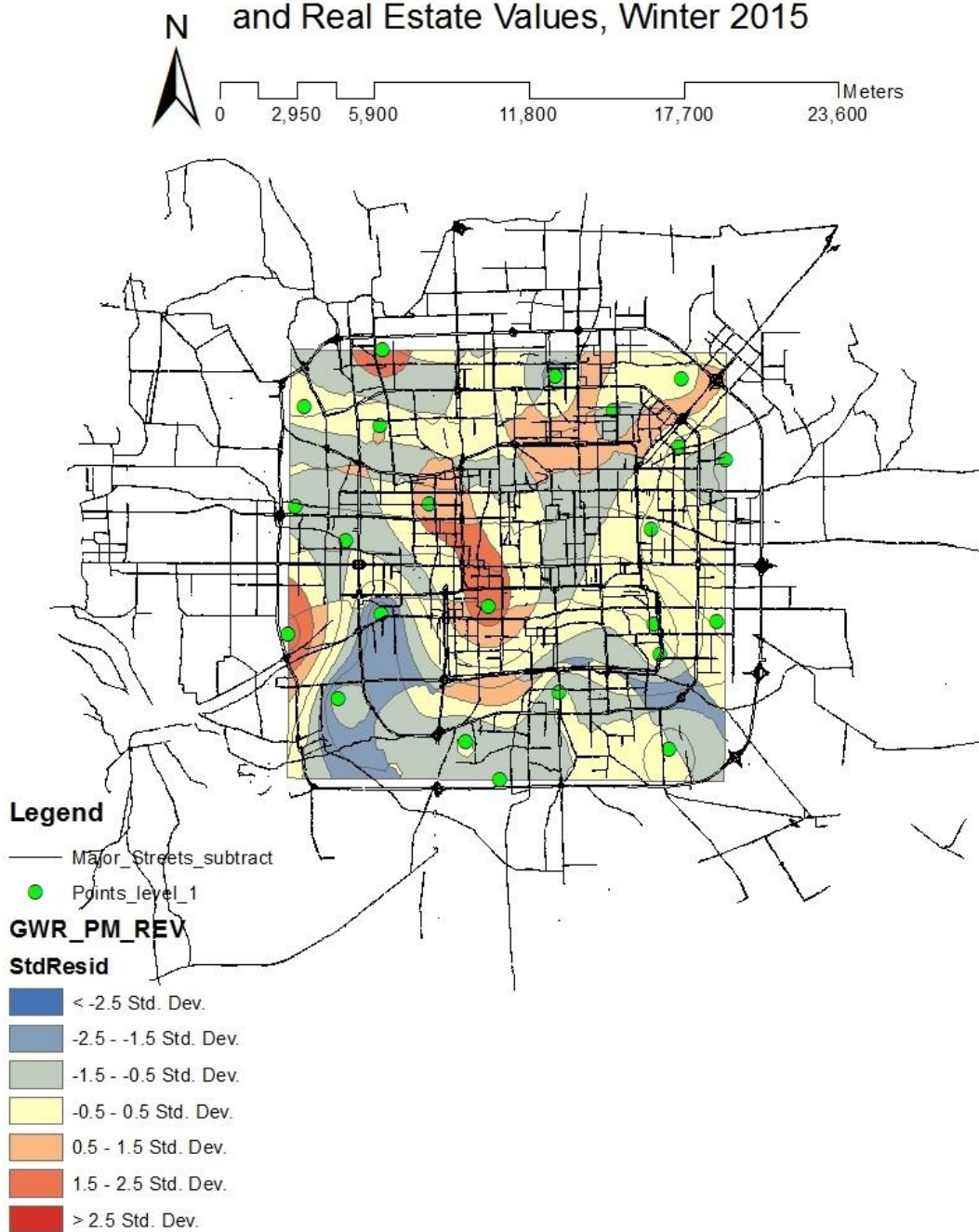
R^2 equals to 0.21 (summer) and 0.17 (winter) The low values indicate that both the two local models are performing poorly. Because of the limited field data of real property values, the current prediction of GWR model might not be accurate. In the future, more real property data and more localized impact analyses of particulate matter concentrations on real property values are needed.

GWR Map of Total PM (\leq PM10) Concentrations and Real Estate Values, Summer 2015



a)

GWR Map of Total PM (\leq PM10) Concentrations and Real Estate Values, Winter 2015



b)

Figure 33: GWR Regression Residual Map
a)summer, b)winter

5. Conclusion

5.1 Temporal Distributions of Air Particulate Pollution

According to the data of field survey, the PM concentrations are significantly different at the different time periods in 10 hours. The trend of PM_{0.5} and PM_{1.0} in 10 hours displayed similar with the trend of PM_{2.5} at both the western part (Yiyuanju) and the eastern part (Shuixingyuan) of Beijing. In addition, the temporal change of PM_{5.0} concentrations displayed the same trend as PM₁₀ concentrations at both the west (Yiyuanju) and the eastern part (Shuixingyuan) of Beijing. Based on the different temporal distributions of PM concentrations, two temporal profiles (Yiyuanju Profile and Shuixingyuan Profile) were conducted in order to normalize the field survey data collected at different times in a day of the twenty-three vertical profiles.

5.2 Two Dimensional (2D) Spatial Distributions of air particulate and Real Property

Values

The field survey shows that PM concentrations are very high both in summer and winter 2015 in Beijing. In this study, the concentrations of PM_{0.5}, PM_{1.0}, PM_{2.5} and PM_{5.0} similarly distributed in summer 2015 in Beijing urban area: the concentrations in the east of Beijing was higher than the concentrations in the west of Beijing; while, the concentrations of PM₁₀ were higher in the northeastern part and southwestern part of

Beijing than the northwestern part and southeastern part of Beijing in summer 2015. In winter 2015, the concentrations of all size PM decreased from the south to the north of Beijing, that is to say, they may had the same sources in the south of Beijing. The spatial distribution of real property values in June 2015 were the same as the spatial distribution of real property values in December 2015. In 2015, the high real property values appeared in the central and northwestern part of Beijing urban area.

Based on the two GWR analysis of air particulate pollution and real property values in the year of 2015 (summer and winter), we found that the total concentrations of PM have some impact on real property values in Beijing urban area, but there is no significant relationship between the two factors, or in other words, they do not have causal relationship. Air particulate pollution is not a criterion of real estate choice. However, the limited field data of real property values may be the reason of the inaccurate prediction of GWR models. Tang et al. (2009) conducted GWR models for analyzing the spatial relationships of air particulate and respiratory diseases in Beijing. They found that spatial concentrations of $PM_{0.5}$, $PM_{1.0}$, and $PM_{3.0}$ have positive impacts on occurrences of residential respiratory diseases in 2008.

5.3 Three Dimensional (3D) Spatial Distributions of Air Particulate Pollution

The vertical distribution of PM concentrations in summer were different from it is in winter. The concentrations of PM_{0.5} did not have significant differences as the elevation increases both in summer and winter 2015; PM_{1.0} concentrations distributed similarly in vertical direction in summer and winter. The highest concentrations of PM_{2.5} and PM_{5.0} appeared on the ground in summer, while the highest concentration of PM_{2.5} and PM_{5.0} appeared at 44.8m in winter. The concentrations of PM₁₀ decreased from the ground to 22.4m and then increased from 22.4m to 44.8m in summer; and they decreased from the ground to 11.2m and then increased to 44.8m in winter. The three-dimensional spatial distribution maps show that the concentration of each PM size in vertical direction had different spatial patterns. The concentrations of PM_{0.5} and PM_{1.0} at the four levels of elevations distributed the same as their spatial distributions on the ground; while, the concentrations of PM_{2.5}, PM_{5.0} and PM₁₀ were different from their spatial distributions on the ground.

5.4 The Further Research of Studying Spatial Relationships of Air Particulate

Pollution and Real Property Values

In this research, we also analyzed the spatial relationships of LULC and the concentrations of air particulate pollution. According to Figure 34 and Figure 35, the blue color represents rivers; black color represents streets and highways; grey color represents

buildings; and green color represents vegetation. The major land use in Beijing urban area within the “Fourth Ring Road” is residential and commercial buildings (Figure 34). By contrast, vegetation cover occupies the major percentage of land use if entire Beijing municipal jurisdiction is accounted (Figure 35). The vegetation distribution in the western and northwestern parts of Beijing may be one of reasons for the relative low concentrations of some particulate matter (such as $PM_{0.5}$) in the west of Beijing. In addition, the high real property values appeared in the central and northwestern part of Beijing urban area that may also because of the vegetation distribution. More evidences (such as the area or percentage of vegetation) need to be provided to run a spatial regression to test the possible relationships of LULC, PM concentrations and real property values in the future.

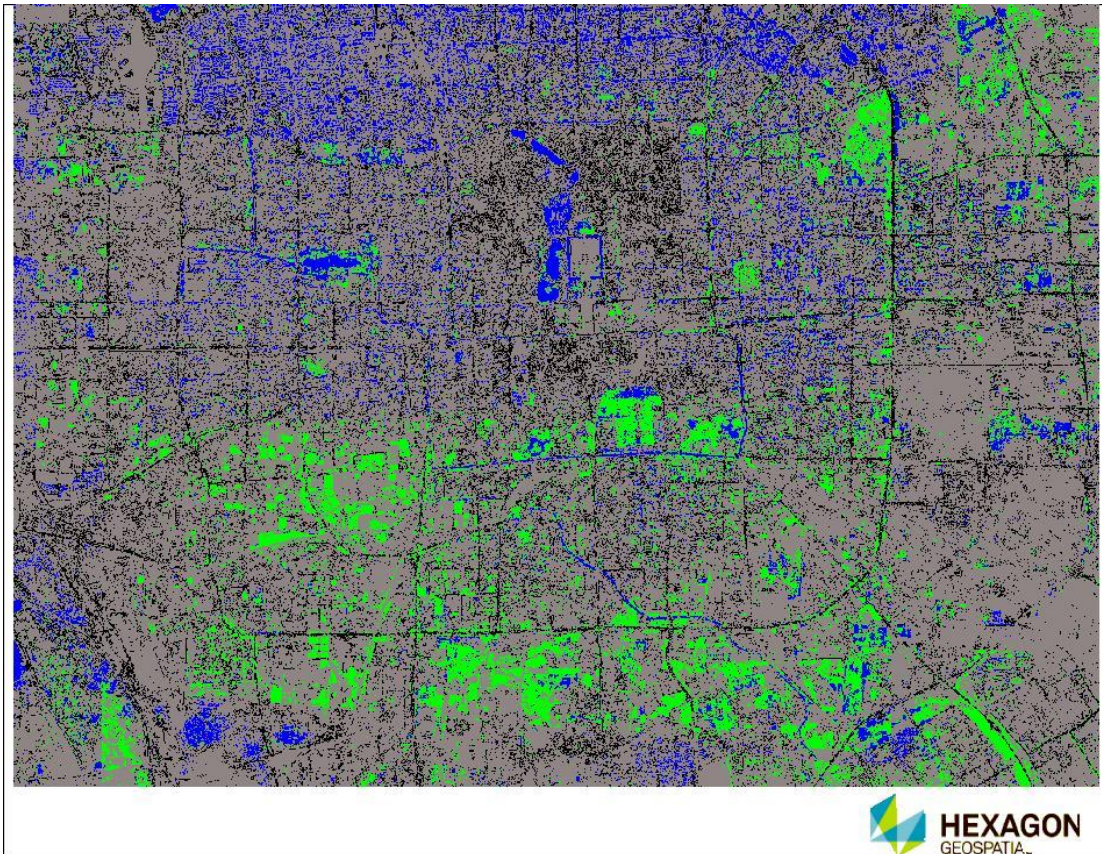


Figure 34: LULC Classification of Beijing Urban Area

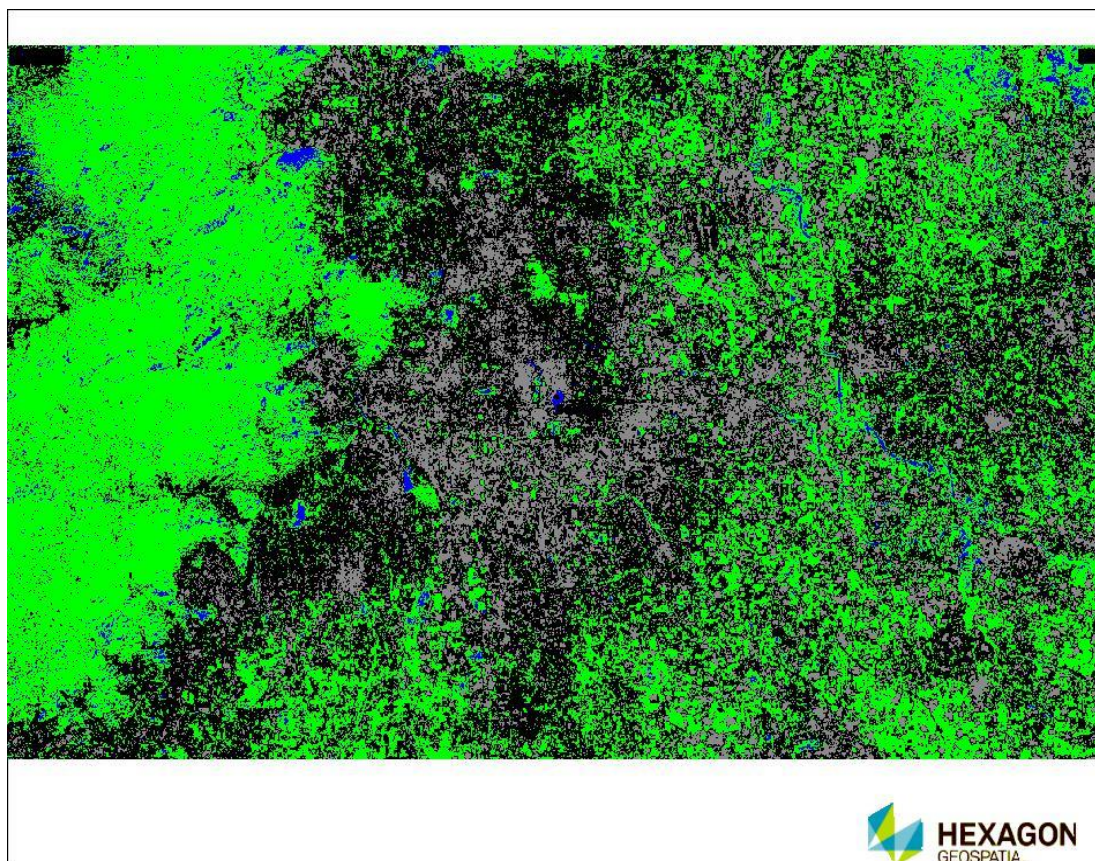


Figure 35: LULC Classification of Beijing (including urban and suburban areas)

5.5 Limitations of the Study

Owing to only one laser particle counter we have, concentrations of air particulate pollutions in the twenty-three sampling profiles in the urban districts in Beijing were not recorded in the same time and same day. However, data collected in 10 hours in one day were utilized to standardize the data collected in the twenty-three profiles. In the future, more air particulate pollution and more real property data should be analyzed for studying the spatial relationships between air particulate pollution and real property values.

6. Bibliography

Adel, G.A., Bamdad, R.Z., and Mahdi, B.M. (2016) *Effects of air pollution on human health and practical measures for prevention in Iran*. J Res Med Sci. 2016; 21: 65.

AirNow (2014) *Particle Pollution (PM)* Retrieved from: <https://www.airnow.gov/index.cfm?action=aqibasics.particle>, Last accessed: 6 September 2017.

Ambient (outdoor) air quality and health (2016) *WHO* Retrieved from: <http://www.who.int/mediacentre/factsheets/fs313/en/>, Last accessed: 17 March 2018

Anderson, J.R., Hardy, E.E., Roach, J.T. and Witmer, R.E. (1976) *A Land Use and Land Cover Classification System for Use with Remote Sensor Data*. Geological Survey Professional Paper 964.

Aneja, V.P., Wang, B., Tong, D.Q., Kimball, H., Steger, J. (2006) *Characterization of major chemical components of fine particulate matter in North Carolina*. J Air Waste Manag Assoc. 56(8): 1099-107.

ArcMap (2016) *Interpreting GWR results*. Retrieved from: <http://desktop.arcgis.com/en/arcmap/10.3/tools/spatial-statistics-toolbox/interpreting-gwr-results.htm> Last accessed: 15 March 2018.

Bank of China (2015) Retrieved from: <http://srh.bankofchina.com/> Last accessed: 17 March 2017.

Barrett, E.W. and Ben-Dov, O. (1967) *Application of the Lidar to Air Pollution Measurements*, Journal of Applied Meteorology 6: 500-515.

Beijing Environmental Statement (2015), *Beijing Municipal Environmental Protection Bureau* Retrieved from: <http://www.bjepb.gov.cn/> Last accessed: 17 March 2017.

Beijing Statistic Bureau (2010) Retrieved from: <http://www.bjstats.gov.cn/English/> Last accessed: 17 March 2017.

Bernosky, J.D. and Vermette, S.J. (2012) *Temporal Characteristics of Airborne Particulate Matter in Phnom Penh, Cambodia*. EnvironmentAsia 5(2), 11-15.

Bezzi, M. and Vitti, A. (2005) *A Comparison of Some Kriging Interpolation Methods for the Production of Solar Radiation Maps*. Geomatic Work.

Bohling, G. (2005) *Kriging* Retrieved from:
<http://people.ku.edu/~gbohling/cpe940/Kriging.pdf>, Last accessed: 15 March 2017.

Brunsdon, C.F., Fotheringham A.S., and Charlton, M.E. (1996) *Geographically Weighted Regression: A Method for Exploring Spatial Non-stationarity*. Geographical Analysis 28: 281-298.

Carlson, T.N.; Azofeifa, S.G.A. (1999) *Satellite Remote Sensing of land Use changes in and around San Jose', Costa Rica*. Remote Sensing of Environment 1999 (70)247–256.

CASA. and ERG. (2008) *3-D Map of Air Pollution in London* Retrieved from:
<http://www.londonair.org.uk/london/asp/virtualmaps.asp?view=maps>, Last accessed: 15 March 2017.

Case, K.E., and Shiller, R.J. (1990) *Forecasting prices and Excess Returns in the Housing Market*, AREUEA Journal, 18(3): 253-273.

Chan, Y., Xu, D., Li, Y.S., Wong, K.H., Ding, L., Chan Y., Cheng, X. H. (2005) *Characteristics of vertical profiles and sources of PM_{2.5}, PM₁₀ and carbonaceous species in Beijing*. Atmospheric Environment 39, 5113–5124.

Charlton, M., Fotheringham, A.S. (2009). *Geographically weighted regression white paper*. National Centre for Geocomputation, Maynooth. 5-8.

Chen, B., Yang, S., Xu, X., Zhang, W. (2013) *The impacts of urbanization on air quality over the Pearl River Delta in winter: roles of urban land use and emission distribution*. Theoretical and Applied Climatology 117, 1-2, pp 29-39.

Chen, T., He, J., Lu, X., She, J., Guan, Z. (2016) *Spatial and Temporal Variations of PM_{2.5} and Its Relation to Meteorological Factors in the Urban Area of Nanjing, China*. International Journal of Environmental Research and Public Health 13(9): 921.

Chen, Y., Ebenstein, A., Greenstone, M., Li, H., (2013) *Evidence on the impact of sustained exposure to air pollution on life expectancy from China's Huai River policy*.

Proc. Natl. Acad. Sci. 110, 12936e12941.

Chen, Z., Ge, S., Zhang, J. (1994) *Measurement and analysis for atmospheric aerosol particulates in Beijing*. Research of Environmental Sciences 7 (3): 1–9 (in Chinese with abstract in English).

Cheng, Y., He, K., Du, Z., Zheng, M., Duan, F. and Ma, Y. (2014) *Humidity plays an important role in the PM 2.5 pollution in Beijing*, Environmental Pollution 197 (2015) 68-75.

China Air Quality Standards (2016) *Ministry of Environmental Protection* Retrieved from: <https://www.transportpolicy.net/standard/china-air-quality-standards/> Last accessed 17 March 2018 GB 3095-2012, phased-in 2012-2016

China's National People's Congress (2016), *Xinhuashe* Retrieved from: http://www.xinhuanet.com/politics/2017lh/2017-03/16/c_1120638890.htm Last accessed: 17 March 2017.

ChinaHighlights (2012) Retrieved from: <http://www.chinahighlights.com/beijing/map.htm> Last accessed: 15 March 2017.

CHINATouristMaps (2010) *Map of Beijing Districts, Beijing Regions Map* Retrieved from: <http://www.chinatouristmaps.com/provinces/beijing.html>, Last accessed: 15 March 2017.

Chivakul, M., Lam W. R., Liu X., Maliszewski W., and Schipke A. (2015) *IMF Working Paper, Understanding Residential Real Estate in China*, 2015 International Monetary Fund WP/15/84.

Colditz, R.R., Schmidt, M., Conrad, C., et al. (2011). *Land cover classification with coarse spatial resolution data to derive continuous and discrete maps for complex regions*. Remote Sensing of Environ, 115: 3264-3275.

Comber, A.J. (2008). *"Land use or land cover?"* J. of Land Use Sci. 3: 199-201.

Corsini K.R. (2009) *Statistical analysis of residential housing price in an up and down real market: a general framework and study of Cobb County, GA* Retrieved from: [https://smartech.gatech.edu/bitstream/handle/1853/31763/Corsini Kenneth R](https://smartech.gatech.edu/bitstream/handle/1853/31763/Corsini%20Kenneth%20R)

200912_mast.pdf Last accessed: 17 March 2017.

Cui, C. (2011) *An Empirical Analysis on the Factors Affecting the Housing Price in Beijing*, Productivity Research 9, 1004-2768.

Dashtpagerdi, M.M., Sadatinejad, S.J., Bidaki, R.Z., Khorsandi, E. (2012) *Evaluation of Air Pollution Trend Using GIS and RS Applications in South West of Iran*, Journal of the Indian Society of Remote Sensing 42(1):179–186.

Deng, C., Ma, Y. and Chiang, Y. (2009) *The Dynamic Behavior of Chinese Housing Prices*, International Real Estate Review 12(2): 121–134.

Deng, X., Li, F., Li, Y., Li, J., Huang, H., Liu, X. (2015) *Vertical distribution characteristics of PM in the surface layer of Guangzhou*. Particuology 20(6): 3-9.

Deligiorgi, D. and Philippopoulos, K. (2011). *Spatial Interpolation Methodologies in Urban Air Pollution Modeling: Application for the Greater Area of Metropolitan Athens, Greece*, Advanced Air Pollution, Dr. Farhad Nejadkoorki (Ed.), InTech, DOI: 10.5772/17734.

Development here will follow that of Pierre Goovaerts, 1997, *Geostatistics for Natural Resources Evaluation*, Oxford University Press.

Donlon, K. (2007) *Using GIS to Improve the Services of a Real Estate Company*. Volume 10, Papers in Resource Analysis. 11 pp. Saint Mary's University of Minnesota Central Services Press. Winona, MN Retrieved from <http://www.gis.smumn.edu> Last accessed: 15 March 2017.

EPA (2012), *National Ambient Air Quality Standards (NAAQS) for Particulate Matter (PM)*, Retrieved from: <https://www.epa.gov/pm-pollution/2012-national-ambient-air-quality-standards-naaqs-particulate-matter-pm> Last accessed: 25 January 2017.

EPA (2013) *Health and Environmental Effects of Particulate Matter (PM)* Retrieved from: <https://www.epa.gov/pm-pollution/health-and-environmental-effects-particulate-matter-pm> Last accessed: 10 April 2018

EPA Particulate Matter (2016) *Particulate Matter (PM) Pollution*. Retrieved from:

<https://www3.epa.gov/pm/https://www3.epa.gov/pm/> Last accessed: 17 March 2017.

EPA (2017) *Positive Matrix Factorization Model for environmental data analyses* Retrieved from:

<https://www.epa.gov/air-research/positive-matrix-factorization-model-environmental-data-analyses> Last accessed: 31 August

Fangjia (2015) Retrieved from: <http://bj.fangjia.com/> Last accessed: 17 March 2017.

Fotheringham, A.S., Brunson C. and Charlton M. (2002) *Geographically Weighted Regression: The Analysis of Spatially Varying Relationships*, Wiley ISBN: 978-0-471-49616-8.

Fisher Box, Joan (1987). *Guinness, Gosset, Fisher, and Small Samples*. *Statistical Science* 2 (1): 45–52.

Giri, D., Krishna Murthy, V. and Adhikary, P.R. (2008) *The Influence of Meteorological Conditions on PM10 Concentrations in Kathmandu Valley*. *Int. J. Environ. Res.*, 2(1): 49-60

GISGeography (2017) Retrieved from: <http://gisgeography.com/> Last accessed: 17 March 2017.

Glaeser, E., Huang, W., Ma, Y. and Shleifer, A. (2016) *A real estate boom with Chinese characteristics*, *Journal of Economic Perspectives* 13(1) 93-116.

Gilliland, F. Avol, E., Kinney, P., Jerret, M., Dvonch, Y., Lurmann, F., Buckley, T., Breysse, P., Keeler, G., Villers, T., McConnel, R. (2005) *Air pollution exposure assessment for epidemiologic studies of pregnant women and children: lessons learned from the Centers for Children's Environmental Health and Disease Prevention Research*. *Environ. Health Perspect.* 113, 1447–1454.

Goovaerts P., (1997) *Geostatistics for Natural Resources Evaluation*, Applied Geostatistics Series, Oxford University Press, New York.

Gorai, A.K., Tuluri, F., Tchounwou, P.B. (2014) A GIS Based Approach for Assessing the Association between Air Pollution and Asthma in New York State, USA, *Int. J. Environ. Res. Public Health* 11, 4845-4869

GrayWolf Sensing Solutions (2011) *Advanced Environmental Instrumentation* Retrieved from: <http://www.wolfsense.com/> Last accessed: 17 March 2017.

Guan, W. J., Zheng, X.Y., Chung, K.F., Zhong, N.S (2016) *Impact of air pollution on the burden of chronic respiratory diseases in China: time for urgent action*. *Lancet* 388, 1939e1951.

Guerschman J.P.; Paruelo, J.M.; Bela, C.D.; Giallorenzi, M.C.; Pacin, F. (2003) *Land cover classification in the Argentine Pampas using multi-temporal Landsat TM data*. *International Journal of Remote Sensing* 24, 3381–3402.

Gundogdu, K.S. and Guney, I. (2007) *Spatial analyses of groundwater levels using universal kriging*. *Journal of Earth System Science*, 116, 49-55.

Guo, S., Hu, M., Zamora, M.L., Peng, J., Shang, D., Zheng, J., Du, Z., Wu, Z., Shao, M., Zeng, L., Molina, M.J., Zhang, R. (2014) *Elucidating severe urban haze formation in China*. *Proc. Natl. Acad. Sci. U. S. A.* 111, 17373e17378.

Habre, R., Coull, B., Moshier, E., Godbold, J., Grunin, A., Nath, A. (2014) *Sources of indoor air pollution in New York city residences of asthmatic children*. *J Expo Sci Environ Epidemiol.* 24: 269–78.

Hadjimitsis, D.G., Retalis, A. and Clayton, C.R.I. (2002) *Water, Air and Soil Pollution, Focus 2*: 631.

Han, H., Yang, C. and Song, J. (2015) *Scenario Simulation and the Prediction of Land Use and Land Cover Change in Beijing, China*. *Sustainability* 2015, 7, 4260-4279

He H., Wang W. and Zeng Q. (2001) *The Application of Geographic Information System on Telecommunication Cable Management System*. *Wuhan University Journal of Natural Sciences* 6(2): 482-485.

He, K., Yang, F., Ma, Y., Zhang, Q., Yao, X., Chan, C., Cadle, S., Chan, T., Mulawa, P. (2001) *The characteristics of PM_{2.5} in Beijing, China*. *Atmospheric Environment* 35(2001): 4959-4970.

History (2009), *Water and Air Pollution* Retrieved from:

<http://www.history.com/topics/water-and-air-pollution> Last accessed: 17 March 2017.

Hoek, G., Beelen, R., Hoogh, K., Vienneau, D., Gulliver, J., Fischer, P., Briggs, D. (2008) *A review of land-use regression models to assess spatial variation of outdoor air pollution*. Atmos. Environ. 42, 7561–7578.

Hopke, P. K. (2003) *Recent developments in receptor modeling*, J. Chemometr., 17, 255–265, 2003.

Hu, M., Jia, L., Wang, J., Pan, Y. (2013) *Spatial and temporal characteristics of particulate matter in Beijing, China using the Empirical Mode Decomposition method*. Science of The Total Environment 458-460C: 70-80.

Huang, R.J., Zhang, Y., Bozzetti, C., Ho, K.F., Cao, J.J., Han, Y., Daellenbach, K.R., Slowik, J.G., Platt, S.M., Canonaco, F., Zotter, P., Wolf, R., Pieber, S.M., Bruns, E.A., Crippa, M., Ciarelli, G., Piazzalunga, A., Schwikowski, M., Abbaszade, G., Schnelle-Kreis, J., Zimmermann, R., An, Z., Szidat, S., Baltensperger, U., El Haddad, I., Prevot, A.S. (2014) *High secondary aerosol contribution to particulate pollution during haze events in China*. Nature 514, 218e222

Jensen, J.R. & Jensen, R.R. (2013). *Introductory Geographic Information Systems*. Pearson Series

Jerrett, M., Arain, A., Kanaroglou, P., Beckerman, B., Potoglou, D., Sahuvaroglu, T., Morrison, J., Giovis, C. (2005) *A review and evaluation of intraurban air pollution exposure models*. J. Exposure Sci. Environ. Epidemiol. 15, 185–204.

Jerrett, M., Finkelstein, M.M., Brook, J.R., Arain, M.A., Kanaroglou, P., Stieb, D.M., et al. (2009) *A cohort study of traffic-related air pollution and mortality in Toronto, Ontario, Canada*. Environ Health Perspect. 2009; 117:772–7.

Johnson, W.B. (1969) *Lidar Applications in Air Pollution Research and Control*, Journal of the Air Pollution Control Association, 19:3, 176-180.

Lee, B.J., Kim, B., Lee, K. (2014) *Air Pollution Exposure and Cardiovascular Disease*, Toxicol Res. 30(2): 71–75.

Lee, Y.C.; Calori, G.; Hills, P.; Carmichael, G.R. (2002) *Ozone Episodes in Urban Hong*

Kong 1994–1999; Atmos. Environ. 36, 1957-1968.

Lefohn, A.S., Knudsen, H.P., Shadwick, D.S. (2005) *Using Ordinary Kriging to Estimate the Seasonal W126, and N100 24-h Concentrations for the Year 2000 and 2003*. A.S.L. & Associates, 111 North Last Chance Gulch Suite 4A Helena, Montana 59601

Li, S., Williams, G., Guo, Y. (2016) *Health benefits from improved outdoor air quality and intervention in China*. Environ. Pollut. 214, 17e25.

Lillesand, T.M., Kiefer, R.W. (2000) *Remote Sensing and Image Interpretation, Ch. 7, Digital Image Processing*, J. Wiley and Sons, Inc.

Lin C., Meng L. and Pan H. (2001) *Applications and research on GIS for the real estate*. The 22nd Asian Conference on Remote Sensing.

Lim, H.S., MatJafri, M.Z., Abdullah, K. and Wong, C. J. (2009). *Air Pollution Determination Using Remote Sensing Technique, Advances in Geoscience and Remote Sensing*, Gary Jedlovec (Ed.), InTech, DOI: 10.5772/8319. Retrieved from: <http://www.intechopen.com/books/advances-in-geoscience-and-remote-sensing/air-pollution-determination-using-remote-sensing-technique> Last accessed: 15 March 2017.

Li, W. and Wu, J. (2015) *Linking Urban Structure and Air Quality: A Geographically Weighted Regression Model for PM2.5 Concentrations in Beijing*, The 14th International Conference on Computers in Urban Planning and Urban Management (CUPUM 2015), MIT, Cambridge, MA., 7-10 July 2015.

Liu, J. (2013) *Institute of Public and Environmental Affairs* Retrieved from: http://www.old.ipe.org.cn/pollution/news_detail.aspx?id=13464 Last accessed: 17 March 2017.

Liu, Z., Huang S., Hallak R., Liang M. (2016) *Chinese consumers' brand personality perceptions of tourism real estate firms*. Tourism Management 52 (2016): 310-326.

Lozano, A., Usero, J., Vanderlinden, E., Ruez, J., Contreras, J., Navarrete, B., Bakouri, H.E. (2009) *Design of air quality monitoring networks and its application to 2 and O3 in Cordova, Spain*. Microchemical Journal, 93 No. 2, (November 2009), 211-219, 0002-6265X

Luo, W., Taylor, M.C., Parker, S.R. (2008). *A comparison of spatial interpolation methods to estimate continuous wind speed surfaces using irregularly distributed data from England and Wales*. *Int. J. Climatol.* 28: 947–959.

Malm, W.C., Bret A., Schichtel, B.A., Pitchford M.L., Ashbaugh L.L., Eldred R.A. (2004) *Spatial and Monthly Trends in Speciated Fine Particle Concentration in the United States*. *Journal of Geophysical Research.* 109 (D3).

Mann-Whitney U Test Calculator (2018) *Social Science Statistics*.

McDonald-Buller, E.C., Webb, A., Kockelman, K.M., Zhou, B. (2010) *Air Quality Impacts of Transportation and Land Use Policies: A Case Study in Austin, Texas*. *Transportation Research Record No. 2158*: 28-35.

Meike, E. (2016) *Project sky nose* Retrieved from:
<http://yoerik.com/Quest/SkyNose/?src=NuevaQuestNightBrochure> Last accessed: 15 March 2017.

Mercer, L.D., Szpiro, A.A., Sheppard, L., Lindström, J., Adar, S.D., Allen, R.W., Avol, E.L., Oron, A.P., Larson, T., Liu, L.J., Kaufman, J.D. (2011) *Comparing universal kriging and land-use regression for predicting concentrations of gaseous oxides of nitrogen (NO_x) for the Multi-Ethnic Study of Atherosclerosis and Air Pollution (MESA Air)*. *Atmos Environ* (1994), 2011 Aug 1; 45(26): 4412-4420.

Mitas, L. and Mitasova, H. (1999): *Spatial interpolation*. In Longley, P.A., Goodchild, M.F., Maguire, D.J. and Rhind, D.W., editors, *Geographical Information Systems*, volume 1: principles and technical issues, New York: Wiley, 481–492.

Mofarrah, A., Husain, T. (2010) *A holistic approach for optimal design of air quality monitoring network expansion in an urban area*. *Atmospheric Environment*, 44 3 (January 2010), 432–440, 1352-2310

Moore, D.K., Jerrett, M., Mack, W.J., Kunzli, N. (2007): *A land use regression model for predicting ambient fine particulate matter across Los Angeles, CA*. *J Environ Monit* 2007, 9: 246-252.

Nejadkoorki, F., Nicholson, K., Hadad, K. (2011) *The design of long-term air quality monitoring networks in urban areas using a spatiotemporal approach*. *Environmental*

Monitoring and Assessment, 172 1-4, (January 2011), 215 223, 1573-2959

Nel A. (2005) *Air pollution-related illness: effects of particles*. Science 308(5723): 804-806.

Nikolaos K., Dimitra V., and Agapi X. (2011) *Real estate values and environment: A case study on the effect of the environment on residential real estate values*, International Journal of Academic Research 3(1) Part III.

Ogneva-Himmelberger, Y., Pearsall, H., and Rakshit, R. (2009) *Concrete Evidence and Geographically Weighted Regression: A Regional Analysis of Wealth and the Land Cover in Massachusetts*. Applied Geography 29(4):478-487.

Pathak, R.K.; Yao, X.; Lau, A.K.H., Chan, C.K. (2003) *Acidity and Concentrations of Ionic Species of PM_{2.5} in Hong Kong*; Atmos. Environ. 37, 1113-1124.

Pearce, J.L., Rathbun, S.L., Aguilar-Villalobos, M. and Naeher, L.P. (2009) *Characterizing the spatiotemporal variability of PM 2.5 in Cusco, Peru using kriging with external drift*, Atmospheric Environment 43 (2009) 2060–2069.

Pelucchi, C., Negri, E., Gallus, S., Boffetta, P., Tramacere, I., La Vecchia, C. (2009) *Long-term particulate matter exposure and mortality: A review of European epidemiological studies*. BMC Public Health. 2009; 9:453.

Penner, J.E., Zhang, S.Y., Chin, M., Chuang, C.C., Feichter, J., Feng, Y. I., Geogdzhayev, V., Ginoux, P., Herzog, M., Higurashi, A., Koch, D., Land, C., Lohmann, U., Mishchenko, M., Nakajima, T., Pitari, G., Soden, B., Tegen, I., Stowe L. (2002) *A comparison of model and satellite-derived optical depth and reflectivity*. Retrieved from: <http://data.engin.umich.edu/Penner/paper3.pdf> Last accessed: 15 March 2017.

People's Daily (n.d.) *Beijing*. Retrieved from: <http://en.people.cn/data/province/beijing.html> Last accessed: 17 March 2017.

Phuleria, H.C., Sheesley R.J., Schauer, J.J., Fine, P.M., Sioutas, C. (2007) *Roadside measurements of size-segregated particulate organic compounds near gasoline and diesel-dominated freeways in Los Angeles, CA*. Atmospheric Environment 41, 4653–4671.

-
- Potepan, M. J. (1996) *Explaining Intermetropolitan Variation in Housing Prices, Rents and Land Prices*, Real Estate Economics 24(2): 219-245.
- Qiao, X. (2010) *A Review of the Chinese Real Estate Market*, Social Impact Research Experience (SIRE) 3, University of Pennsylvania Scholarly Commons Retrieved from: <http://repository.upenn.edu/sire/3> Last accessed: 17 March 2017.
- Reis, S. (2008) *Analyzing Land Use/Land Cover Changes Using Remote Sensing and GIS in Rize, North-East Turkey*. Sensors 2008, 8, 6188-6202.
- Richards, J. A. (1986) *Remote Sensing Digital Image Analysis: An Introduction*. Springer-Verlag, Berlin.
- Robinson, D.L. (2005) *Air pollution in Australia: Review of costs, sources and potential solutions*. Health Promot J Austr. 16:213–20.
- Rogana, J.; Chen, D. (2004) *Remote sensing technology for mapping and monitoring land-cover and landuse change*. Progress in Planning 2004, 61, 301–325.
- Rundquist, B. (2010). Unsupervised classification
- Saadat, H., Adamowski, J., Bonnell, R., et al. (2011). *Land use and land cover classification over a large area in Iran based on single date analysis of satellite imagery*. ISPRS J. of Photogrammetry and Remote Sensing, 66: 608-619.
- Sears, A. and Jacko, J. A. (2008) *The Human–Computer Interaction Handbook: Fundamentals, Evolving Technologies, and Emerging Applications*, Lawrence Erlbaum Associates. Third Edition, ISBN 9781410606723.
- Seinfeld, J.H. (1989) *Urban air pollution: state of the science*. Science 243,745–752.
- Shi, W., Wong, S., Wang, J., Zhao, Y. (2012) *Analysis of Airborne Particulate Matter (PM_{2.5}) over Hong Kong Using Remote Sensing and GIS*. Sensors 12(6): 6825-6836.
- Shen, Z., Cao, J., Arimoto, R., Han, Y., Zhu, S., Tian, J., and Liu, S. (2010) *Chemical characteristics of fine particles (PM₁) from Xi'an, China*, Aerosol Sci. Tech., 44, 461–472.

Shier, R. (2004) *Statistics: 2.3 The Mann-Whitney U Test*. Mathematics Learning Support Centre Retrieved from: <http://www.statstutor.ac.uk/resources/uploaded/mannwhitney.pdf> Last accessed: 15 March 2018.

Sloane, C.S., Watson, J., Chow, J., Pritchett, L., Willard Richards, L. (1991) *Size-segregated fine particle measurements by chemical species and their impact on visibility impairment in Denver*. Atmospheric Environment Part A. General Topics 25, 1013–1024.

Spendley, S.K. & Brehme, C.E. (2014) *GIS Analysis of Factors Influencing Particulate Pollution in Keene, New Hampshire*, International Journal of Undergraduate Research and Creative Activities 6 (4).

Spengler, J.D., Hughes, A.F., Vallarino, J., Agyei-Mensah, S., Ezzati, M. (2013) *Chemical composition and sources of particle pollution in affluent and poor neighborhoods of Accra, Ghana*. Environmental Research Letters 8, 044025 (9pp).

Song, C., Wu, L., Xie, Y., He, J., Chen, X., Wang, T., Lin, Y., Jin, T., Wang, A., Liu, Y., Dai, Q., Liu, B., Wang, Y., Mao, H. (2017a) *Air pollution in China: Status and spatiotemporal variations*. Environmental Pollution 227, 334-347.

Song, Y., Wan, X., Bai, S., Guo, D., Ren, C., Zeng, Y., Li, Y., Li, X. (2017b) *The Characteristics of Air Pollutants during Two Distinct Episodes of Fireworks Burning in a Valley City of North China*, PLoS One. 2017; 12(1): e0168297.

Sun, L., Wei, J., Duan, D.H., Guo, Y.M., Yang, D.X., Jia, C., Mi, X.T. (2016) *Impact of Land-Use and Land-Cover Change on urban air quality in representative cities of China*. Journal of Atmospheric and Solar-Terrestrial Physics 142 (2016) 43–54

Sun, Y., Jiang, Q., Wang, Z., Fu, P., Li, J., Yang, T., Yin, Y. (2014) Investigation of the sources and evolution processes of severe haze pollution in Beijing in January 2013. J. Geophys. Res. Atmos. 119, 4380e4398.

Tang, T., Zhao, W., Zhao, W., Gong, H. and Cai, L. (2009) *GIS analysis of spatial and temporal changes of air particulate concentrations and their impacts on respiratory diseases in Beijing, China* Middle State Geographer 42: 73-82.

Tang, T., Zhao, W., Gong, H., Li, X., Zang, K., Bernosky, J.D., Zhao, W., and Li, S. (2010) *GIS spatial analysis of population exposure to fine particulate air pollution in Beijing*,

China, *Environmental Geosciences* 17(1), 1–16.

Tian, Y., Yin, K., Lu, D., Hua, L., Zhao, Q., Wen, M. (2014) *Examining Land Use and Land Cover Spatiotemporal Change and Driving Forces in Beijing from 1978 to 2010*. *Remote Sens.* 2014, 6, 10593-10611

Tsai, J.H., Chang, L.T., Huang, Y.S., Chiang, H.L. (2011) *Particulate composition characteristics under different ambient air quality conditions*, *J Air Waste Manag Assoc.* 61(7): 796-805.

Tyagi, A. and Singh, P. (2013) *Applying Kriging Approach on Pollution Data Using GIS Software*. *International Journal of Environmental Engineering and Management.* 4(3), 185-190

Wang, G., Wang, P. (2014) *PM_{2.5} Pollution in China and Its Harmfulness to Human Health*, *Science and Technology Review* 32(26).

Wang, G., Zhang, R., Gomez, M.E., Yang, L., Levy Zamora, M., Hu, M., Lin, Y., Peng, J., Guo, S., Meng, J., Li, J., Cheng, C., Hu, T., Ren, Y., Wang, Y., Gao, J., Cao, J., An, Z., Zhou, W., Li, G., Wang, J., Tian, P., Marrero-Ortiz, W., Secret, J., Du, Z., Zheng, J., Shang, D., Zeng, L., Shao, M., Wang, W., Huang, Y., Wang, Y., Zhu, Y., Li, Y., Hu, J., Pan, B., Cai, L., Cheng, Y., Ji, Y., Zhang, F., Rosenfeld, D., Liss, P.S., Duce, R.A., Kolb, C.E., Molina, M.J. (2016) *Persistent sulfate formation from London Fog to Chinese haze*. *Proc. Natl. Acad. Sci. U. S. A.* 113, 13630e13635.

Wang, J., Hu, M., Xu, C., Christakos, G., Zhao, Y. (2013a) *Estimation of citywide air pollution in Beijing*. *PLoS ONE* 8(1): e53400.

Wang, J.F., Hu, M.G., Xu, C.D., Christakos, G. and Zhao Y. (2013b) *Estimation of Citywide Air Pollution in Beijing* Retrieved from: PLOS ONE: www.plosone.org 8(1) Last accessed: 17 March 2017.

Wang, S., Huang, G.H., Lin, Q.G., Li, Z., Zhang, H., Fan, Y.R. (2014) *Comparison of Interpolation methods for estimating spatial distribution of precipitation in Ontario, Canada*. *International Journal of Climatology* 34:3745-3751

Wang, W., Tang, D. and Liu, H. (2000) *Research on Current Pollution Status and Pollution Characteristics of PM_{2.5} in China*, *Research of Environmental Sciences*

13(1):1-5 (in Chinese with abstract in English).

Wang, Y., Zhao, L., Sobkowiak L., Guan, X. and Wang, S. (2015) *Impact of urban landscape and environmental externalities on spatial differentiation of housing prices in Yangzhou City*, Journal of Geographical Sciences 25(9): 1122-1136.

Watson, J. G. (2002) *Visibility: science and regulation*. J. Air Waste Manage. 52(6):628-713.

Wei, F., Teng, E. and Wu, G. (2001) *Concentrations and elemental components of PM_{2.5}, PM₁₀ in ambient air in four large Chinese cities*, Environmental Monitoring in China 17(7):1-6 (in Chinese with abstract in English).

WHO (2013) *Health Effects of Particulate Matter*. Revised from:
http://www.euro.who.int/__data/assets/pdf_file/0006/189051/Health-effects-of-particulate-matter-final-Eng.pdf Last accessed: 10 April 2018

WHO (2018) *Air Pollution*. Revised from:
<http://www.who.int/airpollution/ambient/pollutants/en/> Last accessed: 10 April 2018

Wilson, J. G. and Zawar-Reza, P. (2006) *Intraurban-scale dispersion modelling of particulate matter concentrations: applications for exposure estimates in cohort studies*. Atmos. Environ. 40, 1053–1063.

Wong, W., Yuan, L, Perlin, S.A. (2004): *Comparison of spatial interpolation methods for the estimation of air quality data*. J Expo Anal Environ Epidemiol 2004, 14: 404-415.

Wu, G., Hu, W. and Teng, E. (1999) *PM_{2.5} and PM₁₀ pollution level in the four cities in China*, China Environmental Science 19(2):133-137 (in Chinese with abstract in English).

Yamamoto, J.K. (2005). *Comparing ordinary kriging interpolation variance and indicator kriging conditional variance for assessing uncertainties at unsampled locations*. Application of Computers and Operations Research in the Mineral Industry Dessureault, Ganguli, Kecojevic, & Dwyer editors, Balkema.

Yang, L., He, K., Zhang, Q., Wang, Q. et al. (2005) *Vertical Distributive Characters of PM_{2.5} at the Ground Layer in Autumn and Winter in Beijing*. Reserrch of Environmental

Science,18(2):23-28.

Yang, Z., Cai, J., Ottens, H.F.L., Sliuzas, R. (2013) *Beijing*, Cities 31 (2013): 491-506.

Zahran, E.S., Bennett, L. and Smith, M. (2010). An approach to represent air quality in 3D digital city models for air quality-related transport planning in urban areas. In *Computing in Civil and Building Engineering, Proceedings of the International Conference*, Tizani, W. (Editor), 30 June-2 July, Nottingham, UK, Nottingham University Press, Paper 10, p. 19, ISBN 978-1-907284-60-1.

Zhai, L; Sang, H; Zhang, J; An, F. (2015) *The International Archives of Photogrammetry, Remote Sensing and Spatial Information Sciences* Gottingen XL.7: 209-213.

Zhang R., Jing, J., Tao, J., Hsu, S.C., Wang, G., Cao, J., Lee, C.S.L., Zhu, L., Chen, Z., Zhao, Y. (2013) *Chemical characterization and source apportionment of PM_{2.5} in Beijing: seasonal perspective*. Atmospheric Chemistry and Physics 13, 9953–10007.

Zhang, R., Wang, G., Guo, S., Zamora, M.L., Ying, Q., Lin, Y., Wang, W., Hu, M., Wang, Y. (2015) *Formation of urban fine particulate matter*. Chem. Rev. 115, 3803e3855.

Zhang, P., Hong, B., He, L., Cheng, F., Zhao, P., Wei, C., and Liu, Y. (2015) *Temporal and Spatial Simulation of Atmospheric Pollutant PM_{2.5} Changes and Risk Assessment of Population Exposure to Pollution Using Optimization Algorithms of the Back Propagation-Artificial Neural Network Model and GIS*, International Journal of Environmental Research and Public Health 12171-12195.

Zhao, C.X., Wang, Y.Q., Wang, Y.J., Zhang, H.L., Zhao, B.Q. (2014) *Temporal and spatial distribution of PM_{2.5} and PM₁₀ pollution status and the correlation of particulate matters and meteorological factors during winter and spring in Beijing*. Huang Jing Ke Ji 35(2): 418-427 (in Chinese with abstract in English).

Zhao, H., Che, H., Zhang, X., Ma, Y., Wang, Y., Wang, H., Wang, Y. (2013) *Characteristics of visibility and particulate matter (PM) in an urban area of Northeast China*, Atmospheric Pollution Research 4(4): 427-434.

Zhou, M., Liu, Y., Wang, L., Kuang, X., Xu, X., Kan, H. (2014) *Particulate air pollution and mortality in a cohort of Chinese men*. Environ Pollut. 2014; 186:1–6.

Zhou, Z., Dionisio, K.L., Verissimo, T.G., Kerr, A.S., Coull, B., Arku, R.E., Koutrakis, P., Spengler, J.D., Hughes, A.F., Vallarino, J., Agyei-Mensah, S., Ezzati, E. (2013) *Chemical composition and sources of particle pollution in affluent and poor neighborhoods of Accra, Ghana*, Environ. Res. Lett. 8(4).

Zhu, Y., Zhang, J., Wang, J., Chen, W., Han, Y., Ye, C., Li, Y., Liu, J., Zeng, L., Wu, Y., Wang, X., Wang, W., Chen, J. and Zhu, T. (2016) *Distribution and sources of air pollutants in the North China Plain based on on-road mobile measurements*, Atmospheric Chemistry and Physics 12551–12565.

Zsuzsanna, D.; Bartholy, J.; Pongracz, R.; Barcza, Z. (2005) *Analysis of land-use/land-cover change in the Carpathian region based on remote sensing techniques*. Physics and Chemistry of Earth 2005, 30, 109-115.

Appendix A

PM_{0.5}

```
yi yuanju05<-c(24.16,26.01 ,27.84,23.68,19.28,14.70,16.50,15.38,15.79,28.98,20.92,17.18,16.67,17.02,20.58,26.52,29.07,30.01,31.91,33.62,37.33)
```

```
shuixingyuan05<-c(9.12,11.32,12.76,12.39,11.92,15.03,17.33,19.61,34.33,37.22,35.18,38.01,36.37,33.74,25.62,24.18,25.87,25.34,21.94,22.57,23.99)
```

```
var.test(yi yuanju05,shuixingyuan05)
```

#the result shows that the **p-value is 0.1415 (>0.05)**, which means the two groups have equal variance.

```
t.test(yi yuanju05,shuixingyuan05,var.equal=TRUE)
```

#the result shows that the **p-value is 0.9897**, which means the two groups do not have significant difference of the two means.

PM_{1.0}

```
yi yuanju10<-c(42.97,46.41,50.01,41.27,32.78,24.03,27.06,25.03,25.76,54.05,37.96,28.15,27.34,27.96,34.02,48.24,54.06,56.81,61.55,65.93,75.97)
```

```
shuixingyuan10<-c(15.12,18.65,21.24,20.64,20.07,26.03,31.11,36.08,74.17,83.44,76.47,86.69,82.05,72.70,50.51,46.54,50.59,48.77,41.34,42.84,45.61)
```

```
var.test(yi yuanju10,shuixingyuan10)
```

#the result shows that the **p-value is 0.05368 (>0.05)**, which means the two groups have equal variance.

```
t.test(yi yuanju10,shuixingyuan10,var.equal=TRUE)
```

#the result shows that the **p-value is 0.4273**, which means the two groups do not have significant difference of the two means.

PM_{2.5}

```
yi yuanju25<-c(72.71,74.26,76.71,61.93,50.77,37.55,41.69,37.99,38.41,77.72,69.39,41.26,40.24,41.48,49.66,72.12,81.03,85.28,93.17,100.69,116.51)
```

```
shuixingyuan25<-c(26.30,31.23,36.75,36.46,33.72,41.91,50.59,59.25,123,141.79,127.51,146.95,137.42,118.10,79.48,72.91,78.06,74.90,62.95,65.64,70.05)
```

```
var.test(yiyuanju25,shuixingyuan25)
```

```
#the result shows that the p-value is 0.02077(<0.05), which means the two groups have unequal variance.
```

```
t.test(yiyuanju25,shuixingyuan25,var.equal=F)
```

```
#the result shows that the p-value is 0.2365, which means the two groups do not have significant difference of the two means.
```

PM_{5.0}

```
yiyuanju50<-c(217.05,167.93,142.06,110.40,102.20,82.70,92.47,84.90,75.76,130.01,152.14,84.43,81.99,87.48,97.09,128.55,135.67,137.66,151.37,159.26,184.79)
```

```
shuixingyuan50<-c(55.95,64.50,84.97,85.73,73.34,83.19,97.94,115.66,190.49,212.31,189.33,216.08,202.26,175.44,126.52,120.23,122.65,120.17,104.49,110.59,118.08)
```

```
var.test(yiyuanju50,shuixingyuan50)
```

```
#the result shows that the p-value is 0.2679 (>0.05), which means the two groups have equal variance.
```

```
t.test(yiyuanju50,shuixingyuan50,var.equal=T)
```

```
#the result shows that the p-value is 0.827, which means the two groups do not have significant difference of the two means.
```

PM₁₀

```
yiyuanju100<-c(698.31,454.79,335.26,250.52,268.04,218.16,240.22,224.41,189.35,248.33,265.75,208.40,198.10,230.81,283.59,274.85,249.16,301.07,322.41,349.69)
```

```
shuixingyuan100<-c(136.25,168.92,242.27,236.60,184.25,200.61,246.64,308.30,388.64,408.98,378.29,416.07,382.37,362.09,287.14,288.45,269.23,276.30,261.40,268.64,277.14)
```

```
var.test(yiyuanju100,shuixingyuan100)
```

```
#the result shows that the p-value is 0.1217 (>0.05), which means the two groups have equal variance.
```

```
t.test(yiyuanju100,shuixingyuan100,var.equal=T)
```

```
#the result shows that the p-value is 0.8613, which means the two groups do not have
```

significant difference of the two means.

Appendix B

Summer and Winter

```
summerPM0.5<-
```

```
c(19.37,19.63,23.79,38.02,31.73,21.18,21.10,25.14,31.98,31.40,24.67,36.44,36.54,19.17,26.32,27.07,27.27,30.70,29.65,28.29,26.88,27.81)
```

```
winterPM0.5<-
```

```
c(36.75,35.99,35.76,42.18,42.81,40.69,41.22,28.65,28.69,30.88,30.29,26.54,36.42,36.43,12.88,14.38,16.47,18.30,18.40,17.04,17.12,24.94,20.91)
```

```
var.test(summerPM0.5, winterPM0.5)
```

```
#the result shows that the p-value is 0.01076(<0.05), which means the two groups have unequal variance.
```

```
t.test(summerPM0.5, winterPM0.5,var.equal=F)
```

```
#the result shows that the p-value is 0.6878, which means the two groups do not have significant difference of the two means.
```

```
summerPM1.0<-
```

```
c(27.81,27.34,33.50,80.84,64.81,33.53,30.91,39.04,95.38,100.79,88.37,57.80,110.75,110.37,42.41,69.17,70.42,71.36,110.44,93.60,88.47,83.13,83.46)
```

```
winterPM1.0<-
```

```
c(193.33,186.36,179.74,207.40,194.89,196.76,195.22,130.06,106.46,87.24,57.32,50.42,98.56,90.08,21.59,24.29,27.65,30.64,29.57,30.28,48.00,36.19)
```

```
var.test(summerPM1.0, winterPM1.0)
```

```
#the result shows that the p-value is 7.664e-05(<0.05), which means the two groups have unequal variance.
```

```
t.test(summerPM1.0, winterPM1.0,var.equal=F)
```

```
#the result shows that the p-value is 0.06812, which means the two groups do not have significant difference of the two means.
```

```
summerPM2.5<-
```

```
c(43.52,41.01,50.08,140.03,106.97,53.42,43.37,61.80,202.70,214.83,171.93,99.45,235.96,230.44,70.09,119.24,121.58,268.64,207.93,185.39,167.93,167.84)
```

```
winterPM2.5<-  
c(430.90,320.14,315.90,396.95,347.34,425.02,381.62,304.23,208.84,330.74,119.45,104.4  
6,255.05,209.52,32.69,37.43,41.04,46.95,56.18,58.87,97.89,66.91)
```

```
var.test(summerPM2.5, winterPM2.5)  
#the result shows that the p-value is 0.002536(<0.05), which means the two groups have  
unequal variance.
```

```
t.test(summerPM2.5, winterPM2.5,var.equal=F)  
#the result shows that the p-value is 0.04586 (<0.05), which means the two groups have  
significant difference of the two means.
```

```
summerPM5.0<-  
c(84.38,78.05,100.46,332.10,174.31,102.96,78.21,142.12,299.73,324.37,332.01,112.22,  
166.14,168.01,162.89,341.49,252.81,226.10,209.45,237.56)
```

```
winterPM5.0<-  
c(571.84,496.35,442.03,509.59,522.77,536.57,575.12,552.12,378.03,551.61,177.69,174.  
00,504.13,405.15,65.78,74.05,74.54,81.42,83.08,105.76,105.30,158.02,111.16)
```

```
var.test(summerPM5.0, winterPM5.0)  
#the result shows that the p-value is 0.0007396(<0.05), which means the two groups have  
unequal variance.
```

```
t.test(summerPM5.0, winterPM5.0,var.equal=F)  
#the result shows that the p-value is 0.01869(<0.05), which means the two groups have  
significant difference of the two means.
```

```
summerPM10<-  
c(136.23,126.01,167.36,422.52,282.49,171.57,132.59,304.68,410.05,452.35,388.63,262.  
20,571.56,439.84,164.85,223.91,223.21,206.40,370.73,277.37,251.24,230.26,296.29)
```

```
winterPM10<-  
c(831.67,786.84,700.50,844.41,796.44,869.24,850.73,724.69,649.56,668.95,261.51,325.  
84,677.61,620.34,162.85,183.69,149.78,205.55,137.66,258.58,226.47,278.09,186.40)
```

```
var.test(summerPM10, winterPM10)
```

#the result shows that the **p-value is 0.0001611(<0.05)**, which means the two groups have unequal variance.

```
t.test(summerPM10, winterPM10,var.equal=F)
```

#the result shows that the **p-value is 0.002465(<0.05)**, which means the two groups have significant difference of the two means.